Retromer associated sorting nexins SNX1, SNX4, and SNX27 and the trafficking and basolateral membrane population of the intermediate conductance calcium-activated potassium channel (KCa3.1) in polarised epithelial cells

Elliot Pilmore

May 2017

-

In complete fulfilment of the requirements of the Masters of Science at the University of Otago, Dunedin, New Zealand

Abstract

The intermediate conductance calcium (Ca^{2+})-activated potassium (K^+) channel (KCa3.1) is targeted to the basolateral membrane of polarised epithelial cells, and is also found in many non-epithelial cell types. KCa3.1 performs several fundamental roles, including the promotion of transepithelial ion transport, and the maintenance of a homeostatic equilibrium inside cells. Thus, KCa3.1 is found in a wide range of tissues, from epithelial to neural, and is involved in several disease states. These disease states include sickle-cell anaemia, cardiac fibrosis, and diabetic nephropathy, and paint KCa3.1 as a potential target for novel disease therapies.

In order to create these novel disease therapies, it is vital to understand how KCa3.1 is trafficked within the cell. Functionally, KCa3.1 is trafficked from the ER to the Golgi in a manner dependent on Rab1, and from the Golgi to the plasma membrane in a manner dependent on Rab8. Additionally, KCa3.1 trafficking has been shown to require a functional cytoskeleton, as well as the motor protein Myocin-Vc. One trafficking pathway which may traffic KCa3.1 is the Retromer pathway. This pathway involves multiple protein complexes, including the cargo recognition complex, and the WASH complex, as well as multiple individual sorting nexin proteins. If KCa3.1 is found to interact with components of the Retromer pathway, it could lead to new disease therapies.

This project examined the role of three distinct sorting nexin protein; SNX1, SNX4, and SNX27, on the trafficking and basolateral membrane population of KCa3.1 in polarised epithelial cells. In order to do this, Fischer Rat Thyroid cells transfected to stably express a KCa3.1-BLAP (biotin ligase acceptor peptide) construct, were transfected with SNX1, 4, or 27 specific siRNA, then grown on filters in order to achieve polarity. This allowed for the apical and basolateral membrane populations of KCa3.1 to be independently assessed.

Immunoblots were used to determine the extent to which transfections were successful. In cells where the transfection was successful, the basolateral membrane population of KCa3.1 was determined by immunoblots. Additionally, Ussing chamber experiments were utilised in order to explore the effects of transfections on the KCa3.1 current when stimulated by the KCa3.1 opener 1-EBIO, or the KCa3.1 inhibitor clotrimazole.

This project showed the first evidence of the endogenous expression of SNX1 and SNX27 in FRT cells, and confirmed expression of SNX4 in FRT cells, first discovered in the McDonald Lab. Following this demonstration, cells were transfected with 40 pM of either SNX1, SNX4, or SNX27 siRNA. The transfection with SNX1 siRNA resulted in a 44 ± 8% decrease in SNX1 protein levels, however, showed no significant decrease in the basolateral membrane population of KCa3.1, nor in

the KCa3.1 sensitive current measured by Ussing chamber experiments was observed. The transfection with SNX4 showed a 62 ± 12% decrease in intracellular SNX4, however, similar to SNX1, a decrease in intracellular SNX4 did not appear to affect either the basolateral membrane population of KCa3.1, nor the KCa3.1 sensitive currents. Finally, the transfection of cells with SNX27 siRNA showed a 27 ± 4% decrease in the intracellular protein levels of SNX27. While knockdown of SNX27 did not elicit a significant change in the basolateral membrane population of KCa3.1, it did suggest the possibility of KCa3.1 missorting to the apical membrane, as there was a trend towards a significant increase in the apical membrane population of KCa3.1 in the SNX27 knockdown cells compared to the control cells ($p = 0.0818$; $n=4$). These results appear to be consistent with the notion that KCa3.1 is not recycled in polarised epithelial cells, and suggest that KCa3.1 is not trafficked via the Retromer pathway. While KCa3.1 does not appear to be trafficked via the Retromer pathway, there are still unknown factors regarding the trafficking of KCa3.1 which need to be explored, such as why KCa3.1 appears to be recycled in migratory cells. It is important to fully comprehend the trafficking mechanisms surrounding KCa3.1 in order to develop novel effective therapeutic techniques to combat pathophysiological conditions resulting from dysfunctional KCa3.1.

Acknowledgements

First and foremost, I would like to thank my primary supervisor, Kirk Hamilton, and my secondary supervisor, Fiona McDonald. Thank you both so much for devoting as much time as you have towards me to ensure that I have had the success I have this year. Thank you for always having your doors open, and for always offering me brilliant advice, and for coaxing me in the right direction when I needed it. Thank you especially for the support you both gave me when I fell ill. I will never forget how much it meant to me to have such supportive supervisors.

A special thank you to the chair of my MSc committee, Dr Martin Fronius. Every committee meeting we had you always listened to any problems I had, and you have always given me sound advice. In our last meeting, before I went to Auckland to write my thesis up, you said you believed in me. That meant a lot, even though I didn't say it at the time. Thank you.

Rachel, thank you for putting up with me for a second year in a row. Thank you for helping me out when I managed to get myself stuck, and for being patient when I have had problems. I will always be grateful of the help you have given me, and I wish you the best for your future projects.

Tanya, thank you for being a wonderful teacher. You were always so patient when teaching me new techniques, and you always seemed to be able to answer my questions. Thank you for all your help when I was writing up from a different city, you were invaluable.

Pinky, thank you for all the conversations that we have had. I thoroughly enjoyed spending the summer with you during your summer studentship. I hope you continue to enjoy your lab experience.

I would like to extend special gratitude to the Department of Physiology for awarding me a Master's of Science scholarship. I cannot thank you enough for the financial support you have provided me over the last year.

Finally, thank you to all my friends and family for believing in me. I love you all and I couldn't have done this without all your support.

Table of Contents

List of Figures

List of Tables

List of Abbreviations

-	Negative
+	Positive
±	Plus or minus
%	Percent
©	Copyright
°C	Degrees Celsius
µL	Microlitre ($1x10^{-6}$ Litres)
µg	Microgram ($1x10^{-6}$ grams)
µM	Micromole ($1x10^{-6}$ Moles)
1-EBIO	1-Ethyl-1,3-dihydro-2H-benzimidazol-2-one
Å	Ångstrom
α	alpha
Aβ	amyloid-β protein
AβO	amyloid-β protein oligomer
AD	Alzheimer's disease
ADPKD	Autosomal dominant polycystic kidney disease
AEE	Apical early endosome
AL	Apical membrane specific labelling of KCa3.1-BLAP with streptavidin
AP	Adaptin protein
AQP4	Aquaporin 4
ARE	Apical recycling endosome
ATP	Adenosine triphosphate
β	beta
β2AR	Beta-2-adrenergic receptor
BAR	Bin/Amphiphysin/Rvs
BEE	Basolateral early endosome
BCA	Bicinchronic acid
BirA	Biotin ligase
BK	Big conductance calcium-activated potassium channel
BL	Basolateral membrane specific labelling of KCa3.1-BLAP with streptavidin
BLAP	Biotin ligase acceptor peptide
βME	β-mercaptoethanol
BSA	Bovine serum albumin
$CaCl_2$	Calcium Chloride
CFTR	Cystic Fibrosis transmembrane conductance regulator
CI-MPR	Mannose-6-phosphate receptor
Cl^-	Chloride ion
CLT	Clotrimazole
CMM	Cisternal maturation model
CO_2	Carbon dioxide
COP	Coat protein

COS-7	African Green Monkey kidney cells
CRE	Common recycling endosome
CRC	Cargo recognition core
Cs^+	Caesium ion
CTRL	Cells transfected with 40 pM control siRNA
CTRL AL	Cells transfected with 40 pM control siRNA with the apical membrane population of KCa3.1 labelled with streptavidin
CTRL BL	Cells transfected with 40 pM control siRNA with the basolateral membrane population of KCa3.1 labelled with streptavidin
Cu^{2+}	Copper ion
δ	delta
DCEBIO	5,6-Dichloro-1-ethyl-1,3-dihydro-2H-benzimidazol-2-one
DMEM	Dulbecco's modified Eagle medium
DMSO	Dimethyl sulphoxide
DN	Diabetic nephropathy
DNA	Deoxyribose nucleic acid
DSCR3	Down's syndrome critical regulator 3
EDTA	Ethylenediaminetetraacetic acid
ELU	Elution buffer
EQU	Equilibration buffer
ER	Endoplasmic reticulum
ERQC	Endoplasmic reticulum quality control
ETC	Endosome to trans-Golgi network transport carrier
Fam21	Family with sequence similarity 21
FERM	4.1 protein, ezrin, radixin, moesin
FRT	Fischer Rat Thyroid cell, an epithelial cell line
FRT-KCa3.1-BLAP	Fischer Rat Thyroid cell line stably transfected with the KCa3.1-BLAP plasmid
g	Grams
γ	gamma
GAPDH	Glyceraldehyde 3-phosphate dehydrogenase
GPI-APs	Glycosylphosphatidylinositol-anchored protein
H^+	Hydrogen ion
HbS	Haemoglobin with the sickle cell anaemia mutation
HCl	Hydrochloric acid
HEK293	Human Embryonic Kidney cells
HeLa	Henrietta Lacks cell line
HEPES	4-(2-hydroxyethyl)-1-piperazineethanesulfonic acid
HRP	Horseradish peroxidase
HX	Hereditary xerocytosis
IB	Immunoblots
IK1	Intermediate conductance calcium-activated potassium channel
$IK_{Ca}4$	Intermediate conductance calcium-activated potassium channel
I_{SC}	Short circuit current

K^+	Potassium ion
KCa2.1	Small conductance calcium-activated potassium channel 1
KCa2.2	Small conductance calcium-activated potassium channel 2
KCa2.3	Small conductance calcium-activated potassium channel 3
KCa3.1	Intermediate conductance calcium-activated potassium channel
KCa3.1-BLAP	Intermediate conductance calcium-activated potassium channel containing a BLAP sequence
KCa3.1-HA	Intermediate conductance calcium-activated potassium channel containing a HA tag
KCNN	Gene encoding a small/intermediate conductance calcium-activated potassium channel
KCNN4	Gene encoding KCa3.1 (also known as IK1/$IK_{Ca}1$)
KCl	Potassium chloride
KDEL	Lysine, Aspartic acid, Glutamic acid, Leucine - Endoplasmic reticulum retention motif
KCa	Calcium activated potassium channel
K_{IR}	Inwardly rectifying potassium channel
K_v	Voltage gated potassium channel
L	Litre
LDLR	Low density lipoprotein receptor
LL	Dileucine sorting motif
LYS	Lysis buffer
µ	mu
MA	Macula adherens
mA	milliamps
Mg^{2+}	Magnesium ion
mqH_2O	Water filtered through a Millipore filter
Na^+	Sodium ion
NaCl	Sodium chloride
NEM	N-ethylmaleimide
NEU	Neutralising buffer
NHE	Sodium/Hydrogen exchanger
NKCC	Sodium/Potassium/2Chloride ($Na^+/K^+/2Cl^-$) cotransporter
NSF	N-ethylmaleimide-sensitive factor
PBS	Phosphate buffered saline
PBS/BSA	Phosphate buffered saline with 0.1% bovine serum albumin
PDZ	Post synaptic density protein 95, Drosophila disc large tumour suppressor 1, zonula occludens 1
PKD	Gene encoding for polycystin proteins
pM	Picomoles ($1x10^{-12}$ Moles)
pS	Picosiemens
PtdIns3p	Phosphatidylinositol-3-monophosphate
PVDF	Polyvinylidene Fluoride
PX	Phox domain
Rab	Rab-GTPase

Rb^+	Rubidium ion
RES	Resuspension buffer
RME-1	Receptor mediated endocytosis 1
SCA	Sickle cell anaemia
SDS-PAGE	Sodium dodecyl sulphate polyacrylamide gel electrophoresis
siRNA	Short interfering RNA
SNAP	Synaptosomal-associated protein
SNAP23	Synaptosomal-associated protein 23
SNARE	Soluble NSF attachment protein receptor
SNX	Sorting nexin
STX	Syntaxin
TBS	Tris Buffered Saline
TBS-T	Tris Buffered Saline with 0.1% Tween-20
TEN	Tubular endosomal network
TfNR	Transferrin receptor
TGN	Trans-Golgi network
TJC	Tripartite junctional complex
UC	Ulcerative colitis
VAMP	Vesicle-associated membrane protein
VPS	Vacuolar protein sorting-associated protein
VTM	Vesicular Transport Model
WASH	Wiskott-Aldrich syndrome protein and SCAR Homologue
YXXØ	Tyrosine based endocytosis and sorting motif
ZA	Zonula adherens
ZO	Zonula occludens

1 Introduction

1.1 Overview

The tissues of animals can be separated into four distinct categories; connective tissue, muscular tissue, nervous tissue, and epithelial tissue. While each of these tissue categories are vital, epithelial tissue is perhaps the most significant, as this is the tissue used to isolate compartments of the body, and that conveys the epithelial barrier function which precisely controls the transport of solutes throughout the body (Simons & Fuller, 1985). Epithelial cells form epithelial tissue, and the individual epithelial cells themselves convey many important functions, including, selectively passaging macromolecules, through the use of channels and transporters, including solutes and ions, between body compartments separated by epithelial tissue. The maintenance of this selective passage is of paramount importance, as this selective passage of macromolecules maintains the homeostatic equilibrium of the body.

In vivo, epithelial cells bind together to form a sheet of epithelial tissue, with individual cells connected by proteins found in the tripartite junctional complex (TJC), which also separates the cell membrane into two distinct regions, known as the apical (mucosal), and the basolateral (serosal) membranes (Farquhar & Palade, 1963; Tepass *et al.*, 2001). The apical membrane domain is oriented to face the external environment, which includes the lumens of hollow organs such as the intestine, the kidney, and the lungs, whilst the basolateral membrane domain contacts both the basal lamina and adjacent epithelial cells (Simons & Fuller, 1985; Tepass *et al.*, 2001; Apodaca *et al.*, 2012). One of the main advantages of having two distinct membrane regions is to allow for cellular polarisation. Polarisation occurs when some membrane bound proteins are selectively trafficked to one domain. This is important as polarisation sets up solute gradients, allows for more controlled absorption and secretion of ions and solutes. The mechanisms behind these selective trafficking are discussed later, however, contributing factors to protein sorting include; protein synthesis in the endoplasmic reticulum (ER), posttranslational modifications in the ER and the Golgi apparatus, and cytoskeletal function (Ellgaard & Helenius, 2003).

The main protein channel of interest for this project is the calcium activated potassium channel KCa3.1, which, in epithelial cells, is trafficked to the basolateral membrane (Bertuccio *et al.*, 2014; Farquhar *et al.*, 2017). KCa3.1 functions primarily as a K^+ channel to regulate the intracellular and extracellular K^+ levels (Ishii *et al.*, 1997) However, the exact mechanisms controlling the number of KCa3.1 channels in the membrane remains to be intensively studied. This being said, certain aspects of the KCa3.1 trafficking pathway have been determined, such as the proteins Rab1 and

Rab8 (Babbey *et al.*, 2006; Zhang *et al.*, 2009; Dong *et al.*, 2010), which are responsible for the regulation of KCa3.1 transport from the ER to the cis-Golgi body, and from the trans-Golgi body to the plasma membrane respectively (Bertuccio *et al.*, 2014). Secondary to KCa3.1, this project focusses on proteins involved in a novel protein recycling pathway known as the Retromer pathway. This pathway involves multiple protein complexes that facilitate recycling of membrane proteins back to the cell membrane after their endocytosis, the most prominent of which are the cargo selective complex, which selects and binds the Retromer cargo, and the WASH complex, which connects Retromer to the actin cytoskeleton, facilitating movement (Yang *et al.*, 2005). While Retromer has been studied intensively by multiple groups since its discovery, nobody has studied the possibility of interactions between Retromer and KCa3.1 until now.

1.2 Polarity in Epithelial cells

Epithelial polarity allows for controlled absorption or secretion of ions and molecules across the epithelia, and is the mechanism responsible for basic physiological functions such as the absorption of nutrients and the secretion, and subsequent expulsion of waste. As mentioned previously, the apical membrane faces into the lumen of organs, such as the intestine, and faces into body cavities, however the basolateral domain can be described as two separate membrane domains, the lateral and the basal domains, despite not being physically separate, as the apical and the basolateral membranes are. The lateral membrane domain interacts with epithelial cells which are adjacent to the cell, and contains the TJC on the apical most area of the domain, which defines the border between the apical and the basolateral membranes. The basal membrane domain interacts with subjacent cells, or with the components of the basement membrane though interactions with integrin receptors and dystroglycans (Apodaca *et al.*, 2012). Furthermore, the basolateral membrane contains a relatively high concentration of phosphatidylinositol-3, 4, 5-triphosphate, which has been shown to regulate the formation of the basolateral membrane by acting as a target for basolaterally targeted proteins (Gassama-Diagne *et al.*, 2006). When phosphatidylinositol-3, 4, 5-triphosphate was added to the apical membrane, basolateral proteins were found to target to the apical membrane, Additionally, this was found to not be due to disruption of the TJC, as the TJC was undisturbed by the addition of phosphatidylinositol-3, 4, 5-triphosphate, and the epithelial monolayer did not become “leaky” which would signify disruption to the tight junctions (Gassama-Diagne *et al.*, 2006).

The main protein complex which is involved in creating a scenario where epithelial polarisation can exist is the TJC (Farquhar & Palade, 1963; Tepass *et al.*, 2001), which acts on both the X, and Z-axes, forming a “ring” of membrane bound protein around the circumference of the cell. The TJC comprises of three individual elements; the zonula occludens (tight junction), the

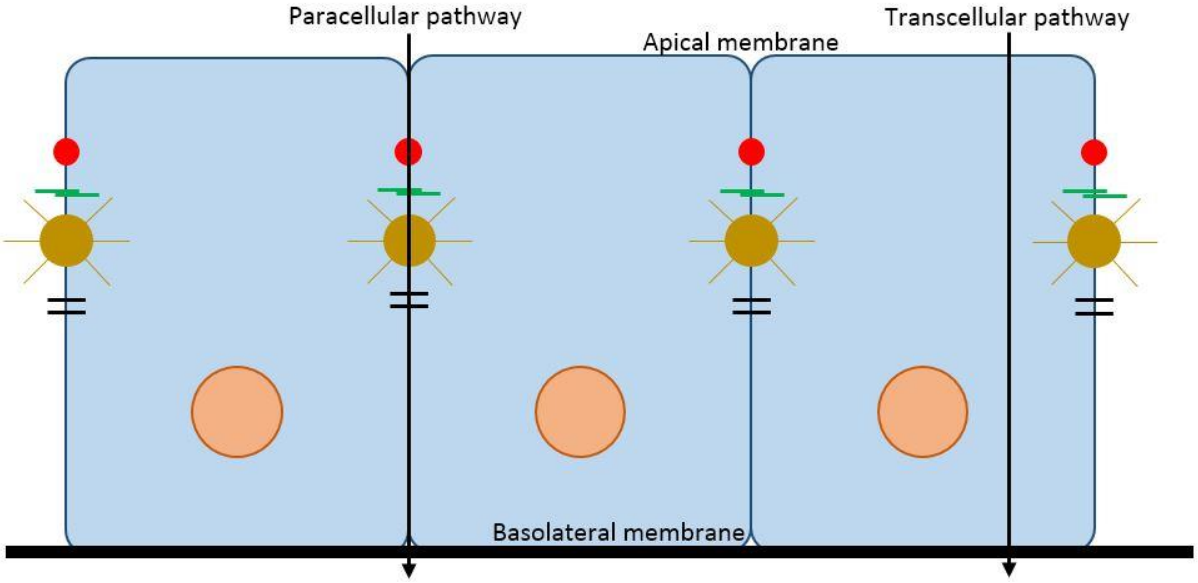

Figure 1.1 – Diagram showing epithelial cells *in vivo* displaying the apical and basolateral membrane, the components of the TJC, and the different transport routes for solutes. The components of the TJC are colour coded as follows; red is the zonula occludens (tight junction), green is the zonula adherens (intermediate junction), gold is the macula adherens (desmosome), and black is the gap junction. Pilmore, Unpublished.

zonula adherens (intermediate junction), and the macula adherens (desmosome) (Figure 1.1). The zonula occludens (ZO) is primarily characterised by the fusion of adjacent cell membranes, which results in the obliteration of the intercellular space. Furthermore, the ZO causes dense leaflets from the external plasma membrane of each cell to interact, forming a dense, single belt (Farquhar & Palade, 1963). Unlike the ZO, the zonula adherens (ZA) does not cause the elimination of the intercellular space, instead, the ZA is characterised by the presence of a small (~200 Ångströms (Å)) gap containing low density material. In some epithelia, the ZA forms a continuous belt, similar to the ZO, however this variable depending on the epithelia, and can be discontinuous (Farquhar & Palade, 1963). Similar to the ZA, the macula adherens (MA) also contains an intercellular space, which is slightly larger than that of the ZA (~240Å). Furthermore, the MA contains a central disc of cytoplasmic plaques, and cytoplasmic fibrils which interact with the plaques in order to anchor the cells together (Farquhar & Palade, 1963). The 3 components of the TJC act together to prevent membrane bound proteins from migrating from one membrane domain to the other (Madara, 1998). Furthermore, the TJC forms a semipermeable barrier, creating a secondary pathway for solutes to move, and controlling the paracellular transport of solutes (Figure 1.1) (Madara, 1998).

1.3 Biosynthetic secretory pathway

The biosynthetic secretory pathway is the cellular process behind the synthesis of cellular proteins. It is, therefore, important to understand the basics of this process when studying cellular protein function. Protein synthesis begins with the ribosomes in the cytosol, which decode

messenger RNA into amino acid sequences. For proteins to enter the secretory pathway, or for proteins that will be secreted or trafficked to the plasma membrane containing a hydrophobic signal sequence, the ribosomes move to the endoplasmic reticulum (ER), where the newly synthesised proteins undergo quality control (ERQC) (Rapoport *et al.*, 1996). The ERQC acts to ensure that newly synthesised proteins are functioning correctly, and to prevent non-functional proteins from progressing in the trafficking pathway (Ellgaard & Helenius, 2003). Ineffective proteins are released into the cytoplasm, where they are degraded into their constituent amino acids through the ubiquitin-proteasome pathway (McCracken & Brodsky, 1996).

Once proteins successfully navigate through the ERQC, they are trafficked towards the cis-Golgi body via anterograde coat protein (COP) II vesicles (Barlowe *et al.*, 1994). The COP II vesicles take proteins to the ER/cis-Golgi intermediate compartment, which acts to increase the concentration of proteins so that only a few vesicles are ultimately required to transport proteins (Figure 1.2) (Klumperman *et al.*, 1998). Additionally, another type of COP vesicle, the COP I vesicle, also transports proteins around the Golgi and back to the ER, however, COP I largely traffics proteins

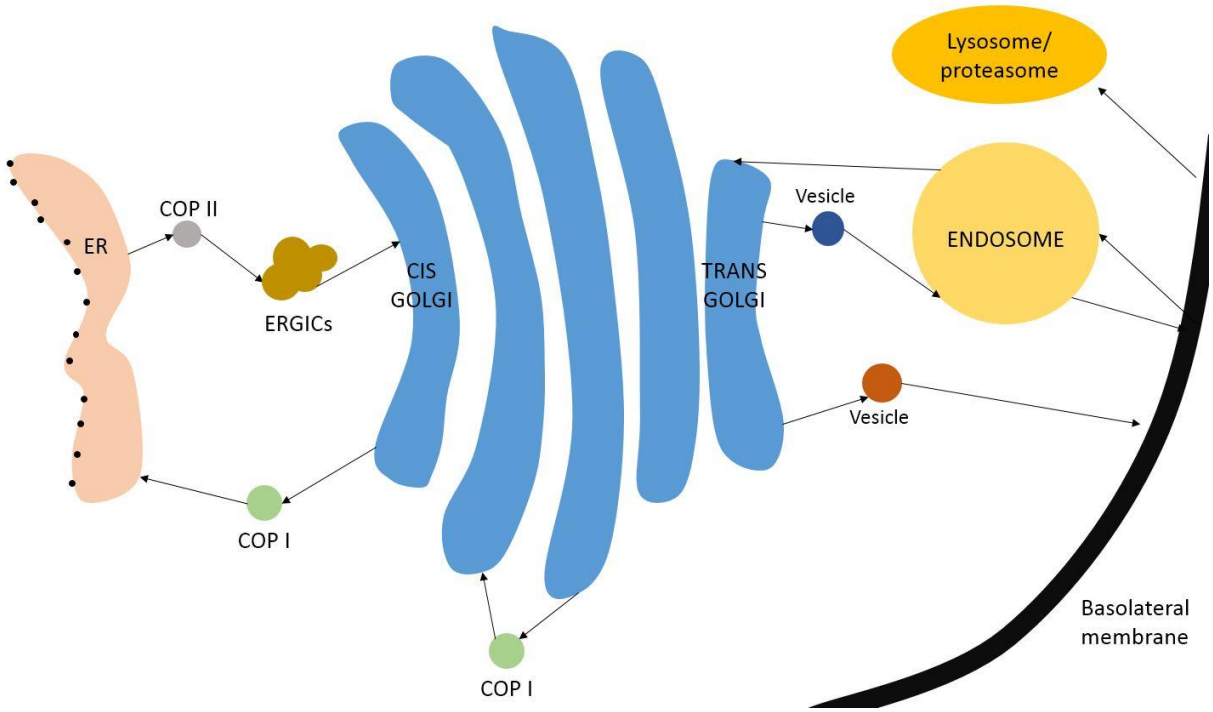

Figure 1.2 – Schematic diagram of the biosynthetic secretory pathway in epithelial cells. Proteins are trafficked from the ER to the cis-Golgi body through two vesicle systems; COP II vesicles travel to the ER/cis-Golgi intermediate compartment (ERGIC), which then travels to the cis-Golgi body. Proteins containing an endoplasmic reticulum KDEL motif are trafficked back to the ER in COP I vesicles. COP I vesicles are also used to traffic proteins in a retrograde fashion between the stacks of the Golgi apparatus. Finally, proteins are released from the trans-Golgi body, and trafficked to the plasma membrane (shown here as the basolateral membrane), either directly or indirectly. Pilmore, Unpublished.

containing an ER retention motif consisting of Lysine, Aspartic acid, Glutamic acid, and Leucine (KDEL) (Figure 1.2) (Majoul *et al.*, 2001).

At the Golgi, proteins undergo further post translational modifications, which ensure that the proteins will be fully functional in the cell. There are two hypotheses as to how the Golgi apparatus traffics and matures proteins; the Vesicular Transport Model (VTM), and the Cisternal Maturation Model (CMM). The VTM proposes that the individual cisterna of the Golgi are static, and that proteins are trafficked between cisternae via COP I vesicles, receiving specific post translational modifications in each cisterna (Pfeffer, 2010). On the other hand, the CMM states that proteins enter the cisterna at the cis-Golgi, which then mature as the proteins inside receive post translational modifications (Figure 1.2). Furthermore, the CMM states that Golgi specific enzymes are trafficked retrogradely by COP I vesicles (Mironov *et al.*, 2003), allowing for the individual cisterna to have a fluid enzymatic composition, compared to the static, but more specialised enzymatic composition seen in the VTM (Pfeffer, 2010). Ultimately, proteins exit the trans-Golgi body complete with post translational modifications which serve the dual functions of improving protein function, and facilitating protein trafficking through sorting signals (Wandinger-Ness *et al.*, 1990).

1.3.1 Apical Trafficking Pathways

In polarised epithelial cells, membrane proteins need to contain specific motifs in order to accurately traffic them to the appropriate membrane (Misek *et al.*, 1984; Fuller *et al.*, 1985). Apical sorting signals are often post translational modifications, most commonly N-linked or O-linked glycosylation (Scheiffele *et al.*, 1995; Yeaman *et al.*, 1997), both of which lead to protein missorting if not present. As these modifications are added in the Golgi apparatus, proteins are trafficked as soon as they exit the trans-Golgi body. In apical anterograde trafficking, proteins are sorted at the Golgi based on their affinities to interact with self-aggregated structures (Lafont *et al.*, 1998; Ohkura *et al.*, 2014) comprised of cholesterols and glycosphyngolipids known as lipid rafts (Hakomori & Handa, 2002; Wang & Silvius, 2003). The apically targeted proteins are sorted into vesicles, which then interact with lipid rafts, which act as the secondary sorting mechanism for apical transport vesicles (Brown *et al.*, 1989; Lisanti *et al.*, 1989; Kenworthy & Edidin, 1998). The main factor by which apical transport vesicles interact with lipid rafts is through the presence of glycosylphosphatidylinositol-anchored proteins (GPI-APs). GPI-APs become incorporated into the lipid rafts as the rafts pick up the apically targeted proteins at the trans-Golgi body (Brown *et al.*, 1989; Lisanti *et al.*, 1989; Tashima *et al.*, 2006).

While many apical proteins are trafficked through the use of lipid rafts, some proteins are not. These proteins still utilise apical transport vesicles, however these do not have the GPI-APs, and do not interact with the glycosphingolipids of the rafts. Irrespective of whether proteins utilise lipid rafts or not, apically targeted proteins either utilise certain endosomes, such as the apical early endosome, or the apical recycling endosome, or are targeted directly targeted to the apical membrane (Figure 1.3). Additionally, all apically targeted vesicles dock to the membrane to release their proteins into the plasma membrane by soluble NSF attachment protein receptor (SNARE) mediated fusion, with the proteins synaptosomal-associated protein (SNAP) 23, and two SNARE proteins; vesicle-associated membrane protein (VAMP) 7, and Syntaxin (STX) 3 (Lafont *et al.*, 1999; Sharma *et al.*, 2006), which are discussed further in section 1.3.2.

1.3.2 Basolateral Trafficking Pathways

Unlike apical sorting signals, basolateral sorting signals are often the result of specific amino acid sequences, rather than from post translational modifications. Furthermore, a large amount of heterogeneity is present between these proteins, meaning that basolaterally targeted proteins largely have differing amino acid basolateral targeting sequences, however there are some common

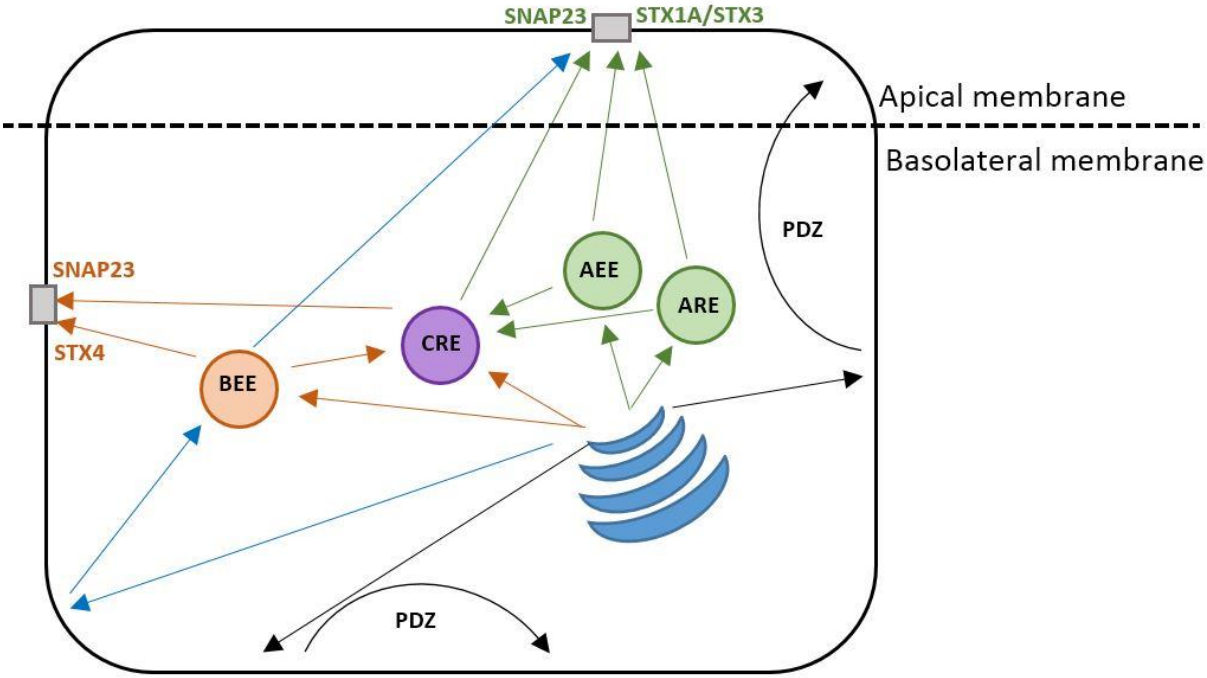

Figure 1.3 **–** Basic anterograde trafficking routes in epithelia. Green shows apical protein sorting, including both the apical early (AEE) and recycling (ARE) endosomes, which can then traffic proteins either to the common recycling endosome (CRE), or to the apical membrane, where SNAP23 and either STX1A or STX3 incorporate the proteins into the apical membrane. Additionally, in some polarised cells, apically targeted proteins can travel via the transcytotic pathway (Blue), where proteins are sent to the basolateral membrane, before being sent to the basolateral early endosome (BEE), then to the apical membrane. Orange shows basolateral protein sorting, including the BEE, which can traffic proteins either to the CRE or to the basolateral membrane, where SNAP23 and STX4 incorporate proteins into the basolateral membrane. Finally, proteins can be sent to a random membrane (Black), which achieves an asymmetric distribution through selective protein retention in the cell membrane through interactions with PDZ proteins. Pilmore, Unpublished.

motifs which have been identified. One of the main motifs involved in basolateral protein trafficking is the tyrosine (YXXØ) motifs, consisting of tyrosine (Y), two nonspecific amino acids (X), and a large hydrophobic residue (Ø) (Matter *et al.*, 1992; Thomas *et al.*, 1993; Sun *et al.*, 2001). A second type of basolateral sorting signal are hydrophobic/dileucine (LL) motifs, which exist on the C-terminal domain (Miranda *et al.*, 2001; Regeer & Markovich, 2004; Guezguez *et al.*, 2006). Additionally, basolateral sorting signals and basolateral sorting machinery share common elements with endocytic sorting machineries (Rodriguez-Boulan & Musch, 2005; Deborde *et al.*, 2008). Furthermore, it is not uncommon for basolateral proteins to have two sorting signals; both the low-density lipoprotein receptor (LDLR) and aquaporin 4 (AQP4) have both a YXXØ motif and an element with an acidic residue cluster (Matter *et al.*, 1992; Madrid *et al.*, 2001). Similarly, the basolateral protein CD147 contains both a mono-leucine motif and an acidic residue cluster (Deora *et al.*, 2004).

There are two main mechanisms behind the basolateral trafficking of proteins; the use of adaptins and the exocyst complex. Adaptins contain heterotetrameric clathrin adaptor proteins, which recognise both the YXXØ and LL motifs through linking clathrin onto the membrane proteins (Yao *et al.*, 2002; Doray *et al.*, 2007). The adaptins AP-1 and AP-2 are two of the major components of clathrin coated vesicles, interacting predominantly with YXXØ and LL motifs, and serve different functions; AP-1 is involved in trans-Golgi body vesicles, while AP-2 is part of plasma membrane vesicles (Jackson *et al.*, 2010; Robinson *et al.*, 2010). Structural and biochemical experiments have shown that the YXXØ motif interacts with the μ subunit of AP-1 and AP-2 (Owen & Evans, 1998), while the LL domain has been suggested to have several interactions; the β subunit of AP-1 and AP-2, the μ subunit of AP-1 and AP-2, the γ/δ hemicomplex of AP-1, and the α/δ hemicomplex of AP-2 (Rodionov & Bakke, 1998; Bonifacino & Dell'Angelica, 1999; Geyer *et al.*, 2002; Coleman *et al.*, 2006; Doray *et al.*, 2007).

The other basolateral trafficking mechanism is the exocyst complex, consisting of eight subunits (Sec3, 5, 6, 8, 10, Exo70, and Exo 84), that acts to regulate the delivery of basolateral cell surface proteins (Lipschutz *et al.*, 2000). The exocyst complex was discovered originally in the yeast *Saccharomyces cerevisiae* through biochemical and genetic experiments (Novick *et al.*, 1980; TerBush & Novick, 1995; TerBush *et al.*, 1996). The mammalian exocyst complex was first purified from rat brain, however it was further found in all the examined tissues (Hsu *et al.*, 1996; Hsu *et al.*, 1998). Most of the exocyst subunits interact with multiple other exocyst subunits, although each individual subunit of the exocyst complex appears to have a unique function (Guo *et al.*, 1999; Matern *et al.*, 2001; Dong *et al.*, 2005). Sec8 inhibition prevents the transport of the LDLR to the basolateral membrane, mutations in Sec5 and 6 hinder the trafficking of D-cadherin to the basolateral membrane, and overexpression of Sec10 reduces the transport of basolateral proteins

(Grindstaff *et al.*, 1998; Lipschutz *et al.*, 2000; Langevin *et al.*, 2005). The exocyst is recruited to areas of membrane expansion and exocytosis, where it mediates vesicle tethering to the plasma membrane, at which point vesicle fusion through soluble N-ethylmaleimide-sensitive factor (NSF) protein receptor mediated membrane fusion can occur (discussed below) (Guo *et al.*, 1999; Guo *et al.*, 2000; Rivera-Molina & Toomre, 2013; Luo *et al.*, 2014). In yeast, the exocyst protein Sec15 interacts with Rab8 (Wu *et al.*, 2005). If this interaction occurs between one of the mammalian exocyst subunits and Rab8 this could suggest a role of the exocyst complex in the trafficking of KCa3.1 to the basolateral membrane.

1.3.3 Fusion of vesicles with the membrane

Once proteins have been successfully trafficked out to the plasma membrane, the cell needs to insert the protein into the plasma membrane for it to function. This is made possible by specialised proteins which lower the energy needed to insert proteins into the membrane. One group of proteins with the primary function of aiding vesicle integration with the plasma membrane are the soluble N-ethylmaleimide-sensitive fusion protein-attachment receptors (SNAREs). SNAREs are classified into two categories; vesicle SNAREs (v-SNAREs), and target SNAREs (t-SNAREs) (Sollner *et al.*, 1993). Both v-and t-SNAREs associate with the plasma membrane, however the v-SNARE reside on the outside of the vesicles, while the t-SNAREs are located on the plasma membrane, allowing for a SNARE complex to form, mediating the specific recognition and fusion of vesicles with membranes (Sollner *et al.*, 1993).

As with many protein groups, there are multiple v- and t-SNAREs. The v-SNAREs are known as vesicle-associated membrane proteins (VAMPs), and display polarity in polarised cells. This acts to stop any missorted vesicles from attaching to the incorrect membrane. VAMP7 is found on apically targeted vesicles, while VAMP3 is found specifically on basolaterally targeted membranes (Lafont *et al.*, 1999; Procino *et al.*, 2008). Unlike VAMP3 and VAMP7, another VAMP, VAMP8 does not show epithelial polarity, suggesting that VAMP8 is involved in exocytosis and recycling pathways (Wang *et al.*, 2007). Similar to the polarity seen by the v-SNARE VAMP proteins, the t-SNARE proteins also exhibit epithelial polarity. STX (Syntaxin) 3 is primarily expressed on the apical membrane, and interacts with VAMP7 on apically targeted vesicles (Lafont *et al.*, 1999), while STX 4 is expressed at the basolateral membrane, and interacts with VAMP3, found on basolaterally targeted vesicles (Procino *et al.*, 2008). However, just as VAMP8 does not present polarity, there are two t-SNAREs not illustrating polarity in epithelial cells; STX 2 and Synaptosomal-associated protein 23 (SNAP23), which are both expressed at the apical and basolateral membranes (Fujita *et al.*, 1998). In particular, SNAP23 interacts with both STX 3 and 4 to form t-SNARE complexes at the apical and the basolateral membranes respectively (Figure 1.3).

1.4 Families of Potassium Channels

Whilst K^+ channels share the ability to traffic K^+ ions with a higher affinity than Na^+ ions (Morais-Cabral *et al.*, 2001), they can be separated out into four general families; voltage gated channels, inward rectifying channels, tandem pore channels, and calcium (Ca^{2+}) activated channels (Jiang *et al.*, 2002; MacKinnon, 2003). Ca^{2+} activated K^+ (KCa) channels, which includes the channel KCa3.1, discussed in section 1.4.1, are activated directly or indirectly by the presence of intracellular Ca^{2+}. The KCa channel family can be further subdivided into three categories, based on their conductance; big conductance (BK) channels, intermediate conductance (IK) channels, and small conductance (SK) channels. The SK and IK channels are both members of the KCNN gene family (Ishii *et al.*, 1997; Joiner *et al.*, 1997), therefore, both the IK and SK channels are relatively similar. Both the IK and SK channels are activated by Ca^{2+} as it binds to a calmodulin domain on the C-terminal complex (Xia *et al.*, 1998; Fanger *et al.*, 1999; Schumacher *et al.*, 2001). Furthermore, both the IK and SK channels exhibit a relatively low conductance; IK has a conductance of ~20-45 pS, while SK is even lower, with a conductance of ~2-20 pS (Ishii *et al.*, 1997; Joiner *et al.*, 1997). For reference, the BK channel has a conductance of ~200 pS (Barrett et al., 1982). The similarities that exists between the IK and SK channels are due to them all being members of the KCNN gene family, with the IK channel (IK1/KCa3.1) exhibiting ~40% similarity at the amino acid level compared to the SK channels (SK1-3/KCa2.1-3) (Ishii *et al.*, 1997; Joiner *et al.*, 1997).

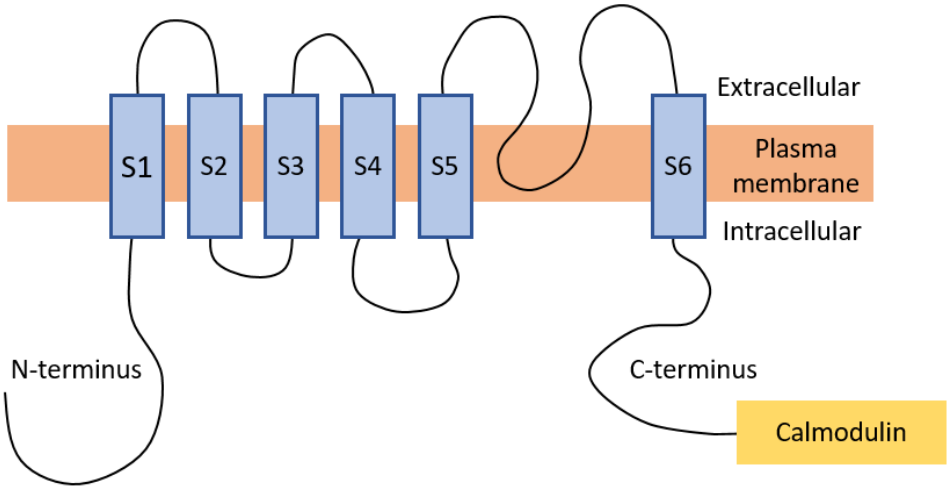

***Figure 1.4* – The KCa3.1 channel.** This diagram shows the KCa3.1 channel, containing six transmembrane domains, labelled S1-S6. KCa3.1 also contains a calcium binding calmodulin domain on the C-terminus, and a pore forming loop between the 5th and 6th transmembrane domains. At the plasma membrane, four of the proteins shown here combine to form a heterotetrameric functional KCa3.1 channel. Pilmore, Unpublished.

The SK channels were first cloned from the mammalian brain (Kohler *et al.*, 1996), and were identified before KCa3.1 was identified (Ishii *et al.*, 1997; Joiner *et al.*, 1997). SK channels contain the

traditional K^+ selectivity pore in their pore loop, which is located between S5 and S6 (Kohler *et al.*, 1996). The trafficking of the SK channel KCa2.3 has been shown to be controlled by a number of factors, including the calmodulin domain used in channel activation (Lee *et al.*, 2003). Additionally, it has been shown that the N-terminal domain, the proximal C-terminal domain, and the calmodulin domain are all vital to traffic KCa2.3 from the ER out to the Golgi body, and that the distal C-terminal domain contains motifs which are required for KCa2.3 to exit the Golgi body and enter transport vesicles (Roncarati *et al.*, 2005).

Importantly for this project, KCa2.3 has been shown to be recycled, which suggests that other members of the KCNN gene family may have also retained the ability for recycling. KCa2.3 has been shown to undergo membrane recycling, which is dependent on RME-1, Rab35, and an N-terminal domain (Gao *et al.*, 2010; Lin *et al.*, 2012). Additionally, KCa2.3 endocytosis has been shown to undergo caveolar trafficking, with endocytosis dependent on GTPases, and exocytosis depending on N-ethylmaleimide (NEM) (Lin *et al.*, 2012), although the experiments performed by Lin and colleagues were in endothelial, rather than epithelial cells. While KCa2.3 has been shown to be recycled, current evidence suggests that KCa3.1 is not, instead, only undergoing a process of slow internalisation followed by degradation (Lin *et al.*, 2012). Furthermore, under the timescale measured by Lin and colleagues (< 30 mins), KCa3.1 was found to not be trafficked from the basolateral membrane (Lin *et al.*, 2012). While these results suggest that KCa3.1 is not recycled, a paper by Schwab and colleagues (Schwab *et al.*, 2012) proposed that KCa3.1 is recycled in migratory cells. This team showed that KCa3.1 is subject to clathrin mediated endocytosis, and calculated that KCa3.1 should be internalised much faster than the 60-90 min half-life which is observed (Balut *et al.*, 2010). This lead Schwab and collaborators to suggest their results were consistent with the notion of channel recycling, despite not producing data showing channel internalisation kinetics.

1.4.1 KCa3.1

In 1958, Gyorgi Gárdos was studying currents in erythrocytes when he observed that the addition of Ca^{2+} resulted in a stimulated electrical current (Gardos, 1958). It was further noted by Gardos that as Ca^{2+} increased, there was a resultant increase in K^+ efflux. Although this Ca^{2+} sensitive K^+ current was first observed in 1958, the current was not accurately shown to be that of KCa3.1 until 2003 (Hoffman *et al.*, 2003). While the intermediate conductance Ca^{2+} activated K^+ channel is primarily referred to nowadays as KCa3.1, in the past it was referred to as IK1, $IK_{Ca}4$, and originally as SK4.

The KCa3.1 channel consists of a tetrameric structure showing rotational symmetry around the channel pore, which, when constructed correctly, forms a voltage and time independent, ligand

binding channel. Each of the four subunits which make up KCa3.1 are comprised of 427 amino acids, arranged to form six transmembrane domains and a P loop between domains 5 and 6 (Figure 1.4) (Jiang *et al.*, 2003; Klein *et al.*, 2007). While it has been mentioned that KCa3.1 is activated by Ca^{2+}, which binds to a calmodulin receptor on the C-terminal domain, KCa3.1 is also known to be activated by ATP, 1-EBIO, and DCEBIO (Devor *et al,* 1996; Joiner *et al,* 1997; Fanger *et al*, 1999; Gerlach *et al*., 2001). Furthermore, KCa3.1 has a number of inhibitors, namely charybdotoxin and clotrimazole (Devor *et al.*, 1997; Ishii *et al.*, 1997; Joiner *et al.*, 1997).

1.4.2 Trafficking of KCa3.1

Much of KCa3.1 trafficking remains to be studied, however, there are certain aspects which have been deciphered. The majority of the knowledge regarding KCa3.1 trafficking is based on the anterograde KCa3.1 trafficking pathway. Recently, Bertuccio and colleagues (2014) examined the role of Rab1 and Rab8 in the trafficking of KCa3.1 to the basolateral membrane. Previously, the roles of both Rab1 and Rab8 in epithelial trafficking had been clearly defined; Rab1 regulates ER → cis-Golgi apparatus trafficking (Zhang *et al.*, 2009), while Rab8 regulates trans-Golgi → basolateral membrane trafficking (Chen *et al.*, 1998). The role of both Rab1 and Rab8 in the trafficking of KCa3.1 was discovered through dominant-negative mutations of Rab1 and Rab8, which resulted in a reduction of the membrane population of KCa3.1 at the basolateral membrane, demonstrating an essential role for both Rab1 and Rab8 in KCa3.1 trafficking. Additionally, it was shown that, following exit from the Golgi apparatus, KCa3.1 is not trafficked through either the transferrin receptor positive recycling endosomes, nor through RME-1, suggesting that KCa3.1 is directly trafficked to the basolateral membrane (Bertuccio *et al.*, 2014).

As mentioned above, there are conflicting studies regarding the possible recycling of KCa3.1; Schwab found that KCa3.1 appeared to be internalised in a manner consistent with channel recycling in migratory cells (Schwab *et al.*, 2012), while Lin found that KCa3.1 was only subject to slow internalisation and degradation in aortic vessels (Lin *et al.*, 2012). While Lin and colleagues did not find any evidence of KCa3.1 recycling, they did find evidence of KCa2.3 recycling (Lin *et al.*, 2012). This suggest that other members of the KCNN gene family may be recycled, such as KCa3.1.

Furthermore, the role of two further aspects have been established in KCa3.1 trafficking; the cytoskeleton and the motor protein myocin-Vc. Inhibiting either cytoskeletal activity or myocin-Vc activity each reduced targeting of KCa3.1 to the basolateral membrane, however it is unknown whether or not KCa3.1 is missorted to the apical membrane, or if it simply never reaches the membrane (Farquhar *et al.*, 2017). In addition, Farquhar and colleagues (2017) stated that it is not understood the exact role that myocin-Vc plays in the trafficking of KCa3.1, and suggested that, it is

likely that myocin-Vc affects KCa3.1 trafficking after KCa3.1 leaves the Golgi apparatus, as both myocin-Vc and the cytoskeleton have been shown to interact with Rab8 (Chabrillat *et al.*, 2005; Watanabe *et al.*, 2008; Xu *et al.*, 2009). Farquhar and collaborators (2017) proposed that, as myocin-Vc has been shown to traffic cargo along the microtubules, it is possible that myocin-Vc allows KCa3.1 to be trafficked along the microtubule cytoskeleton of the cell (Jacobs *et al.*, 2009).

1.4.3 Clinical relevance of KCa3.1

As KCa3.1 is present in a wide variety of tissues, it is able to play a role in a number of pathophysiological states. Under normal physiological conditions, KCa3.1 plays an important role in the homeostasis of both intracellular and extracellular K^+, therefore, if this balance is disrupted, it can lead to serious pathophysiological conditions. As it stands, this makes KCa3.1 out to be an attractive target for disease therapy. However, in order to generate novel therapies, it is vital to obtain a more complete understanding of both KCa3.1 trafficking and KCa3.1 stimulation/inhibition, as different disease states alter KCa3.1 expression in different ways; some states increase the membrane population of KCa3.1, while some decrease it, and some disease states act to alter the open probability of KCa3.1. Current experimental data suggest that altering the membrane population of KCa3.1, thus "resetting" the membrane population of KCa3.1 back to physiological levels, could act as a compensatory mechanism to reduce the effects of certain disease states.

1.4.4.1 Hereditary xerocytosis

Recently, it has been reported that KCa3.1 plays a role in hereditary xerocytosis (HX), which is also known as dehydrated hereditary stomatocytosis. HX is an autosomal dominant disease, resulting in congenital haemolytic anaemia, and is clinically categorised by primary erythrocyte dehydration (Miller *et al.*, 1971). This dehydration is the result of greatly increased K^+ permeability in comparison to Na^+ permeability, which results in the loss of KCl from the cells, leading to cellular water loss in order to maintain the osmotic equilibrium (Miller *et al.*, 1971). There have been three mutations in the KCNN4 gene which codes for KCa3.1 which have been linked to HX; one mutation within the calmodulin binding domain, and the other two on the pore forming domain (Andolfo *et al.*, 2013; Glogowska *et al.*, 2015; Rapetti-Mauss *et al.*, 2015). As the KCNN4 mutations which lead to HX ultimately increase KCa3.1 channel activity, it is believed that the increased K^+ efflux from KCa3.1, leads to Cl^- efflux, and subsequently, water exits the erythrocytes. This mechanism is similar to the erythrocyte dehydration seen in sickle cell anaemia (Lauf *et al.*, 1992; Gibson *et al.*, 1998), where KCa3.1 is activated by increased Ca^{2+} influx, leading to K^+ efflux, and water loss (discussed in section 1.5.3.4).

1.4.4.2 Ulcerative colitis

A second disease state involving KCa3.1 is the inflammatory bowel disease, ulcerative colitis (UC). In the human colon, the dominant driving force of water absorption is electrogenic Na^+ ion transport (Greig *et al.*, 2004). A decrease in the potential difference caused by the electrogenic Na^+ transport is a trademark trait of inflammation in the mucosa, reflecting downregulation of apical Na^+ channels (Amasheh *et al.*, 2004). A further driving force in water absorption are basolateral K^+ channels, such as KCa3.1 (Sandle *et al.*, 1994). These channels determine the intracellular membrane potential, which is an important factor in Na^+ channel activity, and therefore, water absorbance. In UC, unlike in HX, the basolateral membrane concentration of KCa3.1 has been found to be significantly reduced compared to healthy patients (Al-Hazza *et al.*, 2012). This reduction in KCa3.1 was sufficient to incur a 75% decrease in K^+ ion flux, which lead to an impaired Na^+ ion flux, and a subsequent reduction in the ability of affected cells to absorb water across the apical membrane (Al-Hazza *et al.*, 2012). While this does not specifically indicate that a reduction in KCa3.1 expression correlates directly to the pathophysiological symptoms of UC, KCa3.1 was suggested to be a potential target for disease therapy to treat the symptoms of UC.

1.4.4.3 Autosomal dominant polycystic kidney disease

Autosomal dominant polycystic kidney disease (ADPKD) is a monogenic disorder affecting luminal organs such as the liver, pancreas, heart vesicles, and the brain; however ADPKD is best known for its pathophysiological renal effects (Dalgaard, 1957; Torres *et al.*, 2007; Torres & Harris, 2009). ADPKD can be caused by mutations in two individual genes, PKD1, which accounts for roughly 85% of ADPKD cases, and PKD2, which accounts for the remaining 15% of cases (Harris, 2006). The PKD genes encode for the proteins polycystin-1 and polycystin-2, which are believed to interact to form a protein complex located in the primary cilia of epithelial cells, and has been suggested to facilitate Ca^{2+} influx through mechanosensation derived from fluid movement (Qian *et al.*, 1997; Yoder *et al.*, 2002).

1.4.4.4 Sickle cell anaemia

Sickle cell anaemia (SCA) is a genetic disorder affecting the haemoglobin protein in the erythrocytes, where a single amino acid substitution allowing for haemoglobin proteins to adhere to each other under acidic conditions, such as in low oxygen, high carbon dioxide conditions (Nagel & Lawrence, 1991). Under physiological conditions, the intracellular cation homeostasis in erythrocytes is maintained by the active movement of Na^+ and K^+ ions by the Na^+/K^+-ATPase channel, and low passive ion permeability (Joyce, 1958). However, in patients with SCA, the passive cation permeability is substantially higher, causing erythrocytes to shrink, elevating the relative

concentration of the aforementioned mutated haemoglobin (HbS). Furthermore, as the time required for haemoglobin polymerisation is inversely proportional to the concentration of HbS to the power of between 30-50 ($[HbS]^{30-50}$), even small amounts of cell shrinkage severely increase the likelihood of HbS polymerisation (Eaton & Hofrichter, 1987).

There are three main transport systems involved in erythrocyte dehydration; increased conduction of positive ions into the deoxygenated erythrocytes, the K^+-Cl^- cotransporter, and KCa3.1 (Lew & Bookchin, 2005). Under deoxygenation, Ca^{2+} enters the cell (Rhoda *et al.*, 1990), which activates the KCa3.1 channel, and in turn causes K^+ and Cl^- efflux through the both KCa3.1 and the K^+-Cl^- cotransporter, leading to water loss (Lauf *et al.*, 1992; Gibson *et al.*, 1998). Additional studies have shown that hydration of erythrocytes can be increased through the use of KCa3.1 inhibitors, which reduce K^+ efflux, therefore reducing Cl^- efflux and reducing water loss (Brugnara *et al.*, 1993; De Franceschi *et al.*, 1994).

1.4.4.5 Fluid secretion

As discussed above, KCa3.1 is believed to be involved in the dehydration of erythrocytes under deoxygenated conditions, however, KCa3.1 also plays a role in fluid secretions elsewhere in the body. Fluid secretion as a result of Cl^- efflux relies strongly on the activity of basolateral proteins in order to generate a sufficient electrochemical gradient. This gradient is generated in a two-step process; firstly, Na^+/K^+-ATPase uses primary active transport to export Na^+ out of the cell against the concentration gradient, and secondly the $Na^+/K^+/2Cl^-$ cotransporter (NKCC) uses secondary active transport to import K^+ and Cl^- into the cell, driven by Na^+ efflux. (Aleksandrov & Riordan, 1998; Trinh *et al.*, 2008). KCa3.1 then allows for K^+ efflux, preventing build-up of K^+ from NKCC, and maintaining the K^+ concentrations of both the extracellular and intracellular fluids, allowing for Na^+/K^+/ATPase to function optimally. As K^+ efflux occurs, water is drawn out of cells in order to keep the osmotic homeostasis balanced, therefore, if more K^+ occurs, due to increased KCa3.1, cells will have increased fluid secretion.

KCa3.1 is also able to inhibit fluid secretion, for example, in the stomach, where parietal cells rely on K^+ secretion through the H^+/K^+-ATPase channel (Vallon *et al.*, 2005). Upon the activation of KCa3.1 in the stomach, K^+ is able to exit cells on the basolateral side, which leads to a decrease in K^+ efflux at the apical membrane, and inhibiting fluid secretion (Rotte *et al.*, 2011). This was observed when DC-EBIO, a potent KCa3.1 activator, elicited a decrease in gastric secretions, an effect attenuated upon the addition of KCa3.1 inhibitor TRAM-34 (Rotte *et al.*, 2011).

1.4.4.6 Cardiac fibrosis

Fibrosis is the process of scarring, characterised by the accumulation of fibroblasts, resulting in the excess accumulation of the extracellular matrix, distorting the physiological architecture, and function of tissue. Cardiac fibrosis in particular, is a contributing factor in many cardiac diseases (Weber, 2000), and the contribution fibrogenesis plays in the impairment of cardiac function increasingly more recognised (Espira & Czubryt, 2009). Fibrosis itself can manifest in two forms; reactive interstitial fibrosis, or replacement fibrosis (Anderson *et al.*, 1979). It is believed that left ventricular pressure overload leads to reactive interstitial fibrosis, which manifests into replacement fibrosis without the loss of cardiomyocytes (Isoyama & Nitta-Komatsubara, 2002). Acute myocardial infarction, on the other hand, results in myocardial cell death, and a state of replacement fibrosis (Hasenfuss, 1998).

Furthermore, the onset of cardiac fibrosis has been suggested to be the result of an imbalance between the synthesis of collagen in the heart, and the degradation of the myocardium (Banerjee *et al.*, 2006). Interestingly, KCa3.1 has been demonstrated to have a role in both the rate of collagen secretion, and the rate of cardiac fibroblast proliferation (Wang *et al.*, 2013a; Zhao *et al.*, 2015). Zhao and associates (2015) showed that inhibiting KCa3.1 with TRAM-34 in pressure overloaded rats, exhibited a significant reduction in cardiac fibrosis, shown through a decrease in both angiotensin II and in overall myocardial inflammation. These results therefore suggest that KCa3.1 may be a novel target for cardiac fibrosis therapy in humans, particularly in cases of reactive interstitial fibrosis.

1.4.4.7 Diabetic nephropathy

Diabetic nephropathy (DN), also known as diabetic kidney disease, is amongst the most prevalent, and dire long-term complications faced by diabetic patients, affecting between 30-40% of diabetes mellitus patients (Gross *et al.*, 2005). DN is caused by angiopathy of the glomerular capillaries, resulting in a progressive pathological renal condition (Kanwar *et al.*, 2008). Additionally, DN is the leading cause of end-stage renal disease in the United States of America, and is a lead contributing factor towards diabetic morbidity and mortality across the globe (USRD, 2009).

One of the predominant conditions relating to DN is interstitial fibroblast activation; these fibroblasts rapidly proliferate, activating myofibroblasts in the process, leading to a marked increase in deposition of extracellular matrix into the renal interstitial space (Qi *et al.*, 2006). As with cardiac fibrosis, discussed above, KCa3.1 has been known to be in fibroblasts since 1999, when it was cloned from fibroblast cells (Pena & Rane, 1999). Moreover, activated fibroblasts treated with TRAM-34 have shown to have significantly reduced proliferation, suggesting that KCa3.1 may be a potential target for treating the fibrosis stemming from DN in patients (Grgic *et al.*, 2009).

1.4.4.8 KCa3.1 in the neural system

While the focus of KCa3.1 in disease thus far has revolved around cardiac and epithelial tissues, it has been shown, through immunolabelling, that KCa3.1 is expressed in all major neuronal cell types; including in the cingulate and motor cortices, cortical and subcortical neuronal regions, and the olfactory bulb (Turner *et al.*, 2015). Additionally, KCa3.1 has been located in the spinal cord, where it plays a role in fluid secretion in ependymal cells, and in the dorsal root ganglion cells (Boettger *et al.*, 2002; Bahia *et al.*, 2005; Chen *et al.*, 2015). Finally, KCa3.1 portrays an important role in the proliferation and migration of neuronal cells, such as endothelial cells and neuroblasts (Yamazaki *et al.*, 2006; Turner & Sontheimer, 2014), and in the regulation of neuronal input to cerebellar Purkinje cells (Engbers *et al.*, 2012).

1.4.4.9 Alzheimer's Disease

Alzheimer's disease (AD), is an irreversible, neurodegenerative disorder which progresses to slowly abolish patients' cognitive ability. One of the lead factors contributing to AD is age; the incidence of AD is believed to double every 5 years after 65 years of age (Hirtz *et al.*, 2007). One protein involved in the pathophysiology of Alzheimer's disease is the amyloid-β protein (Aβ), which is a hydrophobic protein, which self-aggregates into amyloid fibrils, and deposits as amyloid plaques, which are a hallmark of AD. The Aβ aggregates which form then induce microglial activation, which clears the Aβ aggregates, but directly induces neurotoxicity through the release of inflammatory mediators in the process. (El Khoury *et al.*, 2007; Cameron & Landreth, 2010). Aβ proteins are also expressed as oligomers (AβO), which also induce microglial activation (Maezawa *et al.*, 2011). It was found that use of TRAM-34, a KCa3.1 inhibitor, amended the neurotoxicity caused by AβO induced microglial activation by controlling Ca^{2+} entry, preventing oxidative burst (Maezawa *et al.*, 2011; Maezawa *et al.*, 2012). Additionally, KCa3.1 blockade has been shown to be a target for another neural glial cell, astrocytes, which are also activated by Aβ accumulation (Wei *et al.*, 2016) (Yi *et al.*, 2016). Together, these results suggest that KCa3.1 could be an effective target to prevent or diminish the neurodegradation which occurs upon Aβ accumulation.

1.5 The Retromer pathway

The retromer pathway is a trafficking pathway, which is believed to be involved in the recycling and degradation of plasma membrane proteins, and in the regulation of endosome to trans-Golgi body trafficking (Arighi *et al.*, 2004; Temkin *et al.*, 2011). Retromer was first observed in yeast (Seaman *et al.*, 1998), where it was observed to be essential in the process of retrieving the yeast retromer protein receptor VPS10p (vacuolar protein sorting 10 protein) from the endosome to the Golgi. VPS10p is a transmembrane sorting receptor which shuttles between endosomes and the

trans-Golgi body (Seaman *et al.*, 1997). In yeast, the retromer complex consists of two sub-complexes; the VPS26, 29, 35 trimer, or the cargo recognition complex (CRC) (shown in Figure 1.5), and the VPS17p-VPS5p heterodimer (Horazdovsky *et al.*, 1997; Seaman *et al.*, 1998). While the CRC has been highly conserved between species, the genes encoding for VPS17p and VPS5p have evolved to form four proteins, rather than two, which allows for a greater number of combinations of heterodimers to form. In mammals, these proteins are sorting nexin (SNX) 1, SNX2, SNX5, and SNX6, and these sorting nexin proteins all contain a Bin/Amphiphysin/Rvs (BAR) domain, helping to promote membrane curvature (Carlton *et al.*, 2004). Like in yeast, these proteins still form dimers, however only specific combinations occur; either SNX1 or SNX2 are able to form a dimer with either SNX5 or SNX6 (Rojas *et al.*, 2007).

While the mammalian Retromer complex is largely homologous to the yeast Retromer complex in function (Arighi *et al.*, 2004), the mammalian Retromer complex also regulates the transport of the mammalian homologue of the yeast protein VPS10p, sortilin (Mari *et al.*, 2008; Fjorback *et al.*, 2012). Recently, Retromer was found to play a role in the recycling of proteins from the early endosome to the plasma membrane (Chen *et al.*, 2010). Retromer further uses a range of proteins in order to selectively recycle membrane proteins; for example, the beta-2-adrenergic receptor (β2AR) is recycled when the CRC containing the β2AR interacts with SNX27 (Temkin *et al.*, 2011). Retromer is therefore recognised as a critical regulator of many export pathways from endosomes (Pocha *et al.*, 2011).

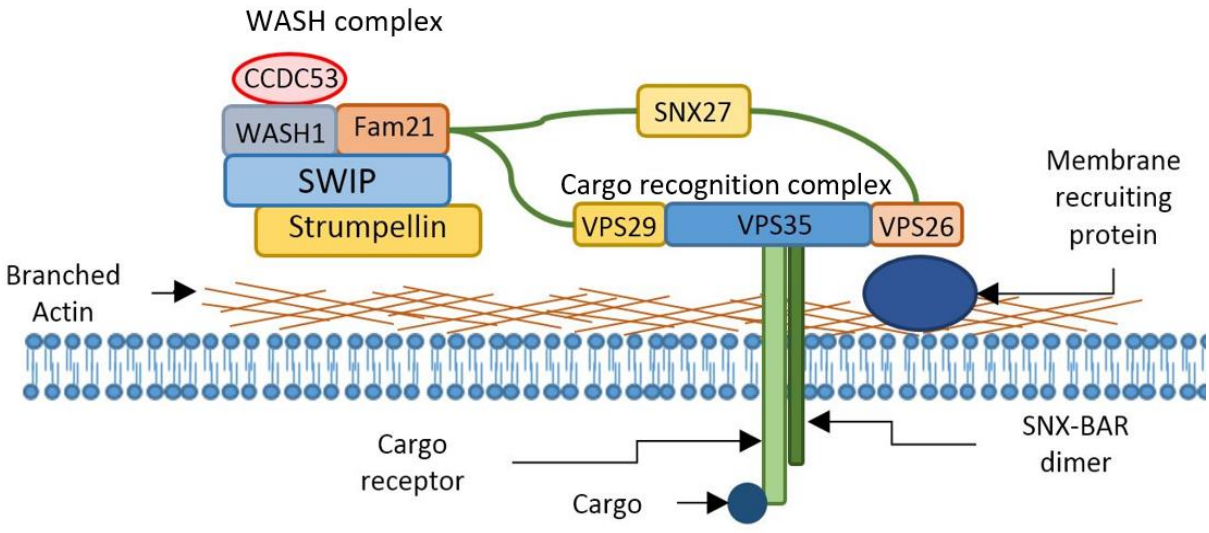

***Figure 1.5* – The Retromer complex.** This diagram of the Retromer complex shows the cargo recognition complex (CRC), consisting of VPS26, 29, and 35, the WASH complex, consisting of CCDC53, WASH1, Fam21, SWIP, and Strumpellin, the SNX-BAR dimer, and SNX27, which is able to interact with both the WASH complex and the CRC. The green links show how proteins are able to interact with each other. Pilmore, Unpublished.

1.5.1 Structure of the cargo recognition complex

The CRC is a complex consisting of three vacuolar protein sorting-associated (VPS) proteins; VPS26, VPS29, and VPS35, which form a heterotrimer in a 1:1:1 ratio (Figure 1.5) (Norwood *et al.*, 2011). While certain areas of the structure of VPS35 remains to be studied, it is known that VPS35 is a 796 amino acid long protein containing a curved surface with six helices and a series of hydrophobic grooves separated by ridges, believed to function as a binding site (Nothwehr *et al.*, 1999). Additionally, the N-terminus of VPS35 contains a Proline, Arginine, Leucine, Tyrosine, Leucine (PRLYL) motif, which interacts with VPS26 (Reddy & Seaman, 2001; Zhao *et al.*, 2007), and the C-terminus of VPS35 contains an α-solenoid fold which binds with VPS29 (Collins *et al.*, 2005). These C- and N-terminal domains allow for VPS35 to function as the central scaffolding for the CRC (Hierro *et al.*, 2007).

The second protein of the CRC is VPS29, which is the smallest protein in the CRC, and associates with the concave face of the C-terminus of VPS35 (Hierro *et al.*, 2007). VPS29 also utilises conserved residues to interact with the α-solenoid fold on the VPS35 C-terminus (Collins *et al.*, 2005). The final protein in the CRC is VPS26, a protein with three known isoforms; VPS26A, VPS26B, and Down's syndrome critical region 3 (DSCR3). VPS26A was the first one of the three whose structure has been analysed, consisting of two sets of two antiparallel β sheets, connected together by a flexible linkage, and by a polar core (Shi *et al.*, 2006). VPS26B has a very similar structure to VPS26A, including an identical binding motif to the A isoform, allowing for both isoforms to compete in binding to VPS35 (Collins *et al.*, 2008). The final isoform of VPS26 is DSCR3, which remains to have its structure studied in depth, although it is believed to be a smaller size than either VPS26A or B (Collins *et al.*, 2008).

1.5.2 The WASH complex

The Wiskott-Aldrich syndrome protein and SCAR Homologue (WASH) complex is an Arp2/3 activating protein located on the endosomal surface. Arp2/3 is a seven-subunit complex which is both a component and regulatory factor of the actin cytoskeleton (Machesky *et al.*, 1999; Marchand *et al.*, 2001; Kelly *et al.*, 2006) (Figure 1.5). As the WASH complex activates Arp2/3, WASH is an integral part of the Retromer pathway, allowing for the formation of branched actin filaments. The mammalian WASH complex consists of five separate subunits, which function as one obligate multiprotein complex; WASH1, Strumpellin, SWIP, CCDC53, and Fam21 (Derivery *et al.*, 2009; Gomez *et al.*, 2012). While these components of WASH are highly conserved across eukaryotes, they are absent in yeast (Derivery & Gautreau, 2010).

WASH is required for Retromer-mediated trafficking, and the CRC recruits the WASH complex into endosomes through multiple LFa motif interactions between VPS35 of the CRC, and Fam21 (Family with sequence similarity 21) of WASH (Harbour *et al.*, 2010; Harbour *et al.*, 2012). Furthermore, these interactions require a fully functional CRC; Fam21 has been shown to only interact with VPS35 when VPS35 has formed an interaction with VPS29, suggesting that this interaction causes a conformational shift to allow for the Fam21-VPS35 interaction to establish (Helfer *et al.*, 2013). The WASH complex has been shown to direct cargo in multiple directions; WASH is required to recycle the β2AR from the early endosome to the plasma membrane (Temkin *et al.*, 2011), and to transport the mannose-6-phosphate receptor (CI-MPR) from the early endosome to the trans-Golgi body (Gomez & Billadeau, 2009). Additionally, WASH has been shown to be responsible for the endosomal sorting of the LDLR (Bartuzi *et al.*, 2016), which is trafficked to the basolateral membrane by the exocyst complex (Grindstaff *et al.*, 1998). This interaction could signify the ability for WASH to traffic other exocyst trafficked proteins.

The largest identified protein of the WASH complex, and a fairly unique member, is Fam21 (Jia *et al.*, 2010), which has a notably long 1100 amino acid tail containing many features, amongst which are 21 LFa motifs (Jia *et al.*, 2012). These LFa motifs are the way in which Fam21 interacts with VPS35; it is believed that the LFa motifs play a crucial role in the detection of the CRC density at the plasma membrane, further allowing for WASH recruitment coordination and the subsequent actin polymerisation which drives vesicle movement (Jia *et al.*, 2012). While the interaction formed with VPS35 is perhaps the most notable formed by Fam21, Fam21 is capable of interacting with multiple proteins, linking the WASH complex with multiple proteins at the same time. Another notable interaction formed by Fam21 is with SNX27, which establishes that SNX27 mediated cargo is incorrectly trafficked if the interaction between SNX27 and Fam21 has not formed (Lee *et al.*, 2016). Lee and collaborators (2016) also showed that this cargo is misstrafficked in different ways depending on if SNX27 or Fam21 are missing; if Fam21 is omitted, the cargo is missorted to the trans-Golgi body, whereas if SNX27 is absent, the cargo is sent to the lysosome for degradation (Lee *et al.*, 2016). The globular head of Fam21 is also used for interactions; binding to both WASH1 of the WASH complex, and to SNX1/2, which further interact with the cargo in the CRC (Gomez & Billadeau, 2009).

1.5.3 Sorting nexins

Sorting nexins (SNX) are a family of proteins with 33 unique members identified in mammals; although more members are apparent in other organisms such as yeast (Cullen, 2008). The members of the SNX protein family are characterised by the presence of a Phox (PX) domain (Teasdale & Collins, 2012), which interact with phosphatidylinositol-3-monophosphate (PtdIns3p) enriched

elements of the early endocytic network (Seet & Hong, 2006). Other domains possessed by SNX proteins, including SNX1, include the BAR domain, which consists of 3 α-domains, together forming a rigid curved structure(Carlton *et al.*, 2004; Peter *et al.*, 2004). This curved BAR domain has been hypothesised to bind optimally to the curvature of membranes, providing the ability to drive membrane curvature, leading to vesicle formation and stabilizing the highly curved membranes found in vesicles (Zimmerberg & McLaughlin, 2004; Frost *et al.*, 2008).

1.5.3.1 Sorting nexin 1

SNX1, along with SNX2 are the mammalian orthologs of the yeast protein VPS5p, which forms an interaction with the VPS17p, who's mammalian orthologs are SNX5 and SNX6 (Carlton *et al.*, 2005; Griffin *et al.*, 2005; Rojas *et al.*, 2007; Wassmer *et al.*, 2009). Structurally, all of SNX1, 2, 5, and 6 contain not only the characteristic PX domain of sorting nexins, but also a BAR domain. Along with PtdIns3P, SNX1 also interacts with phosphatidylinositol-3,5-biphosphate (Ptd (3,5) P_2). This is the interaction required for SNX1 to target the highly-curved subdomains of the early endosome (Carlton *et al.*, 2004). Due to the role SNX1 plays in the early endosome, it is also one of the defining features of the endosome to trans-Golgi network (TGN) transport carrier (ETC) (Bujny et al., 2007) (Figure 1.6).

In the early endosome, SNX1 and another sorting nexin, SNX4, both form sorting tubules, however, these tubules are structurally distinct, and sort specific proteins to specific locations (Traer *et al.*, 2007). The exact process behind how these sorting nexins form such distinct tubules remains to be uncovered, however variations in the affinity and specificity towards different phosphoinositides appears to be a contributing factor towards the formation of these highly-specified sorting tubules (Carlton *et al.*, 2004; Traer *et al.*, 2007). Another factor which may contribute to the highly-specified tubules is that sorting nexins may form higher order complexes, which can specifically exclude other sorting nexins with similar functions (Carlton *et al.*, 2004). It has also been suggested that sorting nexins such as SNX3 are able to utilise the transport structures created by sorting nexins like SNX1 and SNX4 in order to transport their cargo, as they are unable to synthesise transport structures (Strochlic *et al.*, 2007).

In epithelia, the RNA interference of SNX1 expression lead to defective Retromer mediated sorting, however similar experiments with SNX2 have failed thus far to outline a relationship between the two sorting nexins (Carlton *et al.*, 2005; Rojas *et al.*, 2007). SNX1 has been shown to interact with both SNX5 and SNX6, and the suppression of either SNX5 or SNX6 leading to a significant loss in the stabilisation of SNX1, further leading to a decrease in SNX1 expression (Wassmer *et al.*, 2007). This suggests that the SNX-BAR heterodimers formed by SNX1/2 and SNX5/6

act together in order to generate an early endosomal tubular subdomain, allowing for the docking of the CRC.

1.5.3.2 Sorting nexin 4

Aside from SNX1, 2, 5, and 6, there is another SNX protein with a BAR domain; SNX4 (Traer *et al.*, 2007). In yeast, the proteins SNX4, SNX41, and SNX42 act alongside the yeast proteins VPS5 and VPS17. While SNX4 in yeast forms a complex with SNX41 and SNX42, it is unknown if this complex is conserved at all in mammals, or if SNX41 or 42 have mammalian orthologues at all. The mammalian ortholog of yeast SNX4 acts in a similar way to SNX1, 2, 5, and 6, by creating transport tubules from the early endosome (Traer *et al.*, 2007), although it is unknown if SNX4 plays a role in the tubular endosomal network (TEN) in the same way that SNX1 does. It is known that suppression of SNX4 leads to the missorting of the transferrin receptor (TfnR) into the lysosomal degradation pathway, however, it is unknown if this missorting is due to the structural integrity of the TEN being affected, or if TfnR is trafficked through an intact TEN (Traer *et al.*, 2007).

Mammalian SNX4 does not appear to interact directly with TfnR, unlike in yeast, where a direct interaction occurs (Traer *et al.*, 2007). It has been suggested that SNX4 interacts with another protein, reggie-1, which itself interacts with TfnR (Solis *et al.*, 2013). An alternate hypothesis is that SNX4 regulates TfnR through the process of geometry based sorting; which proposes that the bulk

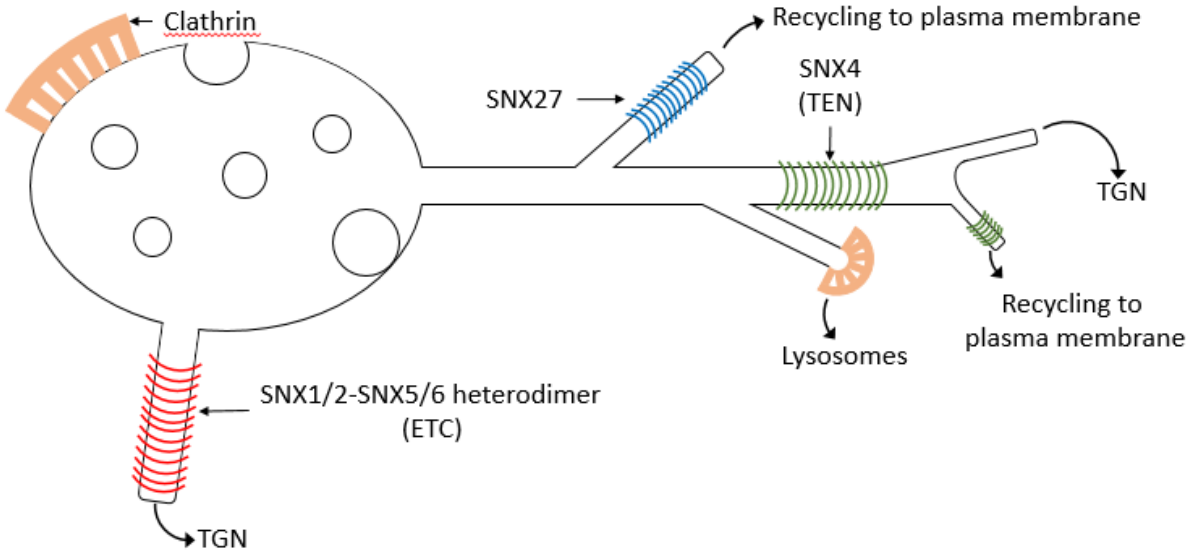

***Figure 1.6* – The early endosome.** Clathrin coated vesicles bind to the surface of the early endosome and to the early endocytic sorting tubules. Tubules also protrude from the early endosome in order to sort proteins in vesicles. The red bands show the tubules formed by the SNX1/2-SNX5/6 heterodimer, which creates the endosome to TGN transport carriers (ETC). The green bands show the tubules formed by SNX4, which create the tubular endosomal network (TEN). The blue bands show SNX27, which utilises tubules in order to recycle proteins such as the β2AR back to the plasma membrane. The early endosome also traffics proteins to both the TGN and along recycling tubules independently of sorting nexins. Modified from a figure by Cullen (Cullen, 2008).

flow of membrane exiting the early endosome does so through membrane tubules with a narrow diameter, similar to those created by SNX4 (Cohen & Pintavirooj, 2004). This allows for any protein lacking a sorting sequence which leaves the membrane by bulk flow, like TfnR, to be indirectly sorted by SNX4 (Traer *et al.*, 2007). There is also evidence that SNX4 may be linked to molecular motors; as SNX4 interacts with the (-) end of the cytoskeletal motor protein dynein (Traer *et al.*, 2007). This interaction is an important factor allowing for long range transport of SNX4 mediated cargo, such as TfnR-enriched domains. This long-range transport extends from simply occurring along early endosomal sorting tubules, as SNX4 cargo can be trafficked from the early endosome to the juxtanuclear endocytic recycling compartment. Dynein may also be used to assist membrane tabulation and membrane fission in SNX4 mediated transport (Day *et al.*, 2015).

1.5.3.3 Sorting nexin 27

SNX27 is a unique sorting nexin in that it is the only sorting nexin currently known to contain a PDZ (post synaptic density protein 95, Drosophila disc large tumour suppressor 1, zonula occludens 1) domain (Kajii *et al.*, 2003). PDZ domains are commonly found in signalling proteins amongst kingdoms of life, including animals, and play critical roles in anchoring membrane bound receptor proteins to their cytoskeletal components (Ponting, 1997; Li et al., 2009). This PDZ domain is vital for the function of SNX27, as it allows for multiple proteins interactions to form, including interactions with ZO-2, a component of the tight junction (Zimmerman *et al.*, 2013). PDZ domains are amongst the most prevalent protein-protein interaction scaffoldings found in trafficking and signalling proteins (Zhang & Wang, 2003). Among PDZ domains, there are two subcategories; canonical domains, which have a conserved cavity recognising different PDZ binding motifs, and noncanonical domains, which promote protein interactions with specific protein partners, involving protrusions from the core PDZ folds (Zhang & Wang, 2003).

SNX27 itself utilises both the canonical and the non-canonical isoforms of PDZ domain in order to simultaneously interact with type1 PDZ ligands, and with the CRC through interactions with VPS26 (Gallon *et al.*, 2014). These unique interactions allow for SNX27 to act as a cargo adaptor protein for Retromer-mediated transport of endosomes to the cell surface (Lauffer *et al.*, 2010; Temkin *et al.*, 2011; Steinberg *et al.*, 2013; Gallon *et al.*, 2014). These SNX27 cargoes include the β2AR (Lauffer *et al.*, 2010), NMDA receptors (Wang *et al.*, 2013b), and ion channels such as the basolaterally trafficked sodium-hydrogen exchanger 3 (NHE3) (Lunn *et al.*, 2007; Balana *et al.*, 2011; Singh *et al.*, 2015).

Furthermore, SNX27 interacts with Fam21 of the WASH complex (Figure 1.5), through a direct interaction with the FERM (4.1 protein, ezrin, radixin, moesin) domain on the N-terminus of Fam21

(Lee *et al.*, 2016). FERM domains are widespread domains specialised in the localisation of proteins to the plasma membrane, and are located in a number of proteins involved in both cytoskeletal movement and the plasma membrane (Chishti et al., 1998; Pearson et al., 2000). This interaction is critical for the correct trafficking of the β2AR, and for NHE3. As mentioned previously, if SNX27 is not present in the cell, the SNX27 mediated cargo is sent to degradation in the lysosome, whereas if Fam21 is not present, the SNX27 mediated cargo is sent to the trans-Golgi body (Lee *et al.*, 2016). The current array of evidence suggests that Retromer is largely involved in recycling of proteins from the plasma membrane to the trans-Golgi network, or to the plasma membrane from the early endosome. Retromer is also believed to play a role in protein degradation. Despite the array of data surrounding Retromer, little is known about how, if at all, KCa3.1 interacts with Retromer, leading to further study being necessary.

2 Aims/Hypotheses

2.1 Aims

1. To determine the effects of SNX1, SNX4, and SNX27 knockdown on the protein levels of SNX1, SNX4, and SNX27 in Fischer Rat Thyroid cells stably transfected with KCa3.1 (FRT-KCa3.1-BLAP cells).

2. To determine if SNX1, SNX4, or SNX27 alter the trafficking of the KCa3.1 channel to the basolateral membrane of polarised epithelial FRT-KCa3.1-BLAP cells.

3. To assess any changes in the functional expression of KCa3.1 when any of SNX1, SNX4, or SNX27 are knocked down in polarised FRT-KCa3.1-BLAP cells through the use of Ussing chamber experiments.

2.2 Hypotheses

1. I hypothesise that knocking down SNX1, SNX4, or SNX27 will result in a decrease of the protein levels of SNX1, SNX4, or SNX27 in Fischer Rat Thyroid cells stably transfected with KCa3.1.

2. I hypothesise that knocking down SNX1, SNX4, or SNX27 will decrease the membrane population of KCa3.1 at the basolateral membrane of polarised epithelial FRT-KCa3.1-BLAP cells.

3. I hypothesise that the function of the KCa3.1 channel of KCa3.1 will be decreased when SNX1, SNX4, or SNX27 are knocked down in polarised epithelial FRT-KCa3.1-BLAP cells.

3 Methods

3.1 Cell models

In this project, immortalised cell lines were used as a model in order to demonstrate the effect of Retromer disruption on the population of KCa3.1 at the basolateral membrane. For this project, two cell lines were used, which allowed for multiple techniques to be used. The main cell line used for this project was FRT-KCa3.1-BLAP cells. These cells are modified from FRT (Fischer Rat Thyroid) cells derived Fischer Rat thyroid glands (Zurzolo *et al.*, 1991; Tasevski *et al.*, 1998), through the stable integration of a plasmid containing KCa3.1-BLAP (Bertuccio *et al.*, 2014) (discussed later), and were used for immunoblot experiments and Ussing chamber experiments. These cells are able to form a polarised monolayer, allowing for the membrane population of KCa3.1 to be measured at the basolateral membrane, making them ideal for both immunoblot and Ussing chamber experiments, while unmodified FRT cells served as control cells. FRT-KCa3.1-BLAP cells were cultured in Nutrient Mixture F-12 (Catalogue# 21700075, Ham's F-12; Invitrogen, Carlsbad, CA, USA), modified with 10% (v/v) foetal bovine serum (FBS), and 1% (v/v) penicillin/streptomycin (penstrep). Cellular media was further modified with the glycopeptide antibiotic Zeocin (850 µg/mL), which prevented the removal of the plasmid from the cells.

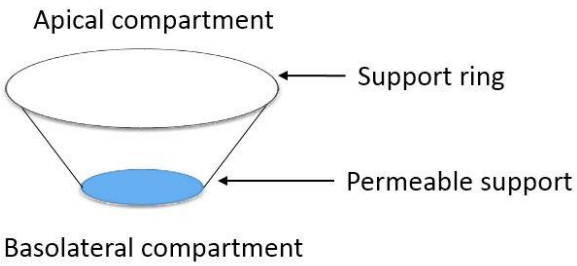

Figure 3.1 – *Schematic diagram showing* Transwell ™/Snapwell ™ permeable support showing the apical and basolateral compartments, the location of the permeable support, and the support ring, which prevents the permeable support from touching the base of the container. Pilmore, Unpublished.

The other cell line used for this project were COS-7 cells. These cells are fibroblast like cells derived from African green monkey kidneys (Gluzman, 1981). These cells were selected due to their high transfection efficiency (Felgner *et al.*, 1987; Aleksic *et al.*, 1996). Unlike the FRT-KCa3.1-BLAP cells used for immunoblot and Ussing chamber experiments, COS-7 cells do not possess the ability to form a polarised monolayer, instead, they were used to transiently express KCa3.1-HA-pcDNA3.1. These cells were cultured in a growth media consisting of DMEM (Catalogue# 12100-046, Dulbecco's Modified Eagle Medium; Gibco, ThermoFisher Scientific, Waltham, Massachusetts, USA) modified with 10% (v/v) FBS.

All cells were grown cultured in 25 cm^2 cell culture flasks (Catalogue# 136196, Nunc™ Cell Culture Treated EasYFlasks™) at 37°C in 5% CO_2. For immunoblot experiments, FRT-KCa3.1-BLAP cells were seeded in Transwell™ permeable supports in order to achieve polarity (Figure 3.1). For Ussing chamber experiments, FRT-KCa3.1-BLAP cells were seeded on Snapwell™ filters in order to achieve polarity on a filter to fit the Ussing chamber apparatus (Figure 3.1). In addition to using lysates from both FRT-KCa3.1-BLAP and COS-7 cells, HEK293 (Human Embryonic Kidney) cell lysate was used as a positive control for both the SNX1 and SNX27 antibodies. HEK293 lysate was obtained from the McDonald Lab.

Finally, the *Escherichia coli* (*E.coli*) bacteria (strain DH5α) transformed with a plasmid coding for KCa3.1 containing an HA tag (KCa3.1-HA) were cultured to amplify this plasmid that was then extracted, purified, and transfected into mammalian COS7 cells. This allowed for non-membrane bound KCa3.1 to be observed by immunoblot, as the KCa3.1-BLAP model exclusively presented membrane bound KCa3.1. Bacteria harbouring the KCa3.1-HA plasmid were grown in a selection media of LB media (10g Bacto-tryptone, 5g yeast extract, 10g NaCl in 1L mqH_2O) containing ampicillin (0.1% v/v) overnight at 37 °C on a shaker. Following this, the plasmid DNA was extracted through the use of a Nucleobond™ Xtra midiprep kit, which contains all of the buffers used in this section unless otherwise stated (Catalogue# 740410.50, Machery-Nagel, Bethlehem, Pennsylvania, USA) as outlined briefly in section 3.5.1.

3.2 Molecular Biology

As stated previously, the FRT-KCa3.1-BLAP cells used for this project originate from unmodified FRT cells that had been transfected with a plasmid containing KCa3.1-BLAP (biotin ligase acceptor peptide) – BirA (biotin ligase enzyme) – KDEL construct using Lipofectamine 2000™ (Catalogue# 11668019, Invitrogen, Carlsbad, CA, USA). This stable transfection introduced the BirA enzyme, which contains an endoplasmic reticulum retention motif (KDEL) behind the human cytomegalovirus (CMV) promoter of the bicistronic, or dual gene, plasmid pBudCE4.1. The pBudCE4.1 plasmid was created by amplifying KCa3.1-BLAP DNA from pcDNA3.1, which was then subcloned into the pBudCE4 plasmids, forming the pBudCE4.1 plasmid (Figure 3.2) (Balut *et al.*, 2010). This plasmid created a cellular model where the KCa3.1 channel undergoes a process known as “internal biotinylation”.

Internal biotinylation was first reported in 2005 by Alice Ting, when she used streptavidin to label cell surface epidermal growth factors in HeLa cells (Chen *et al.*, 2005). The Devor Lab then further developed this technique in order to allow for membrane specific detection of KCa3.1 in polarised epithelial cells (Figure 3.3) (Balut *et al.*, 2010; Gao *et al.*, 2010). In short, KCa3.1 in the cells

contains a biotin ligase acceptor peptide (BLAP) which is located on the extracellular loop between the S3 and S4 domains. This BLAP sequence undergoes biotinylation in the endoplasmic reticulum as a result of BirA, which localises to the endoplasmic reticulum. After leaving the ER, the biotin-tagged KCa3.1 is trafficked to the basolateral membrane. Neither the trafficking nor function of KCa3.1 is changed by the addition of either the BLAP sequence or the extracellular biotin (Gao *et al.*, 2010).

3.3 Transfections

3.3.1 Protein expression knockdowns

For this project, FRT-KCa3.1-BLAP cells were transfected with silencing RNA (siRNA), in order to decrease synthesis of specific proteins. The relative KCa3.1 membrane population was first quantified by immunoblot, following which, differences in membrane populations of KCa3.1 in the knockdown cells compared to the control cells were determined. The FRT-KCa3.1-BLAP cells were used for both IB and Ussing chamber experiments, and these experiments were paired, so that the knockdown of the specific protein caused by transfection with siRNA measured for IB would be the same as the knockdown found in the Ussing chamber experiments. Similarly, the KCa3.1 membrane population was measured through dual experiments of IB and Ussing chamber experiments.

The knockdowns performed in this project were performed through forward transfection of FRT-KCa3.1-BLAP cells. In order to perform a forward transfection, the cells were seeded the day before the transfection, so that cells were in the growth phase during the transfection, increasing the amount of siRNA taken up. The siRNA used for this project (discussed later), was transfected into the cells through the use of two reagents; Lipofectamine 3000 and p3000 (used in a 3:2 ratio) (Catalogue# L3000015, Life Technologies, Thermo Fischer Scientific Inc, Waltham, MA, USA). The oligonucleotide sequences of the siRNA used for this project are shown in table 3.6. Transfections were performed in the presence of F12 Serum Free Media (Catalogue# 21700075, Ham's F-12; Invitrogen, Carlsbad, CA, USA). In order to transfect 40 pM of siRNA, either control siRNA or protein specific siRNA, 50 µL of Serum Free Media was put into two separate 1.5 ml tubes. To the first tube, 3 µL of Lipofectamine 3000 was added, and to the second tube, 2 µL of P3000 was added, followed by 40 pM of siRNA. These tubes were then individually vortexed, before being combined and vortexed again, to ensure that everything mixed. The tube was then incubated at room temperature for 15 min, during which time, the media on the cells being transfected was changed from the growth media discussed earlier to the serum free transfection media. After the incubation period, the media from the tube was added to the apical media of the cells being transfected, and the transfection was left to incubate for 6 hr in the incubator, following which, the media was changed back to growth media and the cells were left to grow for 48 hr to ensure confluence.

3.3.2 Plasmid transfections

In order to express KCa3.1-HA, COS7 cells were transfected with plasmid encoding KCa3.1-HA. Like with the transfections performed earlier, these transfections were forward transfections. The main difference between the plasmid transfection here and the siRNA transfections discussed above, is that the plasmid transfections involved transfecting 1 µg of plasmid protein, while siRNA transfections involved transfecting 40 pM siRNA. The other difference is that plasmid transfections were performed on 6 cm plates seeded with $1x10^6$ cells.

Like the siRNA transfections, 50 µL of transfection media was added to two 1.5 ml tubes, and either 3 µL of Lipofectamine 3000 or 2 µL of P3000 + 1 µg was added to one tube. Each tube was then vortexed, the tubes mixed together, and the final tube vortexed again before being incubated at room temperature for 15 min. The growth media on the cells was then removed, replaced with transfection media, and the transfection media from the tube was added to the cells and incubated for 6 hr.

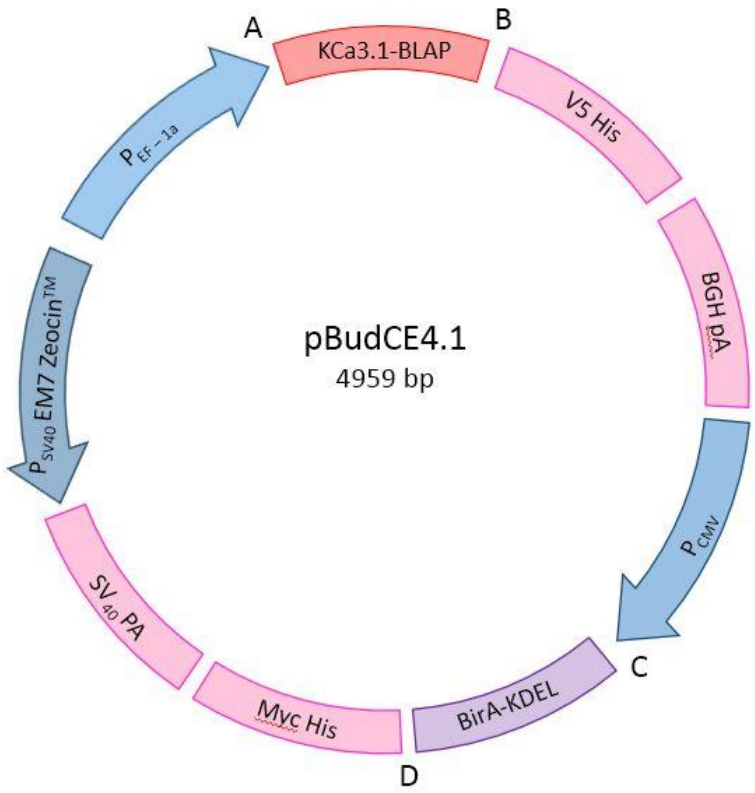

Figure 3.2 – The pBudCE4.1 plasmid. The KCa3.1-BLAP gene is located between Xho1 (A) and Kpn1 (B), and the BirA-KDEL gene is located between Hind3 (C) and Sal1 (D). Pilmore, Unpublished.

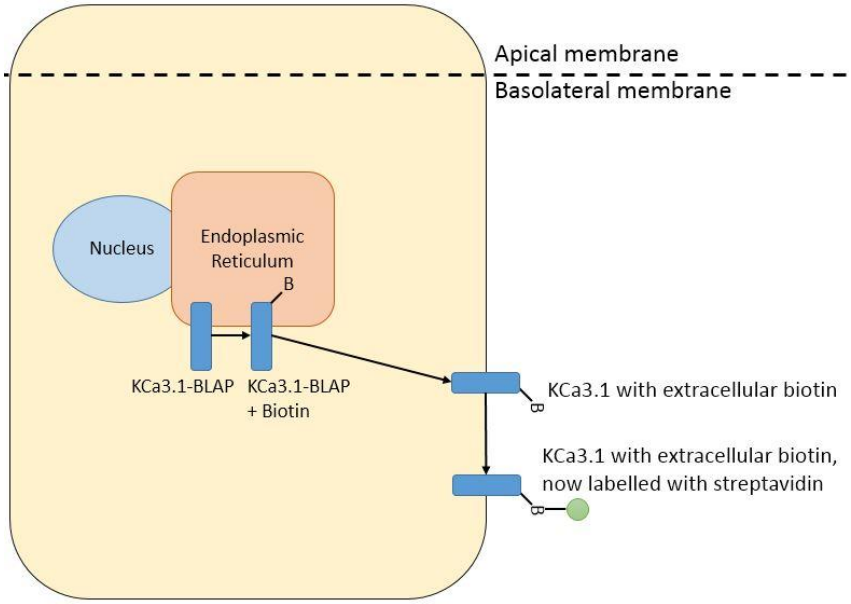

Figure 3.3 – Cellular process outlining the addition of biotin (B) to the biotin ligase acceptor peptide (BLAP) sequence of KCa3.1 in polarised epithelial cells. When KCa3.1 is synthesised in the ER, the biotin ligase enzyme, BirA attaches a biotin molecule to the BLAP sequence, which exits on the loop between the 3rd and 4th transmembrane domains. Following this, KCa3.1 traffics normally to the basolateral membrane, where the loop between the 3th and 4th transmembrane domains is an extracellular loop. When biotin is attached to this loop, it provides an extracellular biotin to label, allowing for membrane selective labelling of KCa3.1 with streptavidin. Then antibodies for streptavidin can be used to detect this KCa3.1-BLAP-streptavidin construct. Pilmore, Unpublished.

3.4 Western Blotting

Western blots or immunoblots (IB) were used to measure the levels of KCa3.1 protein at both the apical and the basolateral membrane of polarised epithelial cells. To produce a successful IB, there are several important steps which must take place, which are outlined below.

3.4.1 Labelling of KCa3.1 and cell lysis

Once the FRT-KCa3.1-BLAP cells are grown to confluency on polarised filters, the membrane bound KCa3.1 is able to be labelled by incubating either the apical or the basolateral membrane in 0.1% streptavidin in PBS/BSA (v/v) for 25 min at 4°C (10% bovine serum albumin in phosphate buffered saline). The cells were then washed in ice cold PBS/BSA three times for five min each wash. A final wash in ice cold PBS for five min was finally carried out to remove any remaining PBS/BSA prior to cell lysis. It was important that both the labelling of KCa3.1 with streptavidin and washing cells with PBS/BSA are carried out at 4°C in order to prevent internalisation of KCa3.1 so that only membrane bound KCa3.1 channels are visualised in immunoblot experiments through the use of an anti-streptavidin antibody. Once the cells have been labelled, the cells are ready to undergo lysis. This was completed by incubating cells in 130 µL lysis buffer on the apical membrane for 15 min (40 µL EDTA free protease inhibitor and 960 µL lysis solution; HEPES 50 mM, EDTA 1 mM, NaCl 150 mM, and Triton 5 mL; made up to 500 mL with ddH_2O). The lysed cells were then scraped off the membrane and transferred to a microcentrifuge tube, which was spun at 14000g for 10 min at 4°C in order to separate the proteins from the lipids. The supernatant, containing the proteins, was transferred to a fresh microcentrifuge tube, while the pellet containing lipids was discarded.

3.4.2 Protein sample analysis

In order to determine the volume of cellular lysate to load for IB the protein concentration of the lysates were analysed in a Bicinchoninic acid (BCA) assay (Smith *et al.*, 1985). The BCA assay determined the protein concentration through the use of three reagents; A, B, and S (Catalogue# 5000111, BioRad, Hercules, Ca, USA), and protein standards of known concentrations. For the BCA assay, 6 µL of protein standard (Bovine Serum Albumin) or cellular lysate was loaded in triplicate into a 96 well plate. This was followed by the addition of either 30 µL of reagent A (for protein standards), or 30 µL reagent AS (1 mL reagent A and 20 µL reagent S, for cellular lysates), and finally the addition of 240 µL reagent B. The absorbance of the BCA assay was the measured through the use of a Synergy 2 Multi-Mode Microplate Reader set to measure absorbance at 630 nm, and the absorbance results quantified using Gen5 software (Biotek, Winooski, VT, USA).

In order to then calculate the concentration of the cellular lysate, first, the absorbance of each of the protein standards were determined, creating a protein concentration curve. Following this,

the absorbance of the lysates were measured and the protein concentration is calculated by using the protein concentration curve set by the protein standards.

3.4.3 Sodium Dodecyl Sulphate Poly-Acrylamide Gel Electrophoresis

Sodium dodecyl sulphate poly-acrylamide gel electrophoresis (SDS-PAGE) is a process that acts to separate proteins based on molecular weight. This occurs because sodium dodecyl sulphate (SDS) has a negatively charged head with a lipophilic tail, which allowing for SDS to bind non-covalently with proteins, conferring a negative change onto them (Weber & Osborn, 1969; Rath *et al.*, 2009). SDS binds proteins in a ratio of 1:4, and acts to linearise proteins, resulting in the secondary, tertiary, and quaternary bonds found in proteins being converted from secondary, tertiary, and quaternary protein bonds into primary bonds (Reynolds & Tanford, 1970; Rath *et al.*, 2009).

The other aspect of SDS-PAGE is the poly-acrylamide gel electrophoresis (PAGE), and is a process whereby proteins that have been loaded into a polyacrylamide gel are separated based on molecular weight. This technique is based on the principle that negatively charged particles will move towards a positively charged region of an electric field (Ganguli, 1956). In PAGE, the negatively charged proteins migrate from the cathode, which itself is negatively charged, to the positively charged anode. This allows for the proteins to be separated by molecular weight, as higher molecular weight proteins will encounter more resistance than lower molecular weight proteins, thus, the high molecular weight proteins will lag behind their smaller molecular weight counterparts (Shapiro *et al.*, 1967; Weber & Osborn, 1969). A protein ladder, which contains a negatively charged, prestained proteins of known sizes is also run on the PAGE, allowing for protein size to be calculated depending on their location relative to the ladder.

SDS-PAGE acrylamide gels were created using the volumes listed below in Table 3.2. The volume of each reagent to make resolving gels changes depending on the desired acrylamide percentage gel, which are shown in Table 3.1. In order to determine what percentage gel to make, it is important to know the sizes of the proteins which are desired to be visualised. Once the desired protein range was calculated, the desired resolving gel was made, for example, the 79 kDa protein KCa3.1 was detected using an 8% gel, as was the 59 kDa protein SNX1, the 60 kDa protein SNX4, and the 61 kDa protein SNX27. This involved preparing the gel solution, and pouring 10 mL of the solution into a watertight gel cassette, followed by 1 mL of water-saturated butanol in order to remove air bubbles and prevent evaporation whilst the resolving gel was setting. After the resolving gel was set, butanol was poured off, and a further 2 mL of stacking gel was added to the gel. A comb was then added before the stacking gel set, so that wells were created in the stacking gel for protein loading (Figure 3.4).

Table 3.1 – Protein size to polyacrylamide gel table. All proteins desired to be visualised by IB should be within the protein size range of the gel being made (Abcam, 2015).

Protein size range (recommended) (kDa)	Polyacrylamide gel percentage
40 – 200	8%
30 – 200	10%
20 – 150	12%

Table 3.2 – Ingredients for the preparation of gels to run SDS-PAGE electrophoresis

Ingredients	8% Resolving Gel 10mL	10% Resolving Gel 10mL	12% Resolving Gel 10mL	Stacking Gel 5mL
H_2O	4.6 mL	3.8 mL	3.2 mL	3 mL
1.5M Tris pH 8.8	2.6 mL	2.6 mL	2.6 mL	
0.5M Tris pH 6.8				1.25 mL
10% SDS	100 µL	100 µL	100 µL	50 µL
30% Acrylamide/Bis-acrylamide	2.6 mL	3.4 mL	4 mL	665 µL
10% APS	50 µL	50 µL	50 µL	25 µL
TEMED	10 µL	10 µL	10 µL	5 µL

Once the gels had set, they were moved to vertical running frames (Catalogue# EC120, ThermoEC, Holbrook, New York) in a gel tank, which was filled with running buffer. 10 µL of prestained protein ladder (Catalogue# 10748010, Benchmark, Invitrogen, Carlsbad, CA, USA) was loaded into the 1st well, followed by protein samples mixed with sample buffer (500µL 5x βME free sample buffer (3 mL 20% SDS, 3.75 mL 1M Tris buffer pH 6.8, 9 mg bromophenol blue, 4.5 mL glycerol, adjusted to 15 mL with H_2O) and 10µL βME) in subsequent wells. The volume of protein

sample loaded were determined via BCA protein assays so that 30 µg of protein was added to each lane. The gels were then run for 90 min at 140 V to completely separate the proteins.

3.4.4 Transfer of Proteins from Gel to Membrane

Once the SDS-PAGE gels have separated out the proteins sufficiently, it was necessary to transfer the proteins from the gel to a more durable structure, such as a polyvinylidene fluoride (PVDF) membrane (Catalogue# 88518, Thermo Fischer Scientific Inc, Waltham, MA, USA). This PVDF membrane is necessary in order to incubate the proteins in primary and secondary antibodies to allow for visualisation. In order to transfer the proteins from the gel to the PVDF membrane so that the proteins retain the separation achieved during SDS-PAGE, the gel with proteins attached and a blank, activated piece of PVDF membrane (PVDF membrane activated via incubation in methanol for 20 seconds) are sandwiched together between pieces of filter paper which have been soaked in transfer buffer (25 mM Tris, 120 mM Glycine; made to 1L with ddH_2O.

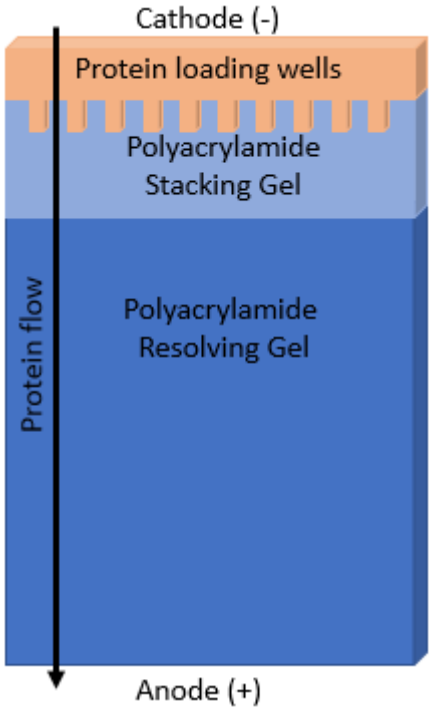

Figure 3.4 **–** SDS-PAGE acrylamide gel. In SDS-PAGE, proteins stack together when moving through the stacking gel, allowing for accurate size based separation when flowing through the resolving gel. Pilmore., Unpublished.

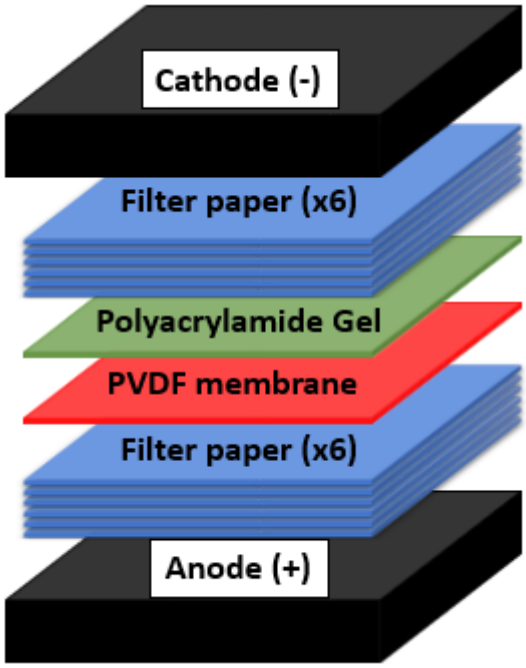

Figure 3.5 **–** Transfer of proteins from the polyacrylamide gel to the PVDF membrane. As it is in SDS-PAGE, protein transfer moves proteins from the cathode to the anode. However, unlike in SDS-PAGE, where proteins are able to run off the gel, the Polyvinylidene fluoride (PVDF) membrane is non-porous, so proteins cannot be transferred through the membrane and onto the filter paper. Pilmore., Unpublished.

It is important to ensure that the filter paper on the cathode side (Figure 3.5) is rolled out thoroughly in order to remove any air bubbles, as these could result in sections of the gel not being

transferred onto the PVDF membrane. Transfers were run using a Semi-Dry transfer system (TE 77 PWR Semi-Dry transfer unit, Amersham ECL Semi-Dry Blotters, GE Healthcare Life Sciences), which was run for 2 hr at 45 mA per gel.

3.4.5 Blocking the PVDF membrane

Once all of the proteins from the SDS-PAGE acrylamide gel have been transferred to the activated PVDF membrane, protein detection is able occur. However the accuracy of protein detection can be significantly improved by first binding non-specific proteins to any empty areas of the PVDF membrane. This is necessary as proteins bind to the PVDF membrane with an extremely high affinity, meaning that proteins can "accidentally" bind to the PVDF membrane (Matsudaira, 1987). In order to bind non-specific proteins to the empty areas of the PVDF membrane, the membrane is immediately immersed in a blocking solution of 5% low-fat (0.1% fat) diary milk powder in Tris-buffered saline – Tween (TBS-T; 10mM Tris-HCL, 100mM NaCl, made to 1L with ddH_2O, 0.1% Tween-20 v/v, pH 7.4) for one hr at room temperature. The proteins in this solution do not react with the primary antibody used for protein detection, meaning that only the proteins detected are from cell lysates.

3.4.6 Antibodies

After the PVDF membrane has been blocked in 5% non-fat dairy milk powder in TBS-T for an hr, the membrane is ready to be incubated in the primary antibody used to detect a specific protein. The primary antibody is diluted in TBS-T at a concentration between 1/1000 and 1/10,000, depending on the antibody (discussed later). In order to obtain optimal visualisation of protein, the PVDF membrane is incubated in primary antibody overnight at 4^{o}C on a shaker. After this incubation, the primary antibody removed and the PVDF membrane was washed in TBS-T for three 10 min washes. The appropriate secondary antibody is then selected, in order to react with the primary antibody. The secondary antibody is required as it is conjugated with horseradish peroxidase (HRP), which fluoresces when activated with a Lumilight™ solution. This secondary antibody is also diluted in TBS-T and incubated for one hr at room temperature on a shaker. Finally, the secondary antibody was removed and the PVDF membrane was washed in TBS-T for three 10 min washes.

***Table 3.3* – Table showing antibodies used.** Antibodies used for this project showing what the antibody reacts to, the animal in which the antibody was purified in, the amount the antibody was diluted in TBS-T by to reach working concentration, and the catalogue number. Additional information regarding these antibodies is in section 2.9.1.

Antibody	Purification	Dilution	Company	Catalogue #
Primary antibodies				
anti-Streptavidin	Rabbit	1:1000	Genscript	A00621-10
anti-GAPDH	Rabbit	1:2000	Sigma Aldrich	g8795
anti-SNX1	Goat	1:1000	Abcam	ab134126
anti-SNX4	Rabbit	1:1000	Abcam	ab170562
anti-SNX27	Rabbit	1:1000	Abcam	ab178388
anti-HA	Rabbit	1:1000	Sigma Aldrich	ab137838
Secondary antibodies				
anti-rabbit	Donkey	1:5000	GE Healthcare	NA934-1ML
anti-goat	Donkey	1:10000	Santa Cruz	sc-2020

3.4.7 Visualisation of proteins

After the proteins of interest on the PVDF membrane have been treated with both primary and secondary antibody, the proteins can be visualised. This is achieved through the use of a Lumilight™ solution (Roche, Basel, Switzerland), which reacts with the HRP conjugated secondary antibody. This reaction causes light to be released due to the oxidation of luminol in the Lumilight solution. This light occurs only where antibodies are bound, and the light is captured by Carestream Kodak Biomax Film (Catalogue# Z350370, Sigma Aldrich, St Louis, Missouri, USA) (Thorpe *et al.*, 1985). As the Kodak Biomax Film is extremely sensitive to light, exposure of the film is minimised to only capturing light released from the PVDF membrane by performing the exposure in a darkroom. The film is then subsequently developed by immersing it in a developer solution (1 part developer: 4 parts water) (Catalogue# 183 8374, Rapid Access Developer, Carestream Dental, Atlanta, Georgia, USA) followed by rinsing any remaining developer solution off in water, and immersion in a fixer solution (1 part developer: 4 parts water) (Catalogue# 183 8374, Rapid Access Fixer, Carestream Dental, Atlanta, Georgia, USA).

3.5 KCa3.1-HA DNA preparation

3.5.1 Bacterial lysis and KCa3.1-HA isolation

For this project, a KCa3.1 channel containing an HA tag was planned to be used for immunoprecipitation experiments. The *KCa3.1-HA* plasmid for this project was generously donated by the Devor Lab from the University of Pittsburgh. The *E.Coli* containing the *KCa3.1-HA* plasmid was stored as a glycerol stock at -80 °C. Bacterial growth is outlined in section 2.1, and, as with all cellular experiments, the first step of this was to lyse the bacteria in order to obtain the plasmid DNA. This was performed by centrifuging the bacteria at 6000g for 15 min at 4 °C to obtain a bacterial pallet, which was then resuspended in Resuspension Buffer RES, and lysed through the addition of 8 mL of Buffer LYS, which contains sodium hydroxide/SDS, and 8 mL of the Neutralising Buffer NEU and incubated for 5 min at room temperature. The addition of Buffer NEU allows for proteins and cellular debris to precipitate out of solution, while plasmid DNA remains soluble. Following this, the lysate was filtered through a Nucleobond™ Xtra Column Filter which had been washed with 15 mL of Equilibration Buffer EQU and allowed to empty by gravity flow. The filter was then washed with 5 mL of Buffer EQU, and the column was subsequently washed without the filter with 8 mL of buffer WASH. Any plasmid DNA bound to the column was then eluted from the column through the addition of 5 mL of Elution ELU Buffer ELU. Isopropyl alcohol was then added to the eluted solution, caused the previously soluble plasmid DNA in solution to precipitate, and the solution was separated by centrifuging the solution at 4 °C for 30 min. The supernant was discarded, and the pellet washed by being resuspended in 2 mL of 70% ethanol, before being centrifuged at 15000g for 5 min at room temperature. Finally the ethanol was carefully removed, and the pellet was allowed to dry at room temperature. The dry DNA pellet was resuspended and stored in TE buffer (10 mM Tris, 1 mM EDTA, pH 8.0), and the concentration of the DNA was determined by Nanodrop.

3.5.2 Restriction digest

Once the plasmid DNA was extracted and stored in TE buffer, a Restriction digest was performed in order to ensure that the plasmid purified indeed contained *KCa3.1-HA*. This was done through the use of two restriction enzymes, EcoR1 (Catalogue# 10703737001, Roche Applied Science, Penzburg, Germany) and Xho1 (Catalogue# 10703770001, Roche Applied Science), as described by Syme and colleagues (Syme *et al.*, 2003). Three digests were performed; a negative control digest (uncut), a single cut digest, and a double digest, as shown in Table 3.4. Each of the digests contained 0.5 µg of plasmid DNA, as determined previously by nanodrop measurement. Additionally, 3 µL of Buffer H (Sigma Aldrich, St Louis, Missouri, USA) was used, as it is the optimised buffer for these restriction enzymes. The 1.5 mL tubes containing each of these mixes were incubated at 37 °C for 1 hr to ensure digestion.

Table 3.4 – Table showing the ingredients used in restriction digests to isolate *KCa3.1-HA*

Ingredients	**Uncut digest**	**Single cut digest**	**Double Digest**
KCa3.1-HA plasmid	0.5 µg	0.5 µg	0.5 µg
Buffer H	3 µL	3 µL	3 µL
EcoR1 enzyme		1 µL	1 µL
Xho1 enzyme			1 µL
Water	26 µL	25 µL	24 µL

The products of the restriction digest were then treated with DNA loading dye (Catalogue# R0611, Thermo Fischer Scientific Inc, Waltham, MA, USA), in order to stop the digestion reaction, and to convey a negative charge onto the plasmid proteins. This loading dye contains both bromophenol blue and xylene cyanol FF in order to track DNA movement, along with EDTA in order to bind divalent metal ions and inhibit metal-dependent nucleases. The proteins from the restriction digest were then run on a 1% agarose gel with TAE (Tris, Acetic acid, EDTA buffer; 40 mM Tris, 20 mM acetic acid, 1 mM EDTA, made to 1L in ddH_2O) for 30 min at 100V, before being visualised through use of ultraviolet light.

3.6 Ussing chamber

In conjunction with IB experiments, which measured the membrane population of KCa3.1, functional studies measuring transepithelial ion transport through the KCa3.1 channel were also performed. These functional studies are vital to understand the effects of knockdown of components of the Retromer pathway on KCa3.1, as the ability of cells to transport K^+ ions is reliant on both adequate membrane populations of KCa3.1, and that KCa3.1 has an adequate open probability. These functional experiments were completed through the use of an Ussing chamber apparatus. The Ussing chamber apparatus consists of two identical chambers, giving the ability to control the extracellular solution on the apical and basolateral membranes independently (Ussing & Zerahn, 1951), as well as a space to put an insert containing cells to measure.

Ussing chambers measure changes in the short circuit current (I_{SC}) across tissue, or, in this case, a cellular monolayer, by measuring the current of the apical and basolateral extracellular fluids. Two current sensing electrodes, one for the apical chamber, and one for the basolateral chamber (Figure 3.6) calculate the transepithelial current and two additional voltage sensing electrodes

calculate the resistance of the cellular monolayer through Ohm's Law ($\text{Resistance} = {}^{\text{Voltage}}/_{\text{Current}}$).

3.6.1 Ussing chamber cell culture

For the Ussing chamber experiments, FRT-KCa3.1-BLAP cells were grown to form a polarised monolayer by seeding cells onto Snapwell™ filters 72 hr prior to the experiment (Figure 3.1). This ensured a fully confluent monolayer without achieving cellular overgrowth. This method of cell growth is similar to the method used to grow a confluent cellular monolayer for IB experiments.

3.6.2 Modified Ringer's Solution

For Ussing chamber experiments, the epithelia is surrounded by a solution known as Ringer's solution. This solution acts to mimic the extracellular fluid, containing ions to be exchanged in the cells, as well as glucose to provide cellular energy. This creates an environment where cells are able to function normally, allowing for ion channel activity to be measured. In the case of KCa3.1, however, standard Ringer's Solution is replaced in favour of a modified Ringer's Solution.

***Table 3.5* – Modified Ringer's Solution.** Ingredients for the modified Ringer's solution used for Ussing chamber experiments. Both the concentration of each ingredient and the weight of each ingredient for 1L of solution are listed, and the Ringer's solutions were adjusted to a pH of 7.4.

Ingredients	**Apical Ringers solution**	**Basolateral Ringer's solution**
Potassium Gluconate	145 mM	5 mM
Sodium Gluconate		145 mM
HEPES	10 mM	10 mM
Magnesium Chloride (hexahydrate)	1 mM	1 mM
Calcium Chloride	4 mM	4 mM
Glucose	10 mM	10 mM

This modified solution is similar to standard Ringer's Solution, however, is modified for use in either the apical or basolateral Ussing chambers, and contains increased $CaCl_2$ (4 mM compared to 1.2 mM found in standard Ringer's Solution) in order to compensate for the Ca^{2+} buffering effect of

the gluconate anions present (Durham, 1983; Ryabov *et al.*, 1999) (Table 3.5). These solutions created an artificial K^+ gradient by exaggerating K^+ concentration differences, as well as removing apical Na^+ transport; which leads to an overall amplified K^+ current through KCa3.1, allowing for more accurate measurement of changes in KCa3.1 activity.

3.6.3 Ussing chamber set up

Prior to use of the Ussing chamber apparatus, some crucial elements must be set up. Firstly, the modified Ringer's solutions outlined in section 3.6.2 must be warmed in a water bath to 37°C in order to keep the "extracellular" environment as close to physiological conditions as possible. Secondly, the current- and voltage-sensing electrodes must be created. This is done by filling the tips of empty plastic electrodes with agar gel (3% agar in 3M KCl (v/v)). Once the agar was set, the remainder of the electrode was filled with 3M KCl solution, and the end capped with either a voltage- or current-sensing electrode. Finally, the completed electrode was checked to ensure that there were no air bubbles, as these would reduce the effectiveness of the electrodes.

Once the Ringer's Solution was warmed and the electrodes were made, wires were plugged into the electrodes, and an empty Snapwell filter was placed into the middle of the Ussing chamber (Figure 3.6). The chambers were then filled with Apical Ringer's Solution, and the electrodes were zeroed in preparation to accurately measure the current and resistance of the cellular monolayer

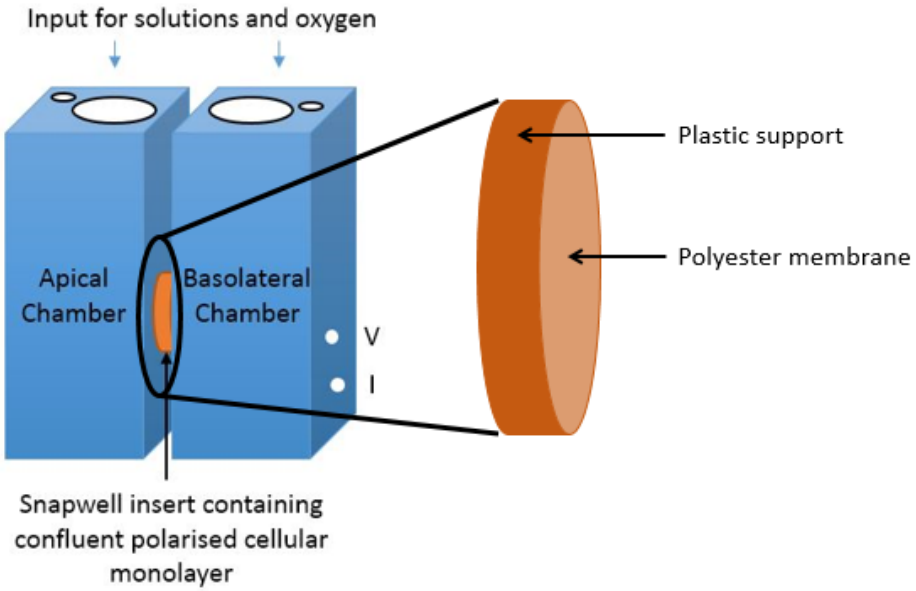

Figure 3.6 **–** Ussing chamber setup. The apical and basolateral chambers are set up to contain distinct solutions, and are connected through the insertion of a Snapwell insert. Current, voltage, and resistance are measured through the use of two pairs of current and voltage sensing electrodes, which are inserted into each chamber, as shown, with V representing the voltage sensing electrode, and I representing the current sensing electrode. Finally, solutions and oxygen are fed into each chamber through the holes at the top of the chamber, with the larger hole for Ringer's Solutions, and the smaller hole to feed oxygen into the chamber. Pilmore., Unpublished.

being tested. A Snapwell filter containing a confluent cellular monolayer was inserted into the system, and apical and Basolateral Ringer's Solutions were added to the apical and basolateral chambers. The recording was then begun, allowing for measurement of the K^+ current.

3.6.4 Measuring K^+ current changes

When the cells have been placed into the Ussing chamber, the electrodes begin to measure both the current and resistance in the Ussing chamber across the monolayer. When the current trace has stabilised, KCa3.1 ligands can be used to either open or close the channel. In order to stimulate KCa3.1, the ligand 1-EBIO was used, which caused an increase in the current, referred to as the 1-EBIO sensitive current (Devor *et al.*, 1996). Conversely, in order to inhibit the channel, clotrimazole was used (Devor *et al.*, 1997), leading to a decrease in the current, denoted as the clotrimazole sensitive current. When measuring the K^+ current, first the current must be stable, or not fluctuating, so that an accurate change in current can be measured, and the transepithelial resistance must be over 500 $\Omega \cdot cm^2$. When both of these criteria were met, 100 µM of 1-EBIO was added to both the apical and basolateral chambers. The current was then allowed to stabilize again, and the change in current was noted. Next, 10 µM of clotrimazole was added to both the apical and basolateral chambers, and the current was allowed to stabilize again. Finally, the clotrimazole sensitive change in current was noted. For this experiment, the change in current was measured by the vertical change in current (Δy) before and after the addition of either 1-EBIO or clotrimazole.

3.7 Chemicals

3.7.1 Zeocin

Zeocin (phleomycin D) (Catalogue# R25001, Life Technologies, Thermo Fischer Scientific Inc, Waltham, MA, USA), is a glycopeptide antibiotic cultivated in *Streptomyces verticillus.* For this project, Zeocin is used as a component of selection media in order to keep the KCa3.1-BLAP plasmid expressed in the FRT cells used, maintaining the FRT-KCa3.1-BLAP cell line (section 3.1). FRT-KCa3.1-BLAP cells contain a Zeocin resistance gene, which prevents Zeocin evoking cell death by fracturing double strands of DNA (Ehrenfeld *et al.*, 1987; Chankova *et al.*, 2007). In the inactive form, Zeocin is bound to a Cu^{2+} ion. Upon entering the cell, on the other hand, the Cu^{2+} ion is cleaved from Zeocin, allowing it to bind to DNA (Oh *et al.*, 2002).

3.7.2 Streptavidin

Streptavidin (Catalogue# 434302, Life Technologies, Thermo Fischer Scientific Inc, Waltham, MA, USA) is a non-glycosylated homotetrameric protein which binds with a high affinity to biotin. This high affinity bond formed to biotin was used in order to tag KCa3.1-BLAP channels present in the membrane, allowing for the membrane population of KCa3.1 to be quantified via IB experiments

(section 3.4.1). This was possible due to the FRT-KCa3.1-BLAP cells expressing KCa3.1 with an extracellular biotin. Streptavidin acts by forming hydrogen bonds with biotin, following which, tryptophan residues interact, stabilizing the hydrogen bonds, and increasing the interaction strength (Kurzban *et al.*, 1990).

3.7.3 1-EBIO

1-ethyl-benzimidazolone (1-EBIO) (Catalogue# SML0034-50MG, Sigma Aldrich, St Louis, Missouri, USA), is a Ca^{2+} activated K^+ channel opener, found to open the KCa3.1 channel by Devor and colleagues (section 3.6.4) (Devor *et al.*, 1996). Alongside Ca^{2+} activated K^+ channels, KCa3.1 has also been shown to activate the cystic fibrosis transmembrane conductance regulator channel (CFTR) (Devor *et al.*, 1996).

3.7.4 Clotrimazole

Clotrimazole (Catalogue# C6019-5G, Sigma Aldrich, St Louis, Missouri, USA), is an antifungal drug which was first found to inhibit the K^+ current seen in cells expressing the KCa3.1 channel by Devor and colleagues (Devor *et al.*, 1997), and was shown to block the KCa3.1 channel with high potency by Wulff (section 3.6.4) (Wulff *et al.*, 2000). As both 1-EBIO and clotrimazole are DMSO soluble, it was important to not exceed a concentration of 0.5% DMSO when reconstituting either 1-EBIO or clotrimazole in DMSO (Adefolaju *et al.*, 2015).

3.7.5 Lipofectamine 3000

Lipofectamine 3000 (Catalogue# L3000015, Life Technologies, Thermo Fischer Scientific, Waltham, MA, USA) is a common transfection reagent. Purchase of Lipofectamine 3000 included the reagent P3000, and these reagents were used together in a 3:2 ratio (Lipofectamine 3000:P3000) in order to increase the transfection efficiency during forward transfections (section 3.3). Lipofectamine 3000 forms a complex with nucleic acid molecules, allowing then to overcome the large electrostatic repulsion of the cellular membrane and enter the cell.

3.8 Plasmids and siRNA

3.8.1 siRNA

For this project, cells were transfected with either 40 pM of control siRNA, or with 40 pM of protein specific siRNA. All the siRNA used in this project was reconstituted in RNAse free water, aliquoted and stored at -20 $^{\circ}$C. Additionally, the three protein specific siRNAs used for this project (SNX1 siRNA (Catalogue# NM_053411), SNX4 siRNA (Catalogue# NM_001127550), and SNX27 siRNA (Catalogue# NM_001110151)) were all purchased from Sigma Aldrich (Sigma Aldrich, St Louis, Missouri, USA). Oligonucleotide sequences for the siRNA used are shown in table 3.6 below.

Control siRNA was used as a negative control for this project, and was transfected into cells at the same concentration as the SNX siRNAs. The control siRNA used for this project was custom made by Sigma Aldrich (Sigma Aldrich, St Luis, Missouri, USA).

Table 3.6 – Oligonucleotide sequences for the siRNA used for knockdown transfections

siRNA	Sequence
SNX1 siRNA	GAAUCAUCCUACCAUGUUA
SNX4 siRNA	CUGUCAUGCAGAUCAGCAU
SNX27 siRNA	GUACUUCUUUCAUCAGGCU
Control siRNA	UGGAGUGAAUACCACGACGAU

3.8.2 KCa3.1-HA

The KCa3.1-HA plasmid for this project was generously donated by the Devor Lab from the University of Pittsburgh. This plasmid contains the gene encoding KCa3.1-HA inserted into the pcDNA3.1 plasmid through the use of EcoR1 and Xho1 restriction enzymes, and the pcDNA3.1 plasmid was transformed into the E-Coli strain DH5α. The E-Coli were stored in a glycerol stock at -80 °C. In order to extract the KCa3.1-HA plasmid, the E-Coli was grown in LB media overnight, and the pcDNA3.1 plasmid extracted through the use of a DNA purification kit. The extracted plasmid was stored in RNAse free water at -20 °C, and transfected into cells via forward transfection with Lipofectamine 3000 as described in section 3.6.2.

3.9 Antibodies

3.9.1 Primary antibodies

3.9.1.1 Anti-Streptavidin

The anti-streptavidin antibody used in this project was developed in rabbits through the use of polyclonal streptavidin, and is purified from rabbit anti-serum by protein G resin (Catalogue# A00621-10, GenScript, Piscataway, NJ, USA). The anti-streptavidin polyclonal antibody binds to streptavidin, which is present on membrane bound KCa3.1-BLAP, and is used at 1:1000 dilution in TBS-T.

3.9.1.2 Anti-GAPDH

GAPDH (Glyceraldehyde-3-phosphate dehydrogenase) is a protein found in FRT cells, and is used as an internal protein control for IB experiments. This is because, unlike other proteins, the concentration of GAPDH in cells remained unaffected by any of the treatments used for this project.

This allowed for the concentration of other proteins to be “normalised”, showing the true concentration of proteins, allowing for comparisons to be made between samples. The anti-GAPDH antibody (Catalogue# g8795, Sigma Aldrich, St Louis, Missouri, USA) was purified in rabbits, and HAbinds directly to GAPDH, and is diluted at 1:2000 in TBS-T.

3.9.1.3 Anti-SNX1

Anti-SNX1 is an antibody which binds directly to sorting nexin 1 (SNX1), and was purified in goats (Catalogue# ab134126, Abcam, Cambridge, UK). The anti-SNX1 antibody binds to the SNX1 present in cell lysate, and was used at 1:1000 concentration, diluted in TBS-T.

3.9.1.4 Anti-SNX4

The anti-SNX4 antibody used binds to sorting nexin 4 (SNX4). This antibody was purified in rabbit (Catalogue# ab170562, Abcam, Cambridge, UK). This antibody was used at 1:1000, diluted in TBS-T.

3.9.1.5 Anti-SNX27

The anti-SNX27 antibody used for this project binds to the C-terminal of sorting nexin 27 (SNX27) was purchased from Abcam (Catalogue# ab178388, Abcam, Cambridge, UK). The anti-SNX27 antibody was purified in rabbit, and was used at a concentration of 1:1000, and was diluted in TBS-T.

3.9.1.6 Anti-HA

The anti-HA antibody used in this project binds to the HA protein tag. Specific proteins were modified to contain an HA tag, allowing for detection with the HA antibody. The anti-HA antibody was purchased from (Catalogue# ab137838, Sigma Aldrich, St Louis, Missouri, USA), and was purified in rabbit. Anti-HA was diluted to 1:1000 for use in immunoblotting.

3.9.2 Secondary antibodies

3.9.2.1 Donkey anti-Rabbit IgG linked Horseradish-peroxidase whole antibody

The donkey anti-rabbit IgG linked Horseradish-peroxidase (HRP) whole antibody was used in order to visualise proteins which used a primary antibody purified in rabbit. These antibodies were anti-streptavidin, anti-GAPDH, anti-SNX4, anti-SNX27, and anti-HA primary antibodies. The donkey anti-rabbit IgG linked HRP whole antibody was purchased from GE Healthcare (Catalogue# NA934-1ML, GE Healthcare, Chicago, IL, USA). As with all HRP linked whole antibodies, the donkey anti-rabbit IgG linked HRP whole antibody reacts with luminol in order to produce a low intensity light in the areas to which it has bound. This light is able to be detected by film, allowing for specific protein

expression to be quantified. The dilutions used for this antibody varied from 1:2000 to 1:10,000 depending on the primary antibody used in order to optimise fluorescence.

3.9.2.2 Donkey anti-Goat IgG linked Horseradish-peroxidase whole antibody

Similar to the donkey anti-rabbit IgG linked HRP whole antibody, the donkey anti-goat IgG linked HRP whole antibody was used in order to visualise proteins bound to primary antibodies purified in goat. This antibody was anti-SNX1 for this project. The donkey anti-goat IgG linked HRP whole antibody was purchased from Santa Cruz Biotechnology (Catalogue# sc-2020, Santa Cruz Biotechnology, Dallas, TX, USA). This antibody was used at a 1:2000 dilution.

3.10 Statistical analysis

The data for this project was analysed through the use of Microsoft Excel™ 2013, ImageJ, and Graphpad Prism 6. In order to analyse IB blot data, the protein of interest was quantified through the use of ImageJ software (imagej.nih.gov/ij), following which, the proteins were normalised to the GAPDH control protein through Microsoft Excel™. This prevented analysis errors as differences in protein loading were able to be easily corrected. Ussing chamber data was analysed by transferring the trace data into Microsoft Excel™ and the change in current was measured upon the addition of both 100 µM 1-EBIO and 10 µM clotrimazole. The results from both of these were uploaded to Prism, in order for statistical analyses to be carried out. In order to gain accurate statistical results, way ANOVA analyses was carried out within each data set for data with more than two groups, while paired t-tests were performed for data sets with only two groups. This allowed for the significance of change between groups to be accurately observed. An additional test for outliers (ROUT outlier test) was also carried out for each data set, and any outliers were omitted from data sets to ensure accurate statistical analysis. Statistical significance for this project was set at $p < 0.05$.

4 Results

Sorting nexins (SNX) are a large group of proteins, with 33 identified members in mammals (Cullen, 2008). SNX proteins interact strongly with the early endocytic network (Seet & Hong, 2006), and some portray a specialised role in vesicle formation through the presence of a BAR domain (Zimmerberg & McLaughlin, 2004; Frost *et al.*, 2008). The presence of this BAR domain presents a role of SNX proteins in channel recycling. While it is unknown if KCa3.1 is recycled, a relationship between SNX proteins and KCa3.1 could indicate the potential for recycling. The aim of this project was to examine the role of three sorting nexins, SNX1, SNX4, and SNX27, which might be involved in the Retromer pathway, in the basolateral trafficking and function of KCa3.1 in a polarised epithelium.

4.1 Confirmation of basolateral localisation of KCa3.1

Before this investigation began, it was important to ensure that KCa3.1 was localised to the basolateral membrane of the polarised FRT-KCa3.1-BLAP epithelial cells. This experiment, known as a sidedness experiment, was accom08plished by seeding cells onto filters, and growing the cells until the cells formed a confluent monolayer, as determined through visualisation by light microscope.

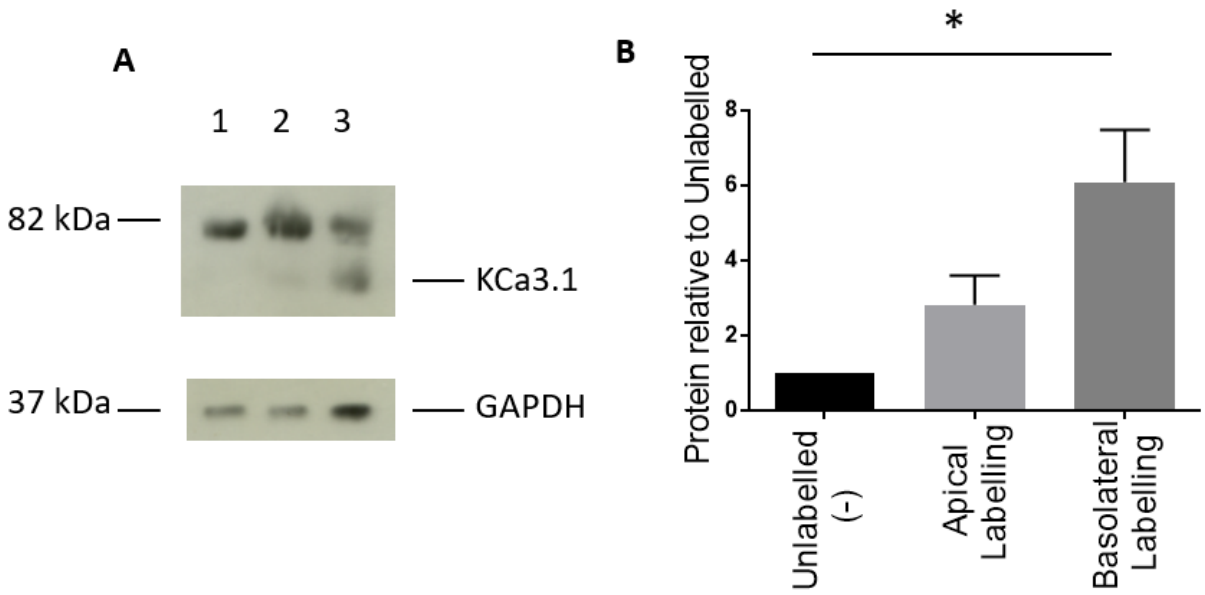

***Figure 4.1* – Sidedness experiment displaying the membrane localisation of KCa3.1. A.** Representative blot demonstrating KCa3.1 at 79 kDa, and the loading control GAPDH at 37 kDa. Lane 1 exhibits the cells without KCa3.1 labelling, which was used as a negative control, lane 2 displays the apical membrane population of streptavidin, and lane 3 presents the basolateral membrane population of KCa3.1. **B.** Quantification of the immunoblots carried out in the sidedness experiments, normalised to the negative control. The results here reveal a significant increase in the basolateral membrane population of KCa3.1 compared to the negative control ($p < 0.05$; n=4), and a trend towards a significant increase in the membrane population of KCa3.1 at the basolateral membrane compared to the population at the apical membrane ($p < 0.05$; n=4). The presence of the non-specific 82 kDa band is consistent with previous results from the Hamilton lab using the KCa3.1-BLAP model, and does not interfere with KCa3.1.ANOVA analyses were performed between each group in B to assess significance between each group.

Once this confluency was reached, the membrane bound biotinylated KCa3.1 was labelled with streptavidin. Streptavidin was added to either the apical or the basolateral membrane, allowing for both the apical and the basolateral membrane populations of KCa3.1 to be labelled and visualised independently of one another. Figure 4.1A displays a representative blot of KCa3.1 during a sidedness experiment, with KCa3.1 at 79 kDa, and GAPDH at 37 kDa. Lane 1 contains the negative control, or lysate from cells without KCa3.1 labelled with streptavidin, from cells that have undergone no streptavidin labelling, whilst lanes 2 and 3 contain lysate from cells with the apical or basolateral membrane populations of KCa3.1 labelled respectively. Figure 4.1B presents the quantification of these immunoblots, which demonstrates the majority of KCa3.1 was present in the basolateral membrane. Additionally, the difference between the apical and the basolateral membrane populations is significant ($p < 0.05$), leading to the possibility that significance would emerge if more experiments were carried out. The nonspecific band at 82 kDa has consistently been identified in immunoblots of the KCa3.1-BLAP channel (Farquhar *et al.*, 2017).

4.2 Antibody tests

For this project, immunoblots were used as a primary experiment, ergo it was essential to ensure that each antibody used for this project was functional with lysate from FRT-KCa3.1-BLAP cells, and, just as importantly, to demonstrate the endogenous expression of the SNX proteins

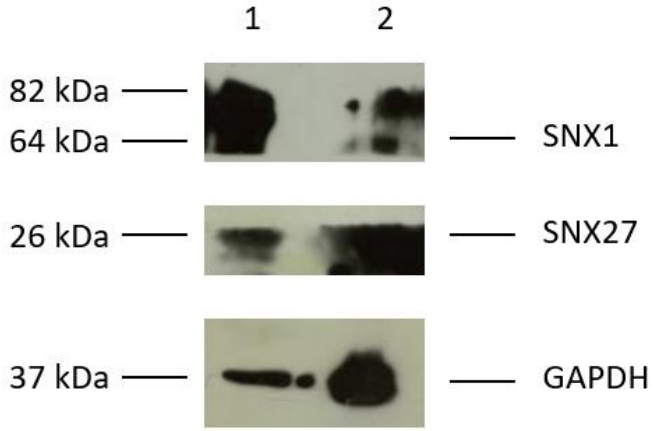

***Figure 4.2* – Antibody test for anti-SNX1 and anti-SNX27.** This figure exhibits immunoblots confirming that anti-SNX1 antibody detects SNX1 protein in FRT-KCa3.1-BLAP cells, and that anti-SNX27 antibody detects SNX27 in FRT-KCa3.1-BLAP cells. Lane 1 contains the positive control, which was lysate from HEK293 cells. Lane 2 consists of lysate from FRT-KCa3.1-BLAP cells, which were not labelled with streptavidin (n=3).

present in the FRT-KCa3.1-BLAP cells. These immunoblot experiments were performed by using cells which the antibody in question had previously been proven to detect SNX1 and SNX27 in the positive control (HEK 293 cellular lysate) provided by members of the McDonald lab, and FRT-KCa3.1-BLAP cells. Figure 4.2 demonstrates the antibody test results for both anti-SNX1 and anti-SNX27 antibodies, which displays lysate from HEK293 cells, a positive control for both the SNX1 and SNX27 antibodies, in lane 1, and FRT-KCa3.1-BLAP cells in lane 2.

4.3 siRNA tests

Aside from the sidedness experiment and the antibody tests, the final preliminary experiment to carry out before the onset of this project was to determine the effectiveness of the SNX1 and SNX27 siRNAs on the protein population of SNX1 and SNX27 respectively. This was done by transfecting cells with increasing concentrations of siRNA, and observing which concentration resulted in the greatest decrease in protein expression of the SNX protein targeted by the siRNA, determined by immunoblot. Figure 4.3 presents the results of the SNX1 siRNA test; with Figure 4.3A presenting a representative immunoblot displaying increasing concentrations of SNX1 siRNA transfected into FRT-KCa3.1-BLAP cells, and Figure 4.3B exhibiting the quantification of the immunoblots from Figure 4.3A. The lanes run in figure 4.3A are all FRT-KCa3.1-BLAP cells, and are transfected as follows; lane 1 has no transfection, lane 2 was transfected with 40 pM control siRNA, and lanes 3-5 were transfected with 10, 20, or 40 pM SNX1 siRNA respectively. This preliminary knockdown of SNX1 proved non-significant up to the transfection with 40 pM of SNX1 siRNA, however, future transfections with 40 pM of SNX1 siRNA proved successful (section 4.4.3; figure 4.9), suggesting these experiments failed due to either poor technique or poor transfection media were the reason behind this.

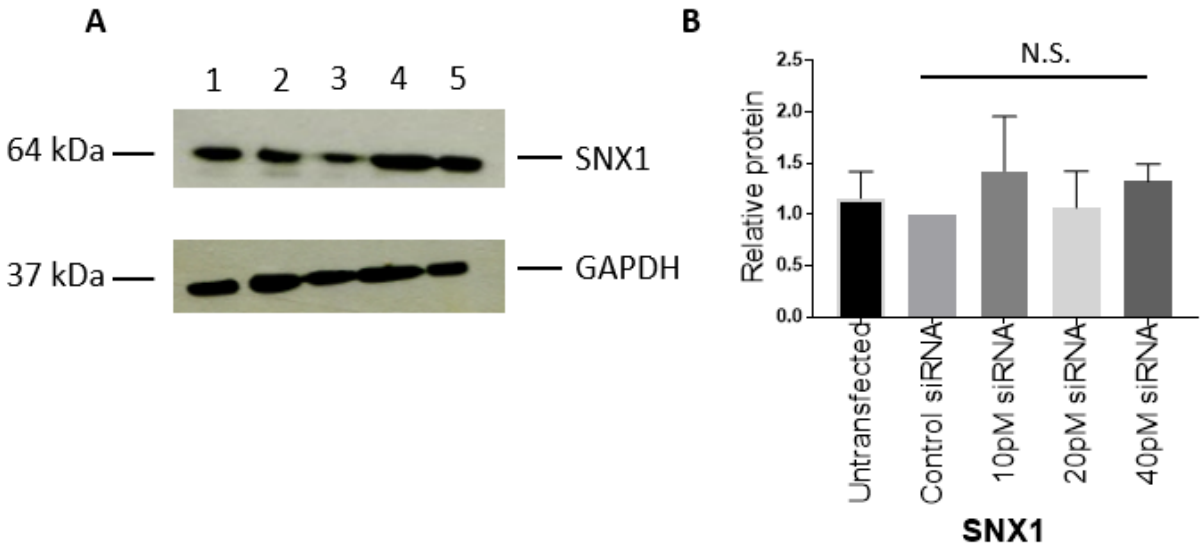

***Figure 4.3* – siRNA optimisation for SNX1.** This figure displays the results of optimising the siRNA for SNX1. **A.** Representative immunoblot for SNX1 siRNA optimisation. Lane 1 contains lysate from untransfected FRT-KCa3.1-BLAP cells, Lane 2 reveals lysate from cells transfected with 40 pM control siRNA, and Lanes 3-5 contain lysate from cells transfected with 10, 20, or 40 pM SNX1 siRNA. **B.** Quantification of the SNX1 immunoblots. These results reveal no significant changes between the control siRNA and any of 10, 20, or 40 pM siRNA transfections on the amount of SNX1 in the cell ($p > 0.1$; n=3). ANOVA analysis was performed between each group in B to assess significance.

The preliminary experiments suggested that the SNX1 siRNA would not lead to a significant decrease in the intracellular protein levels of SNX1 (Figure 4.3), and that the SNX27 siRNA would not lead to a significant decrease in the intracellular protein levels of SNX27. Figure 4.4 presents the results of the SNX27 siRNA test; Figure 4.4A depicts a representative immunoblot with lysates from cells transfected with increasing concentrations of SNX27 siRNA, and Figure 4.4B characterises the quantification of the immunoblots for SNX27, and Figure 4.4C illustrates the quantification for the immunoblots for KCa3.1. Figure 4.4B reveals that transfecting cells with 40 pM SNX27 siRNA lead to the largest decrease in SNX27 protein levels, however, there was no significant difference between any of these groups ($p > 0.05$; n=3).

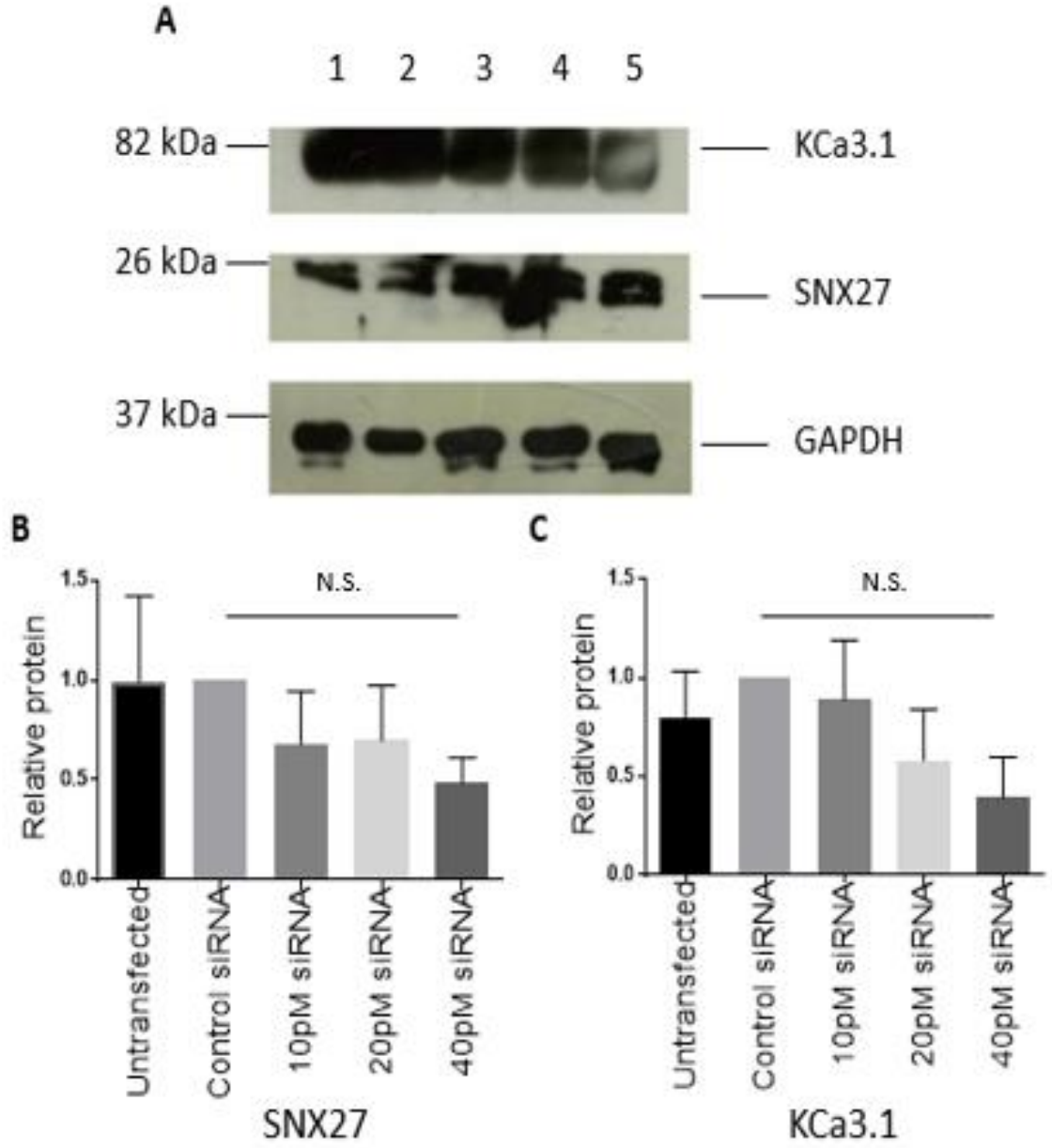

Figure 4.4 **– siRNA optimisation for SNX27.** This figure demonstrates the results of optimising the siRNA for SNX27. For this experiment, FRT-KCa3.1-BLAP cells were transfected with 10, 20, or 40 pM of SNX27 siRNA for 48 hr. **A.** Representative immunoblot revealing the effect of increasing siRNA concentration on both SNX27 expression, and KCa3.1 basolateral membrane population. Lane 1 displays lysate from untransfected FRT-KCa3.1-BLAP cells, Lane 2 displays lysate from cells transfected with control siRNA, Lane 3 displays lysate from cells transfected with 10 pM SNX27 siRNA, Lane 4 displays lysate from cells transfected with 20 pM SNX27 siRNA, and Lane 5 displays lysate from cells transfected with 40 pM SNX27 siRNA. **B.** Quantification of the SNX27 immunoblots. This quantification confers that transfecting cells with 40 pM SNX27 siRNA did not lead to a significant change in the intracellular levels of SNX27 ($p > 0.05$; n=3). **C.** Quantification of the KCa3.1 immunoblots, demonstrating that transfecting cells with 40 pM SNX27 siRNA does not lead to a significant difference in the basolateral membrane population of KCa3.1 ($p > 0.05$; n=3). ANOVA analyses were performed between each group in B and C to assess significance.

4.4 The effect of specific Sorting Nexin proteins on KCa3.1 trafficking to the basolateral membrane

4.4.1 The effect of SNX4 on the trafficking of KCa3.1 to the basolateral membrane

SNX4 is a sorting nexin which transports vesicles by interacting with the (-) end of dynein, allowing for the long range transport of cargo proteins (Traer *et al.*, 2007). It has also been hypothesised that the tubules created by SNX4 may be used to traffic proteins lacking a specific sorting sequence, as they can be trafficked by bulk flow (Traer *et al.*, 2007). For this section, SNX4 is presented first as results are presented in chronological order, allowing for changes in methodology to be more easily followed. In order to determine any effect SNX4 plays on the trafficking of KCa3.1 to the basolateral membrane in polarised epithelial cells, several experiments were required.

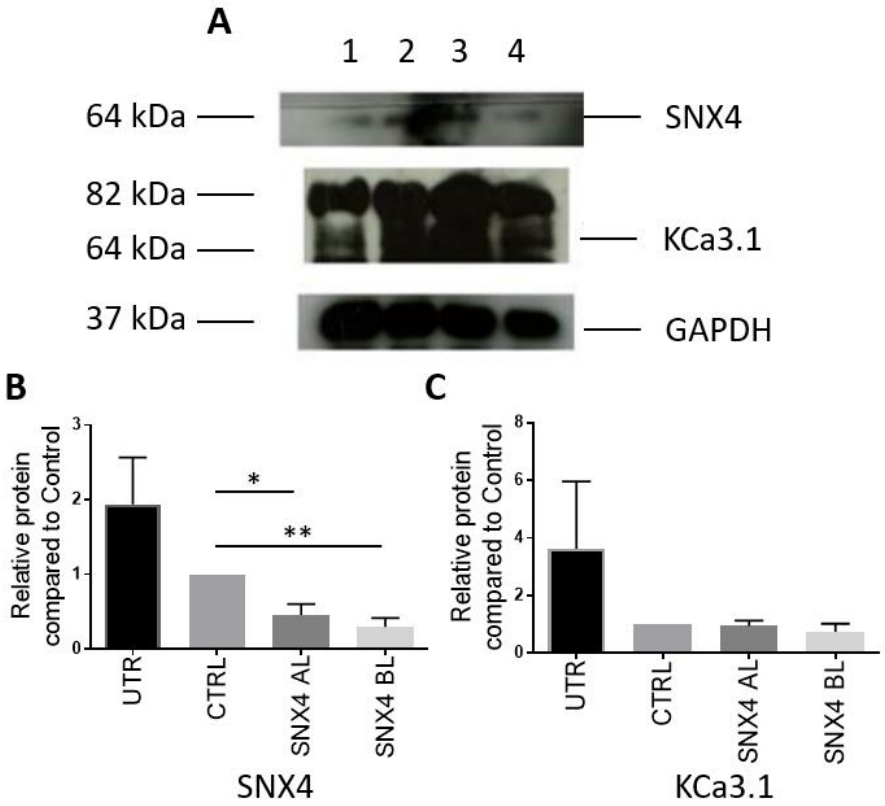

***Figure 4.5* – Effect of SNX4 knockdown on the basolateral membrane population of KCa3.1. A.** Representative blot demonstrating intracellular SNX4 levels and membrane KCa3.1 populations in cells transfected with SNX4 siRNA. Lane 1 contains lysate from untransfected FRT-KCa3.1-BLAP cells, Lane 2 exhibits lysate from cells transfected with control siRNA, Lane 3 presents lysate from cells transfected with 40 pM SNX4 siRNA, with the apical membrane population of KCa3.1 labelled, and Lane 4 displays lysate from cells transfected with 40 pM SNX4 siRNA, with the basolateral membrane population of KCa3.1 labelled. **B.** Quantification of the SNX4 immunoblots, UTR is untransfected, CTRL is control, SNX4 AL is SNX4 knockdown with apical KCa3.1 labelled, and SNX4 BL is SNX4 knockdown with basolateral KCa3.1 labelled. This data revealed that transfecting cells with 40 pM SNX4 siRNA leads to a ~70% decrease in SNX4 protein levels compared to cells transfected with 40 pM control siRNA ($p < 0.001$; n=5). **C.** Quantification of KCa3.1 immunoblots. This data reported that transfecting cells with 40 pM of SNX4 siRNA did not lead to any significant difference in either the apical or the basolateral membrane populations of KCa3.1 ($p > 0.1$; n=5). ANOVA analyses were performed between each group in B and C to assess significance.

Primarily, it was necessary to ensure that a 40 pM transfection with SNX4 siRNA lead to a significant decrease in the intracellular levels of SNX4. It was unnecessary to conduct preliminary experiments regarding the detection of SNX4, or the transfection of SNX4 siRNA into FRT-KCa3.1-BLAP cells, as SNX4 was both found to be present, and knocked down in FRT cells by the McDonald Lab (McDonald, Unpublished Data). The effect of SNX4 on the basolateral membrane population of KCa3.1 was determined by immunoblot, where four samples were analysed; lysate from untransfected cells, lysate from cells transfected with 40 pM control siRNA, and the final two samples of lysate transfected with 40 pM SNX4 siRNA (Figure 4.5). It was demonstrated that transfecting cells with 40 pM of SNX4 siRNA lead to a ~70% decrease in the protein levels of SNX4 compared to the control siRNA ($p < 0.001$; n=5) (Figure 4.5B). Both the untransfected cells and the control cells had the basolateral membrane population of KCa3.1 labelled, as did one of the samples transfected with 40 pM SNX4 siRNA. The other sample transfected with SNX4 siRNA had the apical membrane population of KCa3.1 labelled. This allowed for samples where SNX4 knockdown had been determined to occur to be re-run in order to determine if a subsequent change in the basolateral membrane population of KCa3.1 occurred, and if any KCa3.1 was missorted to the apical membrane (Figure 4.5). These results revealed no significant difference in the basolateral membrane population of KCa3.1 compared to the control ($p > 0.0.5$; n=5) (Figure 4.5C). The apical labelling of KCa3.1 seen here could be due to two factors; KCa3.1 is sorted to the apical membrane, or the epithelial monolayer was not completely formed during the apical labelling, leading to basolateral KCa3.1 being labelled as part of the "apical" labelling. Despite a significant knockdown of SNX4, there was no significant change in the basolateral membrane population of KCa3.1.

Next, electrophysiology was used to determine any functional changes in KCa3.1 caused by SNX4 knockdown. For these experiments, both the 1-EBIO sensitive current and the clotrimazole sensitive current were measured across KCa3.1-BLAP FRT epithelia mounted in an Ussing chamber (Figure 4.6). The 1-EBIO sensitive and clotrimazole sensitive currents were defined by the vertical change in current (Δy) before and after the addition of either 1-EBIO or clotrimazole. These results displayed a significant decrease in the change in current seen when stimulating cells with 100 µM 1-EBIO (1-EBIO sensitive current) in cells transfected with 40 pM SNX4 siRNA compared to cells transfected with 40 pM control siRNA (Figure 4.6B). While a significant ($p < 0.05$; n=5) change in the 1-EBIO sensitive current was seen, there was no significant change seen in the current between cells transfected with 40 pM SNX4 siRNA and control cells when treated with 10 µM clotrimazole (clotrimazole sensitive current) (Figure 4.6C).. Finally, the transepithelial resistance was measured to ensure that a tight epithelia formed for each experiment. The transepithelial resistance at the time which 1-EBIO was taken, and the average resistance of both the control and knockdown traces were

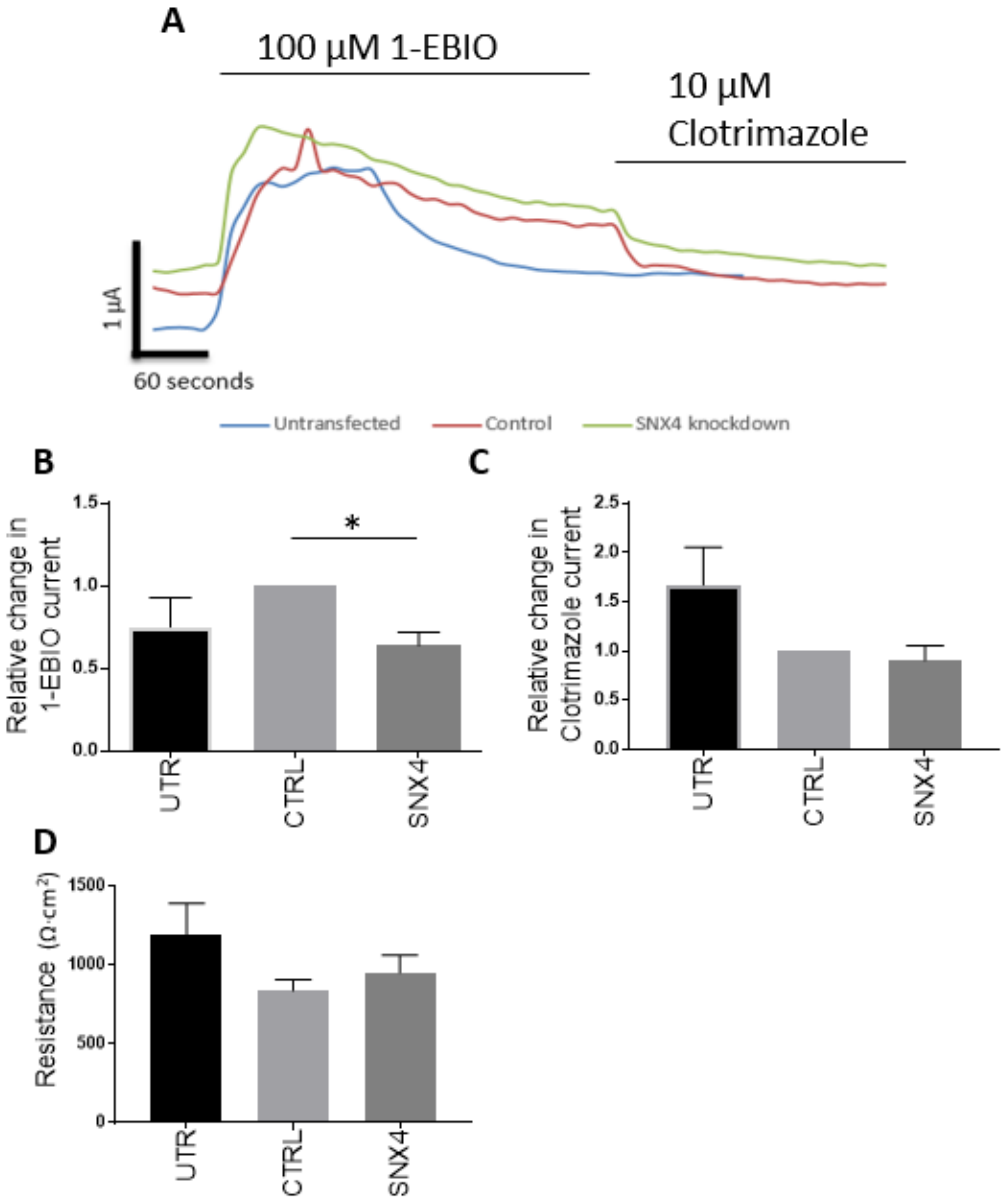

***Figure 4.6* – Effect of SNX4 knockdown on KCa3.1 function. A.** Representative Ussing chamber traces presenting the effect of stimulating cells with both 100 µM 1-EBIO and inhibition by 10 µM clotrimazole, displaying FRT-KCa3.1-BLAP cells without siRNA transfection (Blue), cells transfected with 40 pM control siRNA (Red), and cells transfected with 40 pM SNX4 siRNA (Green). **B.** Quantification of 1-EBIO sensitive current, revealing a significant decrease in the 1-EBIO sensitive current in cells transfecteed with 40 pM SNX4 siRNA (SNX4) compared to the control (CTRL) ($p < 0.05$; n=5). There was no signficant difference seen between the untransfected cells (UTR) and the CRTL. **C.** Quantification of the clotrimazole sensitive current, conceding no significant differences between any of the groups measured ($p > 0.1$; n=5). **D.** Quantification of the transepithelial resistance for Ussing chamber experiments, showing no significant differences betweeen any of the groups ($p > 0.05$; n=5). ANOVA analyses were performed between each group in B, C, and D in order to assess signficance.

compared and analysed. There were no significant differences found between any of the groups ($p > 0.05$; n=5) (Figure 4.6D). The cells used for Ussing chamber experiments in figure 4.6 were paired with cells used for figure 4.5, meaning that all cells were passaged, seeded, and transfected at the

same time to ensure that if a decrease in SNX4 was seen in immunoblots, that same knockdown would be present in the cells used for electrophysiology.

4.4.2 The effect of SNX27 on the trafficking of KCa3.1 to the basolateral membrane

SNX27 is a unique sorting nexin, known to be involved in the trafficking of several proteins, including the tight junction protein ZO-2 (Zimmerman *et al.*, 2013), and the basolaterally trafficked sodium hydrogen exchanger NHE3 (Singh *et al.*, 2015). This trafficking of NHE3 suggests that SNX27 may be able to traffic other basolaterally trafficked proteins, such as KCa3.1. The effect of SNX27 was determined by transfecting cells with SNX27 siRNA, and measuring the intracellular protein levels of SNX27 and membrane bound KCa3.1 via immunoblot, and measuring membrane KCa3.1 through Ussing chamber experiments. Figure 4.7A details the representative immunoblots for both SNX27 and KCa3.1, and the quantifications for these immunoblots are portrayed in Figure 4.7B and 4.7C. Figure 4.7B reveals that transfecting cells with 40 pM SNX27 siRNA led to a significant decrease in the intracellular SNX27 expression compared to cells transfected with 40 pM control siRNA ($p < 0.01$; n=4). Figure 4.7C however, features no significant differences between the control cells and the SNX27 knockdown cells for either the apical or the basolateral populations of KCa3.1. Additionally, there was no significant difference between the apical and basolateral membrane populations of KCa3.1 in cells transfected with 40 pM SNX27 siRNA. Interestingly, there was a trend towards a significant difference between the apical and basolateral membrane populations of KCa3.1 in control cells ($p < 0.1$; n=4).

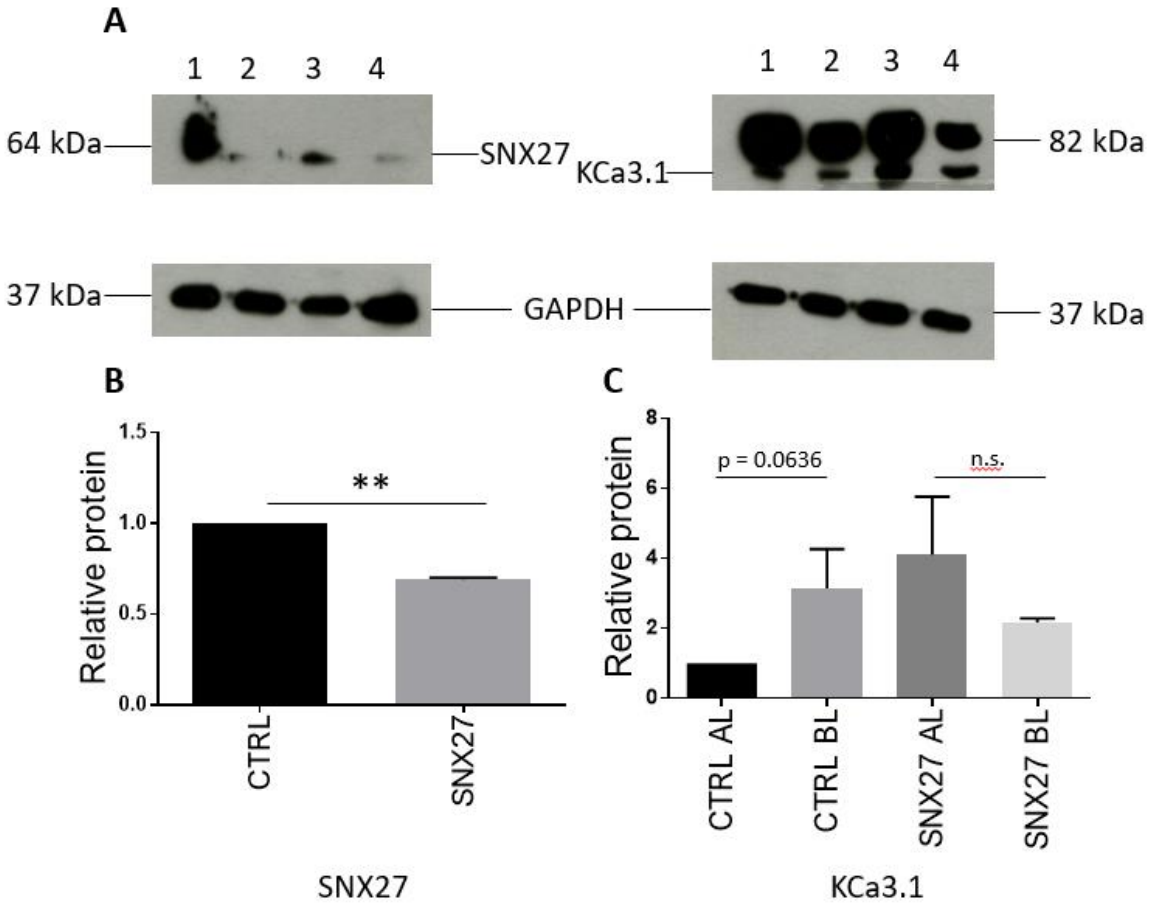

Figure 4.7 – *Effect of SNX27 knockdown on the basolateral membrane population of KCa3.1. A.* Representative immunoblots displaying the SNX27 and KCa3.1 blots for SNX27 knockdown. Lanes 1 and 2 contain lysate from cells transfected with 40 pM control siRNA, with lane 1 containing apically labelled KCa3.1, and lane 2 displaying basolaterally labelled KCa3.1 lysate. Lanes 3 and 4 represent cells transfected with 40 pM SNX27, with lane 3 displaying apically labelled KCa3.1, and lane 4 depicting basolaterally labelled KCa3.1. Both immunoblots contain lysates from the same cells, however were run on different gels. **B.** Quantification of the SNX27 immunoblots, revealing a significant decrease in the intracellular levels of SNX27 in cells transfected with 40 pM SNX27 siRNA (SNX27) compared to cells transfected with 40 pM control siRNA (CTRL) ($p < 0.01$; n=4). **C.** Quantification of the KCa3.1 immunoblots, presenting no significant difference between the CTRL and the SNX27 lysates, for either the apical membrane population of KCa3.1 (AL), or the basolateral membrane population of KCa3.1 (BL). Additionally, there was no significant difference between the AL and the BL in cells transfected with SNX27 siRNA, however there was a trend towards significance between the AL and the BL in the control cells ($p < 0.1$; n=4). A paired two sided t-tests was performed between the groups in B and an ANVOA analysis was performed in group C to assess significance.

As in the SNX4 experiments, Ussing chamber experiments were used to determine any functional changes in KCa3.1 caused by SNX27. Figure 4.8 displays the results of the Ussing chamber experiment conducted with cells paired to the cells used for the immunoblots in Figure 4.7. The Ussing chamber results demonstrate that there is a significant decrease in the effect of treating cells transfected with 40 pM SNX27 siRNA with 100 µM 1-EBIO compared to cells transfected with 40 pM

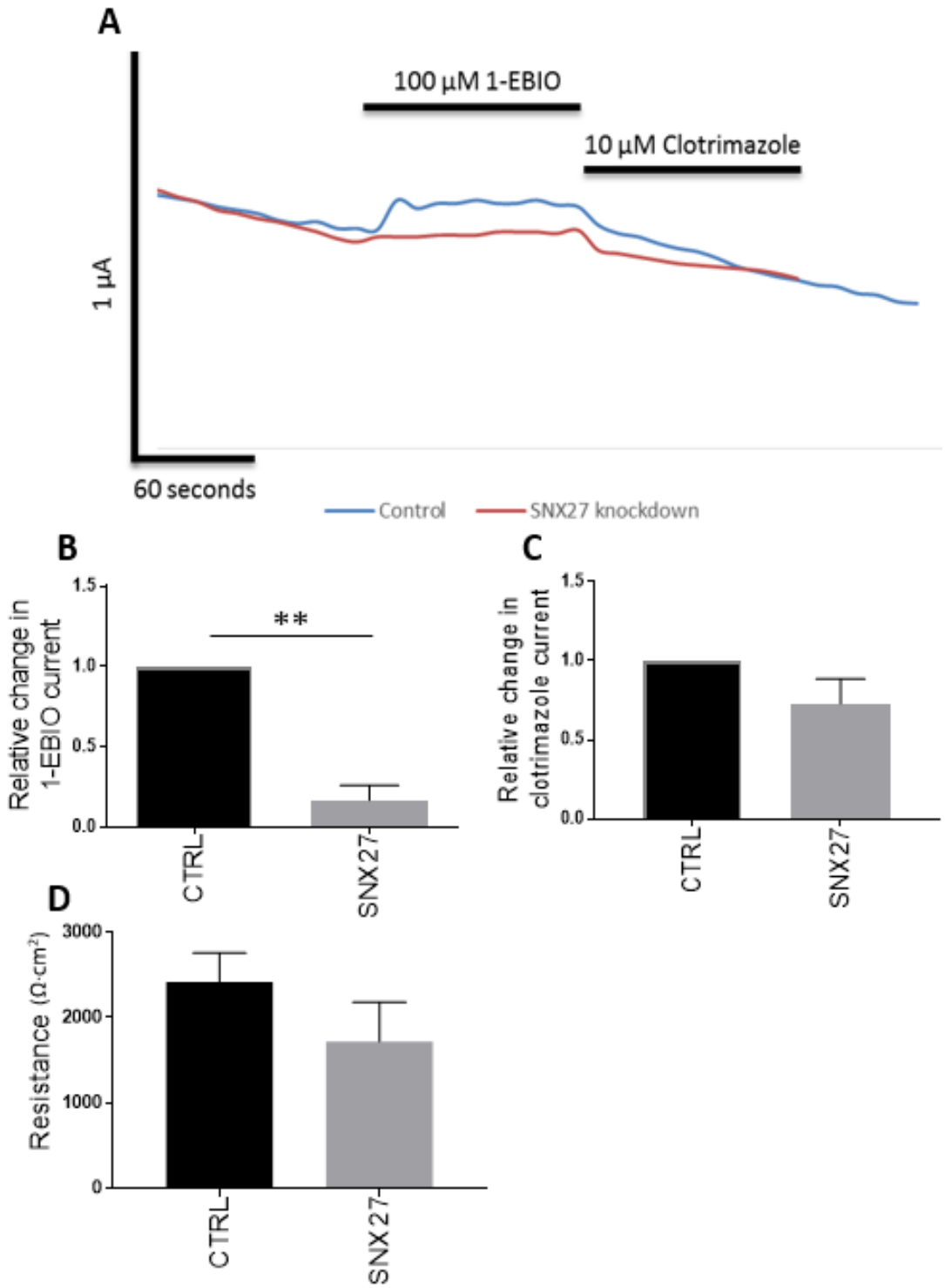

Figure 4.8 **– Effect of SNX27 knockdown on KCa3.1 function. A.** Representative Ussing chamber trace presenting the effect of treating cells with both 100 µM 1-EBIO and 10 µM clotrimazole on cells transfected with 40 pM SNX27 siRNA (Red) compared to 40 pM control siRNA (Blue). **B.** Quantification of 1-EBIO sensitive current. This reveals that cells with significantly less SNX27 had a signfiicantly lower response to the addition of 1-EBIO compared to control cells ($p < 0.01$; n=4). **C.** Quantification of clotrimazole sensitive current, illustrating no signficaint difference in the clotrimazole sensitive response between the control cells or the SNX27 knock down cells ($p > 0.1$; n=4). **D.** Quantification of the transepithelial resistances showing no signficiant change in the transepithelial resistance in the cells transfected with SNX27 siRNA compared to the control cells ($p > 0.1$; n=4). Paired two sided t-tests were performed between each group in B, C, and D to assess significance.

control siRNA ($p < 0.01$; n=4). Contrary to this, there appears to be no significant difference in the

relative function of KCa3.1 in FRT-KCa3.1-BLAP cells transfected with 40 pM control siRNA and 40 pM SNX27 siRNA when treated with 10 µM clotrimazole. Additionally, the reduction in SNX27 did not appear to affect the transepithelial resistance ($p > 0.1$; n=4), revealing that the cells with decreased SNX27 were still able to form a functional, polarised epithelia (Figure 4.8D).

4.4.3 The effect of SNX1 on the trafficking of KCa3.1 to the basolateral membrane

The sorting nexin SNX1 is one of the primary sorting nexin proteins involved in the cargo selection into the cargo retention complex (Wassmer et al., 2007), along with SNX2, 5, and 6. In addition to the PX domain expressed by all SNX proteins, SNX1 contains a BAR domain, which aids in the creation of endosome tubulation vesicles. While there is currently no evidence that KCa3.1 is recruited into the Retromer pathway, a relationship between SNX1 and KCa3.1 could strongly suggest the possibility for KCa3.1 recycling by Retromer. The effect of SNX1 on the trafficking of KCa3.1 to the basolateral membrane was inspected, again through the use of siRNA. Similar to the SNX4 and SNX27 experiments examining KCa3.1, FRT-KCa3.1-BLAP cells were transfected with either 40 pM of control siRNA or SNX1 siRNA. Figure 4.9A displays the representative immunoblot for both KCa3.1 and SNX1, along with the loading control GAPDH. From each of the SNX1 immunoblots, the average of the two control lanes (one with apical KCa3.1 labelled with streptavidin, one with basolateral labelled KCa3.1), and the average of the two SNX1 knockdown lanes was taken, and the averages were used to calculate the average knockdown seen across all immunoblots, presented in figure 4.9B. These results outlined a ~55% decrease in SNX1 protein expression in cells transfected with 40 pM SNX1 siRNA compared to the control cells ($p < 0.05$; n=4). From the KCa3.1 immunoblots, each lane was normalised to the control lane which contained the apical membrane population of KCa3.1 (CTRL AL). Figure 4.9C revealed that there were no significant differences between the control and the knockdown lanes, for either the apical or the basolateral membrane populations of KCa3.1. Additionally, there were no significant differences between the apical and basolateral membrane populations for either the control cells, or the cells transfected with 40 pM SNX1 siRNA.

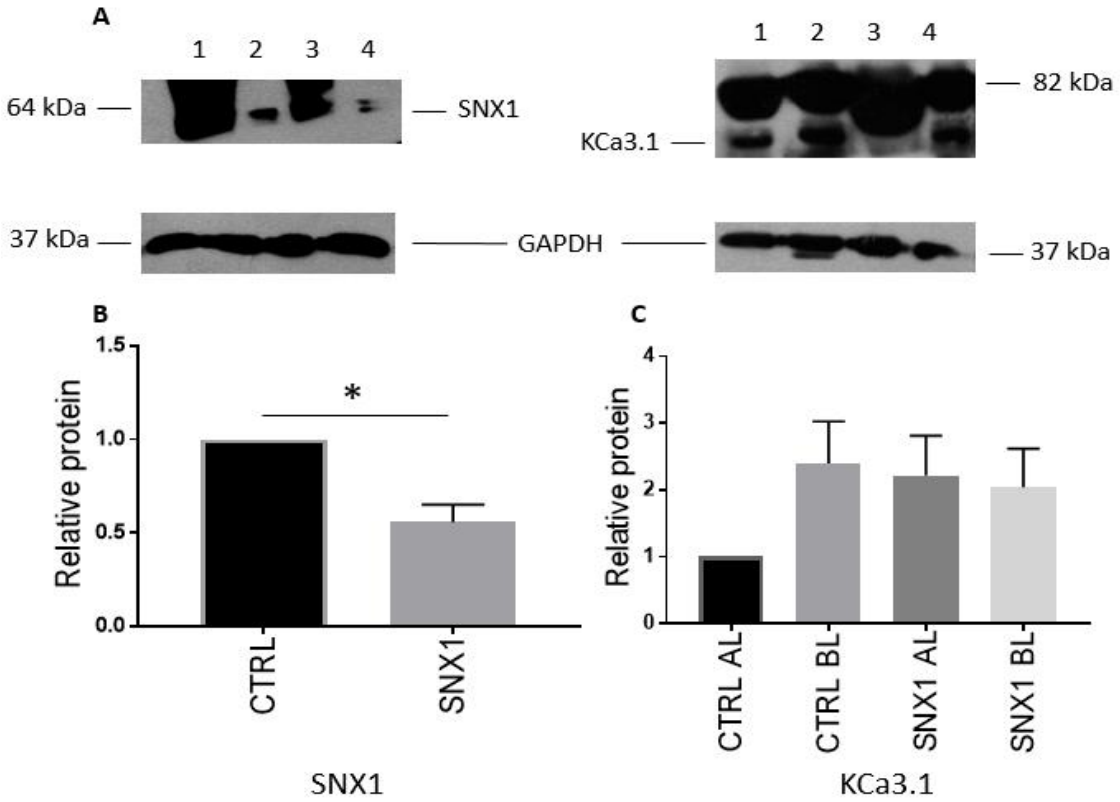

***Figure 4.9* – Effect of SNX1 knockdown on the basolateral membrane population of KCa3.1. A.** Representative blots for SNX1 and KCa3.1. Lanes 1 and 2 display lysate from cells transfected with 40 pM control siRNA, while Lanes 3 and 4 demonstrate lysate from cells transfected with 40 pM SNX1 siRNA. Lanes 1 and 3 represent lysate from cells with apical membrane located KCa3.1, and Lanes 2 and 4 display lysate from cells with the basolateral membrane. **B.** Quantification of the SNX1 immunoblots, revealing a significant decrease in the protein levels of SNX1 in cells transfected with 40 pM SNX1 siRNA compared to control cells ($p < 0.05$; n=4). **C**. Quantification of KCa3.1 immunoblots, demonstrating no significant differences between the control (CTRL) and SNX1 knockdown (SNX1) cells, for either the apical membrane population of KCa3.1 (AL), or the basolateral membrane population of KCa3.1 (BL). Additionally, there was no significant differences found between the CTRL AL and BL, or between the SNX1 AL and BL. Paired two sided t-tests were performed between the groups in B and an ANOVA analysis was performed in group C to assess significance.

Aside from immunoblot experiments, electrophysiology experiments to measure channel functionality were performed. These electrophysiology experiments were in the form of Ussing chamber experiments, and were utilised in order to determine any functional changes on KCa3.1 caused by changed in intracellular SNX1. The representative trace for these Ussing chamber experiments is exhibited in Figure 4.10A. These traces boast a significantly reduced (~60%, $p < 0.05$; n=4) 1-EBIO sensitive current in cells transfected with 40 pM SNX1 siRNA compared to control cells, however, this decrease was not matched in the clotrimazole sensitive current ($p > 0.1$; n=4). As the decrease in the 1-EBIO sensitive current was not matched in the clotrimazole sensitive current, therefore it is unlikely that SNX1 plays a functional role in KCa3.1 trafficking. Additionally, as no significant change was observed in the basolateral membrane population of KCa3.1 in cells with decreased SNX1, it is unlikely that SNX1 portrays a role in the trafficking of KCa3.1 in polarised epithelial cells. Furthermore, the traces showed no significant change in the transepithelial

resistance when cells were transfected with SNX1 siRNA ($p > 0.1$; n=4) (Figure 4.10D). As with the previous experiments, the resistance was measured at the point 1-EBIO was added. These results verify that the FRT-KCa3.1-BLAP cells formed a polarised monolayer effectively regardless of SNX1 inside the cell.

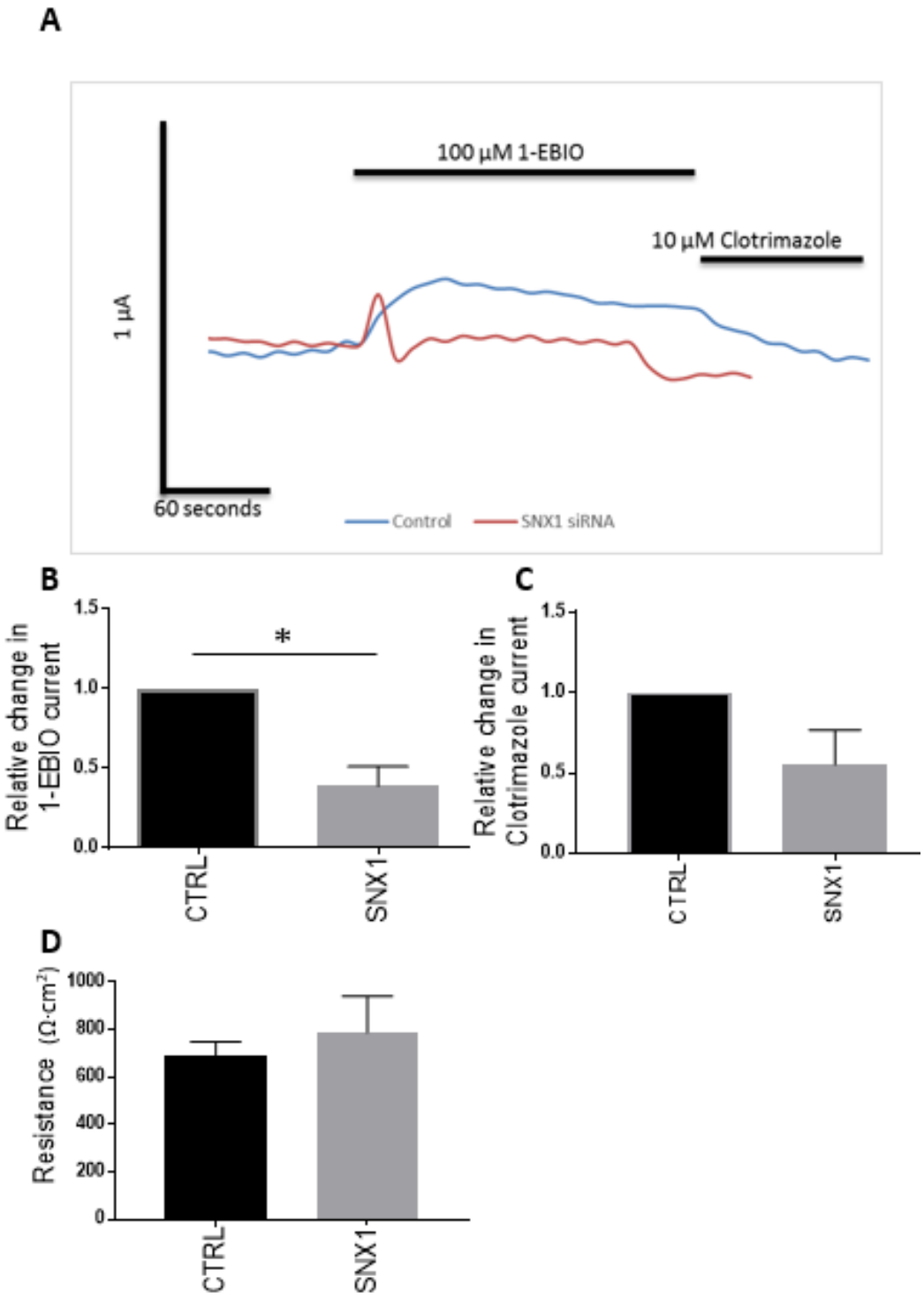

Figure 4.10 **– Effect of SNX1 knockdown on KCa3.1 function. A.** Representative trace displaying the effect of 100 µM 1-EBIO and 10 µM clotrimazole on cells transfected with either 40 pM control siRNA or 40 pM SNX1 siRNA. **B.** Quantification of the 1-EBIO sensitive current, revealing that transfecting cells with 40 pM SNX1 siRNA lead to a significant reduction in the 1-EBIO sensitive current compared to cells transfected with 40 pM SNX1 siRNA ($p < 0.05$; n=4). **C.** Quantification of the clotrimazole sensitive current. These results demonstrate no significant differences in the clotrimazole sensitive current between the control cells and the SNX1 knockdown cells. **D.** Quantification of the transepithelial resistance showing no significant change in the transepithelail resistance between the control and SNX1 knockdown cells ($p > 0.1$; n=4). Paired two sided t-tests were performed between each group in B, C, and D to assess significance.

4.5 Summary of Results

This project found that transfection of FRT-KCa3.1-BLAP cells with 40 pM of SNX(x) (where (x) = SNX1, SNX4, or SNX27) siRNA lead to a significant decrease in the intracellular levels of SNX(x) respectively, as measured by immunoblot. In contrast to this, there was no significant difference found in the basolateral membrane population of KCa3.1 in FRT-KCa3.1-BLAP cells that were transfected with 40 pM of either SNX(x) siRNA. There was no significant difference in the apical membrane population of KCa3.1 in the FRT-KCa3.1-BLAP cells transfected with 40 pM of SNX1 or SNX27 siRNA. I hypothesise that there would be no significant change in the apical membrane population of KCa3.1 in FRT-KCa3.1-BLAP cells transfected with 40 pM of SNX4 siRNA, however this was not measured due to time constraints. In electrophysiology experiments, treating cells with 100 µM of the KCa3.1 stimulator 1-EBIO showed a significant decrease in current in FRT-KCa3.1-BLAP cells transfected with 40 pM of either SNX(x) siRNA when compared with control cells. In contrast, treating cells with 10 µM of the KCa3.1 inhibitor clotrimazole showed no significant change in the current in FRT-KCa3.1-BLAP cells transfected with either SNX(x) siRNA when compared to control cells.

Finally, a plasmid containing *KCa3.1-HA-pcDNA3.1* was extracted from *E.coli*. A restriction digest was performed to ensure that the extracted plasmid contained the correct genetic information. When the plasmid was incubated with the restriction enzymes EcoR1 and Xho1, the plasmid split into two portions of the appropriate sizes to be *KCa3.1-HA* and the remaining plasmid. A transfection experiment was then carried out to determine the optimal transfection time and concentration for KCa3.1-HA expression. 1 or 2 µg of *KCa3.1-HA-pcDNA3.1* was transfected into COS-7 cells for either 24 or 48 hours, however the results proved inconclusive, and the experiment was discontinued due to time constraints.

5 Discussion

5.1 Preface

The intermediate conductance calcium-activated potassium channel, KCa3.1, is a channel expressed throughout the body, where it plays a variety of roles. Amongst these are; an active role in both smooth muscle (Neylon *et al.*, 1999) and fibroblast proliferation (Neylon *et al.*, 1999; Wang *et al.*, 2013a), which can affect cardiac fibrosis (Wang *et al.*, 2013a; Zhao *et al.*, 2015). Additional roles of KCa3.1 include fluid secretion, resulting in dysfunction of KCa3.1 being fully or partly responsible for the phenotypes of diseases such as hereditary xerocytosis (Andolfo *et al.*, 2013; Glogowska *et al.*, 2015; Rapetti-Mauss *et al.*, 2015) and sickle cell anaemia (Lew & Bookchin, 2005), a role in ulcerative colitis (Al-Hazza *et al.*, 2012), and a role in at least two renal diseases; autosomal polycystic kidney disease (Yoder *et al.*, 2002), and diabetic nephropathy (Qi *et al.*, 2006; Grgic *et al.*, 2009). KCa3.1 has also been portrayed as a potential therapeutic target in several cancers, such as gliomas (Abdullaev *et al.*, 2010), lung cancers (Bulk *et al.*, 2015), hepatocellular carcinomas (Liu *et al.*, 2015), and renal clear cell carcinomas (Rabjerg *et al.*, 2015). Moreover the use of the pharmacological KCa3.1 inhibitor Senicapoc, has been studied as a therapy for both hereditary xerocytosis (Rapetti-Mauss et al., 2016), and in sickle cell anaemia (Ataga et al., 2008), suggesting that KCa3.1 can be targeted safely to reduce the pathophysiological symptoms of disease.

The diversity of tissues in which KCa3.1 can be found, along with the still growing list of pathological conditions, has created a need to discover the mechanisms surrounding both KCa3.1 trafficking to and from the plasma membrane. As previously discussed in the introduction, little is known about KCa3.1 trafficking, although both the Devor (University of Pittsburgh) and Hamilton (University of Otago) laboratories have made substantial advancements in this area. Two separate Rab proteins, Rab1 and Rab8, are known to be involved in the anterograde trafficking of KCa3.1 (Bertuccio *et al.*, 2014). Rab1 is responsible for trafficking of proteins from the ER to the cis-Golgi body (Zhang *et al.*, 2009), while Rab8 is responsible for trafficking from the trans-Golgi body to the plasma membrane (Dong *et al.*, 2010). KCa3.1 was also shown to not traffic through either RME-1 or transferrin receptor positive recycling endosomes, which suggest direct trafficking from the Golgi body to the basolateral membrane in polarised epithelial cells (Bertuccio *et al.*, 2014). Recently, both the cytoskeleton and the motor protein myocin-Vc also have been implicated in the trafficking of KCa3.1 (Farquhar *et al.*, 2017). The inhibition of either the cytoskeleton or of myocin-Vc leads to a significant decrease in the basolateral membrane population of KCa3.1. Additionally, both myocin-Vc and the cytoskeletal elements are known to interact with Rab8 (Chabrillat *et al.*, 2005; Watanabe *et al.*, 2008; Xu *et al.*, 2009). This led Farquhar and colleagues to suggest that myocin-Vc simply allows

KCa3.1 to travel along the microtubule cytoskeleton to the basolateral membrane, rather than directly trafficking KCa3.1 to the basolateral membrane (Farquhar *et al.*, 2017).

An area of cellular physiology which has gained traction recently is the Retromer pathway that is involved in both the recycling and degradation of plasma membrane protein (Arighi *et al.*, 2004; Chen *et al.*, 2010; Temkin *et al.*, 2011), and helps to regulate endosome to trans-Golgi body (Arighi *et al.*, 2004). This pathway consists of multiple protein complexes, namely the cargo recognition complex (CRC), consisting of VPS26, VPS29, and VPS35 (Norwood *et al.*, 2011), and the Wiskott-Aldrich syndrome protein and SCAR Homologue (WASH) complex (Derivery *et al.*, 2009; Gomez *et al.*, 2012). The protein complexes involved in Retromer interact with each other, and interact with multiple individual proteins, such as sorting nexin (SNX) proteins (Wassmer *et al.*, 2009).

While Retromer is involved in the recycling of proteins such as the basolaterally located β2 adrenergic receptor (β2AR), which is recycled by SNX27 directly to the plasma membrane from the early endosome (Lauffer *et al.*, 2010; Temkin *et al.*, 2011), KCa3.1 has been shown to not traffic through the recycling endosome (Lin *et al.*, 2012). However, there is some evidence that KCa3.1 may be recycled. Schwab and colleagues found that KCa3.1 was subject to clathrin mediated endocytosis in migratory cells, and discovered that KCa3.1 appeared to be residing in the plasma membrane for longer than expected, a finding which Schwab and co-workers believe is consistent with the notion of channel recycling (Schwab *et al.*, 2012). Furthermore, another member of the KCNN gene family, KCa2.3, is recycled in polarised both endothelial and epithelial cells (Gao *et al.*, 2010; Lin *et al.*, 2012). This recycling has been shown to be partially dependent on an amino acid sequence within the N-terminus. While this 12 amino acid sequence (GQPLQLFSPSNP (Gao *et al.*, 2010)) is not conserved in KCa3.1, there is a possibility of a recycling domain on KCa3.1, as some groups believe that KCa3.1 can be recycled in certain cell types (Schwab *et al*., 2012).

In order to study the effect of the Retromer on KCa3.1 recycling in epithelia, in this project the SNX proteins SNX1, SNX4, and SNX27 were studied. FRT-KCa3.1-BLAP cells were transfected with 40 pM of either control siRNA or SNX(x) (where (x) = SNX1, SNX4, or SNX27) siRNA in order to decrease intracellular expression of a specific SNX protein. The effectiveness of this knockdown was then measured by immunoblot, as was the membrane populations of KCa3.1, and the quantified results were normalised and compared to the cells transfected with 40 pM control siRNA. Furthermore, KCa3.1 function at the basolateral membrane was measured through Ussing chamber experiments, where the change in current was measured after stimulating or inhibiting the KCa3.1 channel, and differences in the change in current between the control and knockdown cells were analysed. I hypothesised that transfecting FRT-KCa3.1-BLAP cells with SNX(x) siRNA would lead to a

significant decrease in the intracellular expression of that SNX protein. Additionally, I hypothesised that this significant decrease in the SNX protein levels would lead to a significant decrease in the basolateral membrane population of KCa3.1, as measured by immunoblot, and a significant decrease in both the 1-EBIO and clotrimazole sensitive currents, compared to control epithelia.

5.2 Technical approach

For this project, a robust, reliable KCa3.1 labelling system was required, as accurate determination of the membrane population of KCa3.1 was vital to observe the channel at the basolateral membrane. The labelling system used in this study was based on the internal biotinylation method developed by Alice Ting (Chen *et al.*, 2005), and modified to biotinylate KCa3.1 by Devor and colleagues (Balut *et al.*, 2010). This method of internal biotinylation centres around cells stably transfected with KCa3.1 which has been modified to contain a biotin ligase acceptor peptide (BLAP) sequence on an extracellular loop between the 3rd and 4th transmembrane domains. The plasmid these cells were transfected with also contains a biotin ligase enzyme (BirA), modified to contain an endoplasmic reticulum retention motif (BirA-KDEL) (Figure 3.2). In the cell, this system allows for KCa3.1 to be synthesised in the ER by ribosomes, then subsequently biotinylated by BirA on the BLAP sequence. At the plasma membrane, KCa3.1 functions normally, whilst exhibiting an extracellular biotin, which can be detected by selective labelling with streptavidin, allowing for immunoblots where only membrane bound KCa3.1 is shown. Gao and colleagues compared KCa3.1 to KCa3.1-BLAP, and found that the addition of BLAP did not significantly affect the activation of KCa3.1 by DCEBIO, nor the inhibition of KCa3.1 by clotrimazole (Gao *et al.*, 2010). Moreover, it has been published that neither KCa3.1 trafficking nor function is adversely affected by the addition of the BLAP sequence (Gao *et al.*, 2010).

This plasmid was stably transfected into Fischer Rat Thyroid (FRT) cells, which are able to form a polarised epithelial sheet (Winter et al., 2011). The resultant cell line in known as FRT-KCa3.1-BLAP cells. As FRT-KCa3.1-BLAP cells retain the ability to form polarised epithelial sheets, the cells were cultured onto semi-permeable membranes for experimental procedures, allowing for both the apical and basolateral membrane populations of KCa3.1 to be independently observed.

5.3 Experimental overview

This study was undertaken with four experimental goals to be competed. The base aspect of this project was the preliminary experiments; the sidedness experiment, where the basolateral localisation of KCa3.1 was confirmed (Figure 4.1), the SNX antibody tests, where antibodies confirmed that each SNX protein was present in FRT cells (Figure 4.2), and the SNX siRNA tests, where the ability of each SNX siRNA to decrease the corresponding protein was determined (Figures

4.3 and 4.4). The sidedness experiment served to ensure that KCa3.1 was being trafficked to the basolateral membrane, as reported in previous studies (Bertuccio *et al.*, 2014; Farquhar *et al.*, 2017). The SNX antibody tests ensure that the antibodies were able to detect endogenously expressed SNX proteins in FRT cells. Finally, the SNX siRNA tests served to find the optimal concentration of siRNA to transfect into cells.

The second area of this project was to ensure that transfecting cells with 40 pM of SNX(x) siRNA led to a significant decrease in SNX(x) protein expression compared to cells transfected with 40 pM control siRNA. If a passage of cells were found to have no decrease in the SNX(x) intracellular protein levels, the neither the apical nor the basolateral membrane populations of KCa3.1 were measured. Changes in the relative intracellular protein levels of SNX(x) were measured through immunoblot experiments.

The third part of this project observed the membrane populations of KCa3.1 in cells transfected with 40 pM SNX(x) siRNA or control siRNA. For cells transfected with 40 pM SNX(x) siRNA, the apical and basolateral membrane populations of KCa3.1 were independently measured, and were compared to the membrane population of KCa3.1 in cells transfected with 40 pM control siRNA. As previously mentioned, these experiments were only carried out on cells with a decrease in intracellular SNX(x) protein expression due to transfection of cells with SNX(x) siRNA.

The final aspect of this project was to observe the functional expression of KCa3.1 in FRT-KCa3.1-BLAP cells transfected with 40 pM SNX(x) siRNA, then measuring the relative change in current, as determined by Ussing chamber experiments. The change in current was measured following the addition of either 1-EBIO or clotrimazole, in order to detect the 1-EBIO sensitive current or the clotrimazole sensitive current in both epithelia transfected with 40 pM control siRNA and cells transfected with 40 pM SNX(x) siRNA. The differences in both the 1-EBIO sensitive current, and the clotrimazole sensitive current were measured in both the control epithelia and the SNX(x) knockdown epithelia.

While four aspects of this project have been outlined, the final three were carried out simultaneously, and in parallel. Cells for these experiments were all seeded from the same passage of cells, and transfected with 40 pM of siRNA. Additionally, all the cells were cultured in the same environment, eliminating many variables which may reduce consistency. This allowed for the assumption that the Ussing chamber experiments experienced the same SNX(x) knockdown as the immunoblot experiments, where the level of knockdown was easily measured. It was imperative that the SNX(x) knockdown was identical in the Ussing chamber experiments, as it allowed for

changes in current seen when the KCa3.1 at the cell membrane was simulated with 1-EBIO or inhibited with clotrimazole to be matched to a % decrease in the intracellular SNX(x) protein levels.

5.3.1 Preliminary experiments

As mentioned above, the preliminary experiments for this project consisted of the sidedness experiment, the antibody tests, and the siRNA tests. The sidedness experiment (Figure 4.1) revealed that the majority of KCa3.1 was expressed at the basolateral membrane compared to both the cells where no membrane bound KCa3.1-BLAP channels were not labelled through the use of streptavidin (hereafter referred to as unlabelled cells) ($p < 0.05$; n=4), and to apically labelled cells (cells where the apical membrane population of KCa3.1 was labelled with streptavidin) ($p < 0.05$; n=4). While the difference between the apical and basolateral membrane populations of KCa3.1 was not significant, there was a trend towards significance seen, suggesting that significance may emerge with more experiments. Previous studies have shown that KCa3.1 is located solely in the basolateral membrane (Bertuccio *et al.*, 2014; Farquhar *et al.*, 2017). This suggests the possibility that the small, non-significant amount of KCa3.1 detected at the apical membrane compared to the negative control was due to streptavidin. If the cellular monolayer was not fully confluent when streptavidin was placed on the apical membrane, some of the basolaterally located KCa3.1 may have been accidentally labelled. Alternatively, if not all the streptavidin was removed by washing steps, then streptavidin on the apical membrane could bind to the basolaterally located KCa3.1 during cell lysis. As there was a trend towards a significant difference seen between the apical and basolateral membranes in the sidedness experiment, this difference was considered to be the baseline for other experiments. Ergo, apical expression akin to what was seen in Figure 4.1 was considered to be normal, and siRNA experiments with only a small amount of apical expression were not considered to be caused by KCa3.1 missorting to the apical membrane. Furthermore, later in this project, the apical expression of KCa3.1 was measured in both the control and knockdown cells. This allowed for relative changes in the apical KCa3.1 signal to be measured, ensuring that any perceived apical missorting of KC3.1 in cells where Retromer was disrupted was actually occurring.

The antibody test (Figure 4.2) for this project proved two things. Firstly, these results revealed that both the anti-SNX1 and the anti-SNX27 antibody indeed identified endogenously expressed proteins in FRT cells, as protein bands appeared in the lysate from FRT cells. Secondly, these results demonstrated that both SNX1 and SNX27 were present in FRT cells, as the protein bands occurred at the correct molecular weight. These protein bands appeared in both the positive control lysate (lysate from HEK293 cells, as shown by immunoblot provided by the manufacturer) and in the lysate from FRT cells.

The SNX27 siRNA test (Figure 4.4) for this project determined the optimal siRNA concentration for transfecting cells with SNX27 siRNA, showing that transfecting cells with 40 pM SNX27 siRNA led to the largest decrease in SNX27 protein levels compared to the cells transfected with 40 pM of control siRNA, however this was not a significant change ($p > 0.05$; $n=3$).

Additionally, the antibody used to detected the C-terminus of SNX27, and suggested that SNX27 run at 28 kDa, rather than 61 kDa. The antibody purchased for detection of SNX27 stated that SNX27 run at 28 kDa, however, after the preliminary experiments, it was revealed that other SNX27 antibodies detected SNX27 at 61 kDa. My preliminary experiments were not able to detect SNX27 at 60 kDa, as the PVDF membrane was sectioned horizontally with reference to the protein ladder to allow for simultaneous detection of both SNX27 (28 kDa) and GAPDH (37 kDa). This meant that any higher molecular weight bands of SNX27 were located on the GAPDH portion of the membrane. SNX27 was detected at 61 kDa by a member of the McDonald Lab. This allowed for the accurate detection of the whole SNX27 protein at 61 kDa using the antibody available, rather than detecting a portion of the SNX27 protein at 28 kDa, as detected in Figures 4.2 and 4.4.

I believe that the detection of SNX27 at 28 kDa was insufficiently accurate for the preliminary experiments, ergo the more accurate detection at 61 kDa was required in order to determine a more accurately calculated knockdown of SNX27. When determining the effect of SNX27 on the basolateral membrane population of KCa3.1, it was vital to accurately determine if a transfection with SNX27 siRNA was successful, as any experiments where a siRNA transfection did not elicit a significant decrease in the protein levels were not accepted to measure changes in the membrane populations of KCa3.1.

On the other hand, the SNX1 siRNA test (Figure 4.3) for this project did not show any significant decrease in SNX1 expression in any of the SNX1 siRNA transfections, up to 40 pM. There are a number of possibilities as to why these transfections did not yield a significant decrease in the intracellular expression of SNX1, including unrefined transfection technique, bad transfection reagents or media, or non-specific protein binding for SNX1. Figure 4.3 showed the representative immunoblot for SNX1, and also shows a faint band underneath the perceived SNX1 band, suggesting the possibility of nonspecific protein bands being detected by anti-SNX1 in FRT cells. This non-specific binding did not occur in the SNX1 experiments discussed in section 5.3.4.

5.3.2 The effect of SNX4 on the trafficking of KCa3.1

The first sorting nexin protein whose effect I studied on the trafficking of KCa3.1 was SNX4; a protein involved in the trafficking of vesicles from the early endosome to the trans-Golgi body and back to the plasma membrane (Traer *et al.*, 2007). Silencing of SNX4 expression results in the

transferrin receptor being sent into the lysosomal degradation pathway, rather than being recycled (Traer *et al.*, 2007). If decreasing the protein levels of SNX4 indeed affects the membrane population of KCa3.1, it could suggest that KCa3.1 is recycled by a previously unknown mechanism. Therefore, it is important to examine the possibility that SNX4 plays a role in the trafficking of KCa3.1.

Before any effect of SNX4 on the trafficking or membrane population of KCa3.1 could be established, a significant decrease in the intracellular expression of SNX4 had to be observed. FRT-KCa3.1-BLAP cells were seeded onto semipermeable filters, then were transfected with 40 pM of either control siRNA or SNX4 siRNA. This transfection resulted in a 62 ± 12% decrease in the intracellular protein levels of SNX4 compared to the control, which was highly significant (Figure 4.5B) ($p < 0.001$; n=5).

When immunoblots detected that a successful SNX4 siRNA transfection occurred, a second sample of this cellular lysate was run on immunoblot in order to measure the apical and basolateral membrane populations of KCa3.1. This was possible as both the apical and basolateral membrane populations of KCa3.1 were labelled prior to cell lysis. It was hypothesised that, by decreasing the intracellular protein levels of SNX4, the basolateral membrane population of KCa3.1 would also be reduced. As both the apical and the basolateral membrane populations of KCa3.1 were measured in cells transfected with SNX4 siRNA, any KCa3.1 missorted from the basolateral to the apical membrane would be able to be detected. Figure 4.5C shows no significant change in the basolateral membrane population of KCa3.1 between the control cells and the cells transfected with SNX4 siRNA. Interestingly, there was also no significant difference between the basolateral membrane population of KCa3.1 in the control cells and the apical membrane population of KCa3.1 in the SNX4 knockdown cells (Figure 4.5C). This could suggest that some KCa3.1 was missorted from the basolateral membrane to the apical membrane, however, it is possible that the FRT-KCa3.1-BLAP cells did not completely cover the filter they were grown on. This could have led to some of the basolateral membrane population of KCa3.1 to be labelled in the apically labelled samples. Additionally, this experiment highlighted the need to measure the apical membrane population of KCa3.1 in the cells transfected with 40 pM control siRNA. The apical membrane population of KCa3.1 was not measured in the control cells for this experiment as previous experiments have shown the basolateral localisation of KCa3.1 (Bertuccio *et al.*, 2014; Farquhar *et al.*, 2017). Following this experiment, the apical membrane population of KCa3.1 was labelled in order to allow for changes in not only the basolateral membrane population of KCa3.1 to be measured, but for changes in the apical membrane population of KCa3.1 to be measured as well.

The final aspect of detecting any effect which SNX4 plays on the trafficking and membrane populations of KCa3.1 was performing Ussing chamber experiments. This was performed by seeding and transfecting cells at the same time and with the same concentrations of siRNA as the immunoblot experiments discussed above, to ensure that any changes detected were indeed due to a change in SNX4. Additionally, both the 1-EBIO and the clotrimazole sensitive currents were measured, to ensure that any changes seen in the current were truly due to changes in the membrane population of KCa3.1, and not due to contaminating factors, such as other potassium channels, which may be activated by 1-EBIO (Bahia *et al.*, 2005). It was shown that, in cells transfected with 40 pM SNX4 siRNA, there was a significant 36 ± 8% decrease in the 1-EBIO stimulated current than in control cells (Figure 4.6B) ($p < 0.05$; n=5). In contrast to this, cells transfected with 40 pM SNX4 siRNA did not show any significant difference in the clotrimazole sensitive current compared to the control cells (Figure 4.6C) ($p > 0.1$; n=5). As the change in the 1-EBIO sensitive current was not consistent with the clotrimazole sensitive current, nor by the immunoblot experiments, it is likely that the basolateral membrane population of KCa3.1 is not affected by SNX4. It is may be possible that the change in the 1-EBIO sensitive current is due to the presence of another EBIO-sensitive K^+ channel, for example, an SK channel, which are also stimulated by the presence of 1-EBIO (Pedarzani *et al.*, 2001), although no reports could be found of SK channels present in FRT cells. On the other hand, clotrimazole does not appear to inhibit SK channels (Malik-Hall *et al.*, 2000). It is known that the SK3 (KCa2.3) channel is recycled in endothelial cells (Lin *et al.*, 2012), although KCa3.1 was revealed to not be recycled in endothelial cells. However, it is may be possible that KCa3.1 is recycled in FRT cells, as KCa3.1 is closely related to KCa2.3, as both channels are from the KCNN gene family. KCa3.1 was hypothesised to be recycled in migratory cells (Schwab, 2012), which may further increase the possibility of KCa3.1 recycling in FRT cells.

Finally, it was determined that there was no change in the transepithelial resistance when cells were transfected with SNX4 siRNA ($p > 0.05$; n=5) (Figure 4.6D). This strongly suggests that the FRT-KCa3.1-BLAP cells used for this experiment were able to form a confluent tight epithelial monolayer when SNX4 was knocked down. This is important as a tight epithelia is vital for the success of Ussing chamber experiments.

I hypothesised that decreasing the intracellular protein levels of SNX4 would decrease the basolateral membrane population of KCa3.1, as measured by both immunoblots and Ussing chamber experiments. Immunoblot experiments showed no significant decrease in the basolateral membrane population of KCa3.1 in cells with less SNX4. Additionally, the Ussing chamber experiments did not show a significant decrease in the basolateral membrane population of KCa3.1. These results prove that my hypotheses were incorrect, and strongly suggest that SNX4 does not

appear to play a role in the trafficking of KCa3.1. Furthermore, it appears that KCa3.1 is not trafficked by bulk flow along the tubules formed by SNX4, as the basolateral membrane population of KCa3.1 did not significantly change when SNX4 was knocked down. Certain proteins, such as TfnR, are trafficked through SNX4 tubules while not directly interacting with SNX4 itself, instead being sorted into these tubules in a geometrical manner (Cohen & Pintavirooj, 2004). These results suggest that, unlike TfnR, KCa3.1 is not indirectly sorted by SNX4, nor directly interacts with SNX4 to be trafficked between the plasma membrane and the early endosome. While it appears that KCa3.1 trafficking in unaffected by SNX4, it is possible that other SNX proteins with similar roles, such as SNX1/2, which are also involved in cargo selection and trafficking (Wassmer *et al.*, 2009). Additionally, as SNX1 and SNX4 both form sorting tubules in the early endosome, it is possible that KCa3.1 is not trafficked by SNX proteins in order to reach the early endosome for its degradatory pathway (Carlton *et al.*, 2004; Traer *et al.*, 2007). The effect of SNX1 on the trafficking of KCa3.1 is further discussed in section 5.3.4.

5.3.3 The effect of SNX27 on the trafficking of KCa3.1

SNX27 is a unique sorting nexin protein, containing a PDZ domain, a domain unseen amongst other SNX proteins. SNX27 has been shown to aid in trafficking the β2AR (Lauffer *et al.*, 2010), and the sodium-hydrogen exchanger NHE3, which is trafficked to the basolateral membrane (Singh *et al.*, 2015). SNX27 utilises both its FERM domain and its PDZ domain in order to selectively traffic its cargo (Lauffer *et al.*, 2010; Temkin *et al.*, 2011; Steinberg *et al.*, 2013; Gallon *et al.*, 2014). Additionally, in SNX27 depleted cells, it was shown that cargo was sent into a lysosomal degradation pathway (Lee *et al.*, 2016).

As with the effect of SNX4, the effect of SNX27 on KCa3.1 trafficking and basolateral membrane population could not be examined before a SNX27 knockdown was observed. FRT-KCa3.1-BLAP cells were transfected with either 40 pM control siRNA or 40 pM SNX27 siRNA, and the cellular lysates were run on an immunoblot. These results showed a 27 ± 4% decrease in the intracellular levels of SNX27 compared to the control cells (Figure 4.7B) ($p < 0.01$; n=4). While this knockdown appeared smaller than the SNX27 knockdown (51 ± 10% decrease) seen in the SNX27 siRNA test ($p > 0.05$)(Figure 4.4), this knockdown was significant, unlike the SNX27 knockdown of the siRNA test. It is possible that this difference in the transfections was because the original immunoblots detected SNX27 at 28 kDa, as per the manufacturer's instructions, rather than detecting the protein at 61 kDa, the size of SNX27 published by other groups. When SNX27 was detected at 61 kDa in FRT-KCa3.1-BLAP cells transfected with 40 pM of SNX27 siRNA, using the same antibody, a significant decrease in the intracellular levels of SNX27 was observed ($p < 0.01$; n=4) (Figure 4.7B).

Just as with looking at the effect of SNX4 on the membrane population of KCa3.1, the cellular transfections where a decrease in the intracellular protein levels of SNX27 was observed were used to observe the apical and basolateral membrane populations of KCa3.1. Unlike with the SNX4 experiments, these immunoblots studied both the apical and basolateral membrane populations of KCa3.1 in the control cells as well as in the SNX27 siRNA transfected cells. This allowed for any differences in the apical membrane population of KCa3.1 to be measured, rather than making the assumption that no KCa3.1 would be detected at the apical membrane of control cells. When the immunoblots were analysed, there was no significant difference detected in the basolateral membrane population of KCa3.1 between the control cells (CTRL BL) and the cells where a SNX27 knockdown was performed (SNX27 BL) (Figure 4.7C). This suggested that SNX27 was not involved in the trafficking of KCa3.1 to the basolateral membrane.

Interestingly, the apical membrane population of KCa3.1 in the cells transfected with 40 pM SNX27 siRNA appeared to be higher than the apical population of KCa3.1 in the control cells, with what was approaching significance (Figure 4.7) ($p = 0.0818$; $n=4$). As these results are from only 4 experiments, this could suggest that without SNX27, the basolaterally targeted KCa3.1 is missorted to the apical membrane. However more experiments would be required before any conclusions could be drawn. If the apical membrane population of KCa3.1 is indeed increased when SNX27 is decreased, but the basolateral membrane population is decreased, it could suggest that surplus KCa3.1 is produced under normal conditions, and there is a cellular process to limit the basolateral membrane population of KCa3.1, however the apical membrane is free to be occupied.

Additionally, the basolateral membrane population of KCa3.1 in the control cells was almost significantly higher than the apical membrane population of KCa3.1 in the control cells (Figure 4.7C) ($p < 0.1$; $n=4$), which appears to suggest that the FRT-KCa3.1-BLAP cells seeded for this experiment formed a near confluent monolayer, with very little streptavidin leaking through to the basolateral membrane KCa3.1, although this is unconfirmed. The results seen in Figure 4.7C suggest that the SNX27 siRNA knockdown which caused a 27 ± 4% decrease in SNX27 was unable to significantly decrease the basolateral membrane population of KCa3.1, however a more substantial reduction in the intracellular protein expression of SNX27, or an increased number of experiments may have shown that KCa3.1 was able to be missorted to the apical membrane. This being said, no conclusions can be drawn from the immunoblots in Figure 4.7.

Again, like with SNX4, the SNX27 immunoblot experiments were paired to Ussing chamber experiments. These results showed an 83 ± 8% decrease in the 1-EBIO sensitive current, which is highly significant ($p < 0.001$; $n=4$) (Figure 4.8B). While this decrease in current appears promising, it

is likely that this result is not solely due to changes in the membrane population of KCa3.1, as only a 27 ± 4% decrease in SNX27 was observed (Figure 4.7B). As with SNX4, this amplified 1-EBIO sensitive current may be the result of other SK channels, which are stimulated by 1-EBIO alongside KCa3.1 (Pedarzani *et al.*, 2001) however, the presence of SK channels in FRT cells must first be confirmed by immunoblot, as there were no published reports of any SK channels present in FRT cells at the time of writing of this report. If SK channels, including KCa2.3, are present in FRT cells, and if a decrease in SNX27 leads to a decrease in basolateral membrane population of KCa2.3, this could aid in the magnitude of change seen, and this could be even more significant if KCa2.3 was missorted to the apical membrane. In order to test this hypothesis, it is vital to first observe endogenous KCa2.3 in FRT cells, a gap in the current literature. This is because the Ussing chamber set up for this experiment had an artificial K^+ gradient designed to amplify the basolateral K^+ current of KCa3.1, ergo if KCa3.1, or a similar channel, was missorted to the apical membrane, it would have an amplified negative effect on the 1-EBIO sensitive current. While an 83 ± 8% decrease in the 1-EBIO sensitive current was seen in cells transfected with 40 pM SNX27 siRNA compared to the control (Figure 4.8B), this decrease was not seen in the clotrimazole sensitive current. While there was a slight decrease seen in the clotrimazole sensitive current (27 ± 14%), this was not significant ($p > 0.1$; n=4) (Figure 4.8C). This further suggests that the 1-EBIO sensitive current seen is not solely due to changes in the basolateral membrane population of KCa3.1.

Finally, there appeared to be no significant differences between the transepithelial resistance of the control cells and the SNX27 deficient cells ($p > 0.1$; n=4) (Figure 4.8D), demonstrating that the cells were able to form a tight epithelial monolayer with significantly decreased intracellular levels of SNX27 (Figure 4.8D). This is especially important in the case of SNX27, as SNX27 has been shown to traffic ZO-2 (Zimmerman, 2013), suggesting that cells with less SNX27 may not form tight junctions as efficiently, which may allow for the streptavidin used to label the apical population of KCa3.1 to leak through to the basolateral membrane more easily. If there was a significant decrease in the transepithelial resistance, it could signify that the increase in the apical membrane population of KCa3.1 was due to more streptavidin leaking through the transcellular pathway. As there is no significant change in the transepithelial resistance, it is possible that the almost significant increase in the apical membrane population of KCa3.1 in the SNX27 scarce cells is due to KCa3.1 being missorted to the apical membrane from the basolateral membrane, however more experiments are required to confirm this.

For this aspect of the project, my first hypothesis was correct, and transfecting cells with 40 pM SNX27 siRNA lead to a significant decrease in the intracellular levels of SNX27 (Figure 4.7B). My second hypothesis was not correct, as there was no significant change in the basolateral

membrane population of KCa3.1 in the SNX27 knockdown cells compared to the control cells (Figure 4.7C). However, it is possible that some KCa3.1 was missorted to the apical membrane without leading to a decrease in the basolateral membrane population of KCa3.1. Finally, my third hypothesis, that both the 1-EBIO sensitive current and the clotrimazole sensitive currents would be decreased in cells transfected with 40 pM SNX27 siRNA, was incorrect, as there was no significant change in the clotrimazole sensitive current, despite the change in the 1-EBIO sensitive current (Figure 4.8). These results suggest that KCa3.1 does not interact with SNX27. Additionally, it appears unlikely that the KCa3.1 channel is trafficked along SNX27 specific tubules. This is consistent with the current literature on KCa3.1, as SNX27 is involved in the recycling pathway from the early endosome to the plasma membrane, as shown in Figure 1.6 (Lauffer et al., 2010; Temkin et al., 2011; Gallon et al., 2014; Lee et al., 2016). Previously, it has been shown that KCa3.1 is not recycled in endothelial cells, unlike the similar KCa channel, KCa2.3 (Lin *et al.*, 2012). Additionally, KCa3.1 trafficking in epithelial cells is recycling endosome independent (Bertuccio et al., 2014), instead being trafficked directly to the basolateral membrane (Bertuccio et al., 2014). The results shown here suggest that KCa3.1 is not recycled in a SNX27 dependent mechanism, strengthening the hypothesis that KCa3.1 is not recycled in epithelial cells. The results seen here, and the results published by Lin and colleagues (2010), and Bertuccio and collaborators (2014), are not supported by the work of Schwab and contemporaries (2012), who suggest that KCa3.1 is recycled in migratory epithelial cells, however, do not provide evidence of a specific mechanism, instead stating that their observations were consistent with the notion of channel recycling, however noting the lack of channel internalisation kinetics data. This could suggest that KCa3.1 is trafficked differently in migratory cells compared to stationary cells.

5.3.4 The effect of SNX1 on the trafficking of KCa3.1

Finally, the effect of SNX1 on the trafficking of KCa3.1 was measured. *In vivo* SNX1 forms a dimer with either SNX5 or SNX6, as does the similar SNX2 (Griffin *et al.*, 2005; Rojas *et al.*, 2007; Wassmer *et al.*, 2007). SNX1 contains a BAR domain, which aids in the formation of vesicles and the internalisation of membrane bound proteins (Peter *et al.*, 2004; van Weering *et al.*, 2012). Furthermore SNX1 has been shown to recycle the basolaterally trafficked protein E-cadherin (Bryant *et al.*, 2007), suggesting that SNX1 is capable of recycling other basolaterally trafficked proteins.

When FRT-KCa3.1-BLAP cells were transfected with 40 pM SNX1 siRNA, compared to cells transfected with 40 pM control siRNA, a significant decrease in the intracellular protein levels of SNX1 were detected (Figure 4.9B) ($p < 0.05$; n=4). This decrease in SNX1 is significantly more than was detected in the SNX1 siRNA test ($p < 0.01$) (Figure 4.3). The increased transfection efficiency seen in Figure 4.9 compared to Figure 4.3 is likely due to multiple factors, including; more refined

transfection technique due to months more practice, and the use of a different batch of transfection media. As each batch of transfection media is made by hand, small differences in the pH or concentration may occur, which could have upset the delicate balance needed for successful siRNA transfections.

In the SNX1 knockdown cells where a decrease in SNX1 was detected were then used to observe the apical and basolateral membrane populations of KCa3.1 in both the control and the SNX1 depleted cells (Figure 4.9C). These results showed no significant difference in the basolateral membrane population of KCa3.1 in either the control cells or the cells where SNX1 was reduced. This suggests that SNX1 is not involved in the trafficking of KCa3.1 to the basolateral membrane. Similarly, there was no significance seen in the differences in the apical membrane population of KCa3.1 between the control cells and the cells transfected with SNX1 siRNA. As KCa3.1 is not expected in the apical membrane in control cells, this suggests that a reduction in SNX1 did not lead to missorting of KCa3.1 from the basolateral membrane to the apical membrane. Following the trend of non-significance, there was no significance seen between the apical or basolateral membrane populations of KCa3.1 in the cells transfected with either 40 pM control siRNA or 40 pM SNX1 siRNA, suggesting the possibility that the FRT-KCa3.1-BLAP cells did not completely form a monolayer on the filters used for immunoblot experiments, allowing for apical streptavidin to label the basolateral membrane population of KCa3.1. As mentioned previously, it is known that, in a confluent epithelial monolayer, KCa3.1 is localised to the basolateral membrane (Farquhar *et al.*, 2017).

Just as with the SNX4 and SNX27 experiments, this experiment utilised functional experiments in the form of Ussing chamber experiments (Figure 4.10). These experiments showed a significant decrease in the 1-EBIO sensitive current in the cells transfected with 40 pM SNX1 siRNA compared to the cells transfected with 40 pM control siRNA ($p < 0.05$; n=4) (Figure 4.10B). This 61 ± 11% decrease in the 1-EBIO sensitive current was not matched by the clotrimazole sensitive current, which only has a 45 ± 19% decrease in the SNX1 knockdown cells compared to the control cells, a decrease which is statistically non-significant ($p > 0.1$; n=4) (Figure 4.10C). As the cells did not exhibit a change in the clotrimazole sensitive current, nor in the basolateral membrane population of KCa3.1 when transfected with SNX1 siRNA, it is highly unlikely that SNX1 is involved in the trafficking of KCa3.1. Additionally, there was no significant change in the transepithelial resistance when cells were transfected with SNX1 siRNA ($p > 0.1$; n=4) (Figure 4.10D). This signifies the formation of a tight epithelial monolayer in the cells with less SNX1. The formation of a tight epithelial monolayer proves that the Ussing chamber results are not due to a leakier or defective epithelia.

The results seen here strongly suggest that SNX1 is not involved in the trafficking of KCa3.1, either to or from the plasma membrane. Additionally, combined with the results presented in section 4.4.1, which examined the potential role of SNX4 in the trafficking of KCa3.1, it is unlikely that any SNX proteins are involved in the trafficking of KCa3.1 between the plasma membrane and the early endosome. This is suggested as both SNX1 and SNX4 are key proteins in the formation of SNX sorting tubules, and both branch from the plasma membrane to the early endosome for membrane protein transport (Carlton et al., 2004; Traer et al., 2007). As KCa3.1 does not appear to be internalised by a SNX1 specific mechanism, it is unlikely that KCa3.1 is transported from the endosome to trans-Golgi body, as SNX1 is one of the defining features of this pathway (Bujny et al., 2007). Furthermore, it is unlikely that either SNX5 or SNX6 play a role in the trafficking of KCa3.1, as SNX1 possesses a well-documented interaction with both SNX5 and SNX6, with suppression of either SNX5 or SNX6 leading to a decrease in SNX1 expression (Wassmer *et al*., 2007). It is also unlikely that SNX2 portrays a role in the trafficking of KCa3.1, due to its similarity to SNX1, as these proteins are believed to have interchangeable roles in trafficking (Rojas *et al*., 2007), however, as SNX2 is similar to SNX1, it is possible that the effect of SNX1 knockdown is blunted by the upregulation of SNX2. Finally, it is improbable that SNX3 plays a role in the trafficking of KCa3.1, as SNX3 has been suggested to utilise the tubules created by SNX proteins such as SNX1 (Strochlic et al., 2007). This is because SNX3 is unable to synthesise their own transport structures (Strochlic et al., 2007).

When the intracellular protein levels of either SNX1, SNX4, or SNX27 are reduced by siRNA transfection, a significant decrease in the 1-EBIO sensitive current was observed. This would suggest that the functional expression of KCa3.1 is reduced, however none of these transfections lead to a significant, or trended towards a significant decrease in the clotrimazole sensitive currents. This suggests that another factor was responsible for the change in the 1-EBIO sensitive current. I hypothesise that another member, or members of the KCNN gene family may be responsible for this, providing that this channel is endogenously expressed in the FRT cell line. As mentioned earlier, the small conductance calcium activated K^+ channel KCa2.3 has been shown to be recycled in epithelial cells (Gao *et al.*, 2010; Lin *et al.*, 2012).

5.4 Limitations

In this project, there were several limitations, which were minimised where possible. Of these limitations, perhaps the most prevalent was that the KCa3.1 activator, 1-EBIO, is not completely specific to KCa3.1, instead also activating the KCa3.1 relatives, KCa2.1, KCa2.2, and KCa2.3 (Pedarzani *et al.*, 2001), which appeared to cause a misleading change in the 1-EBIO sensitive current. While KCA2.3 is found in human thyroid tissue, a search of the NCBI Geo database revealed no evidence of

any of the KCa2.1, KCa2.2, or KCa2.3 channels being present in rat thyroid tissues. Additionally, no literature confirming either the presence or the absence of these channels in rat thyroid tissues was uncovered, therefore the presence of SK channels in rat thyroid tissue must be confirmed before this hypothesis can be examined. Another limitation for this project was streptavidin labelling KCa3.1-BLAP at the basolateral membrane when put onto the apical membrane, due to an incomplete epithelial monolayer, leading to false detection of KCa3.1 at the apical membrane, as shown in Figure 4.1. This limiting factor was minimised in the SNX27 and SNX1 experiment by measuring the apical membrane population of KCa3.1 in both the control and the SNX diminished cells, however this was not controlled for in the SNX4 experiment, and time was not permitting for this to be repeated.

Furthermore, it would have been prudent to reduce the amount of apical labelling of KCa3.1 in the sidedness experiments (Figure 4.1). This could have been completed in two ways. The first would have been to alter the original number of cells seeded onto the Transwell filters. By increasing the original number of cells onto the Transwell filter, cells will require less time to grow in order to form a confluent monolayer, ensuring that there were no gaps in the epithelial monolayer for streptavidin to move through. While this may have generated a confluent monolayer, seeding a higher number of cells may have reduced the cellular transfection efficiency as cells will have more surface area in contact with surrounding cells, ergo less contact with the surrounding media, which limits the ability of cells to take up the siRNA transfection. The second strategy would be similar to the first strategy; changing the cellular growth time. By increasing the time between seeding cells and cellular lysis, the cells will have more time to grow and ergo more likely to form a confluent monolayer. The final approach would be to use cells of a lower passage, as cells of a higher passage did not perform as well. However, by increasing growth time or initial seeding densities, the risk of overgrowing cells increases. FRT cells were observed forming domes by growing vertically once a confluent monolayer has been formed. The resulting cells may not be polarised, meaning that KCa3.1 is not localised to the basolateral membrane and would be able to be labelled at the apical membrane.

Finally, a major limitation for this project was the deterioration of the currents seen in the control traces between experiments. This can best be seen between the control traces between figures 4.6A and 4.8A. It is unknown why there was such variation in the control current, as under ideal conditions, the control current would have been identical each time. In order to minimise the problems this may cause, during analysis, the knockdown current was normalised to the control, allowing for any changes to be seen more accurately. It is possible that using DCEBIO, a stronger KCa3.1 channel opener that 1-EBIO, would have resulted in greater changes in current, allowing for more accurate results to be obtained.

Aside from these specific limitations, there were also more general limitations, such as background fluorescence in the immunoblots and oxidation occurring in the electrodes used for the Ussing chamber. Background fluorescence was minimised by using smaller amounts of Lumilight solution, which made excess Lumilight easier to drain off by touching the edges of the PVDF membrane to a paper towel before fluorescence was detected. While this reduced the prevalence of excess background fluorescence, one had to be careful to ensure that the whole PVDF membrane was covered in Lumilight solution in order to ensure that the experiment was accurate. The oxidation seen on the electrodes of the Ussing chamber was minimised in two ways. The first way was to ensure that the agar used to plug the end of the electrode was fresh when new electrodes were made, so that it would form an effective plug. The second way was to create new electrodes regularly, as the agar plugs in the electrodes degraded over time and with use. This helped to prevent electrodes from oxidising in the middle of an experiment, leading to electrodes being required to be remade, and extra, unnecessary errors being present.

Another limitation to this project was the use of only one cell line; Fischer rat thyroid cells. It is possible that results could vary if a different cell line was utilised, however due to time constraints, this was not possible. If time were not an issue, the use of multiple cell lines to confirm that findings were consistent would have been ideal.

5.5 Future directions

This study has left two main questions which need to be answered in order to completely understand the results gained. The first question is regarding the trend towards a significant increase in the apical membrane population of KCa3.1 in cells with less SNX27. As mentioned above, the possibility of KCa3.1 missorting to the apical membrane needs to be examined. This could be done in two parts; firstly using fluorescently tagged KCa3.1 to determine if any KCa3.1 is located in the apical membrane when SNX27 is diminished, and secondly performing immunoprecipitation experiments to determine if SNX27 and KCa3.1 interact. One problem experienced with this project regarding immunoprecipitation experiments was the inability to transfect cells with the *KCa3.1-HA* construct. I believe that this can be avoided by utilising the already available KCa3.1-BLAP present in FRT-KCa3.1-BLAP cells. By lysing the cells prior to labelling the membrane bound KCa3.1 with streptavidin, then incubating the lysis in the streptavidin solution, the intracellular KCa3.1-BLAP would be labelled. This would allow for any intracellular interactions between KCa3.1 and the Retromer proteins to be detected, even if the interaction has ceased when KCa3.1 gets to the membrane.

The second question I believe needs to be answered is regarding the increased change in 1-EBIO sensitive current compared to the change in the clotrimazole sensitive current. As mentioned

above, it appears that transfecting cells with any of the three SNX siRNAs used for this project resulted in an unknown protein being decreased, which lead to a significant decrease in the 1-EBIO sensitive current. I believe a strong contender for this is the KCa2.3 channel, which is related to KCa3.1, and is opened by 1-EBIO (Pedarzani *et al.*, 2001). KCa2.3 is present in human thyroid tissue (Fagerberg *et al.*, 2014), suggesting that it would be present in FRT cells, however no data has been published regarding this. I believe it would be prudent to examine if KCa2.3, or either of the other two small conductance calcium activated potassium channels (KCa2.1 or KCa2.2), are present in FRT-KCa3.1-BLAP cells. If any of these channels are present, it would be wise to inspect if the trafficking of these channels are affected by changes in retromer components, specifically the sorting nexin proteins used in this project.

In future, I believe that it would be beneficial to perform immunoblots measuring the cell surface levels of the β2-AR as a positive control to confirm that the retromer pathway has been interrupted. The β2-AR was not used in this project due to time constraints surrounding the ability to measure cell surface β2-AR. Additionally, the McDonald laboratory had previously shown measurable changes in ENaC when components of the Retromer complex were knocked down. This suggested that, not only were the individual components of the Retromer pathway were knocked down, but that the overall trafficking pathway was being interrupted.

Another experiment that I believe would be beneficial to perform in future is to look at the effect of Senicapoc; a KCa3.1 channel inhibitor, on the effect of KCa3.1 trafficking. Senicapoc has been proposed as a potential treatment for Sickle Cell Anaemia (Ataga et al., 2008). I believe it would be interesting to investigate if treating cells with Senicapoc, combined with Retromer knockdowns, could have an effect on surface levels of KCa3.1.

Aside from these experiments, which investigate the questions unanswered thus far by this project, I believe it would be beneficial to investigate several other factors. Primarily, it would be prudent to examine if decreasing the intracellular levels of multiple SNX proteins affects the basolateral membrane population of KCa3.1. Some Retromer proteins may be able to perform multiple roles if other proteins are knocked down, which would decrease any effects seen by knocking down that protein. In this project, SNX1 was knocked down, however, SNX2 plays a similar role to SNX1, and forms a complex with the same proteins as SNX1. Therefore, SNX2 may blunt the potential effects of knocking down SNX1. If both SNX1 and SNX2, or multiple other Retromer proteins were simultaneously knocked down, a change in the basolateral membrane population of KCa3.1 may emerge. However it would be important to follow these experiments with immunoprecipitation experiments. By immunoprecipitating KCa3.1 with the protein(s) knocked

down, it can be determined whether or not KCa3.1 has a direct interaction with these proteins, or if a detected change is due to a contaminating factor.

5.6 Conclusion

This project studied the effects of three sorting nexin proteins, SNX1, SNX4, and SNX27, on the membrane population of the intermediate conductance Ca^{2+} activated K^+ channel. SNX1, SNX4, and SNX27 were selected for this project as each of these sorting nexins had unique functions, however, are all linked closely to the Retromer pathway. Primarily, this project was the first to reveal endogenous expression of both SNX1 and SNX27 in Fischer Rat Thyroid cells, and was the first to present that the intracellular protein levels of SNX1 and SNX27 could be reduced by transfecting these FRT cells with either SNX1 or SNX27 siRNA. In order to measure the changes in the basolateral membrane population of KCa3.1 when SNX1, SNX4, or SNX27 protein levels were decreased, both immunoblot and Ussing chamber experiments were utilised. This proved my first hypothesis, that SNX1, SNX4, and SNX27 would be knocked down when FRT-KCa3.1-BLAP cells were transfected with SNX1, SNX4, or SNX27 siRNA, to be correct.

While my first hypothesis was correct, my second and third hypotheses; which stated that both the basolateral membrane population of KCa3.1 (second hypothesis) and the functionality of KCa3.1 as determined by the 1-EBIO and clotrimazole sensitive currents (third hypothesis) would be significantly reduced when one of SNX1, SNX4, or SNX27 were not proven correct. It was found that the basolateral membrane population of KCa3.1 was not significantly changed when cells were transfected with any of SNX1, SNX4, or SNX27 siRNA.

When the intracellular protein levels of either SNX1, SNX4, or SNX27 were reduced by siRNA transfection, a significant decrease in the 1-EBIO sensitive current was observed. This would suggest that the functional expression of KCa3.1 is reduced, however none of these transfections lead to a significant, or trended towards a significant decrease in the clotrimazole sensitive currents. This suggests that another factor was responsible for the change in the 1-EBIO sensitive current. I hypothesise that another member, or members of the KCNN gene family may be responsible for this. As mentioned earlier, the small conductance calcium activated K^+ channel KCa2.3 has been shown to be recycled in epithelial cells (Gao *et al.*, 2010; Lin *et al.*, 2012). These results are consistent with previous results suggesting the KCa3.1 is not recycled in nonmigratory cells (Gao *et al.*, 2010; Lin *et al.*, 2012). Additionally, these results suggest that none of SNX1, SNX4, or SNX27 are involved in the anterograde trafficking of KCa3.1 to the basolateral membrane.

As it appears that neither SNX1, SNX4, nor SNX27 are involved in the trafficking of KCa3.1 to the basolateral membrane, some specific trafficking routes seem less likely to be utilised by KCa3.1.

Both SNX1 and SNX4 form unique sorting tubules (Traer et al., 2007), which transport proteins to specific locations. As the basolateral membrane population of KCa3.1 did not significantly change when either SNX1 or SNX4 were downregulated, it is unlikely that KCa3.1 is trafficked by either the SNX1 or SNX4 sorting tubules. Furthermore, the possibility of KCa3.1 being transported through a sorting tubule by bulk flow through a SNX4 sorting tubule is also unlikely, as there would be fewer tubules when SNX4 was downregulated (Cohen & Pintavirooj, 2004). While there is no evidence that SNX27 forms sorting tubules, it appears unlikely that KCa3.1 is trafficked by either SNX27 or Fam21. Lee and collaborators (2016) found that SNX27 and Fam21 form a close interaction. In systems where the SNX27/Fam21 dimer are trafficking cargo, the cargo is sent along the lysosomal degradation pathway when SNX27 is removed (Lee et al., 2016). As there was no significant change in the basolateral membrane population of KCa3.1 when the intracellular levels of SNX27 were reduced, it is unlikely that Fam21 is involved in the trafficking of KCa3.1.

While these results appear conclusive, I believe that more research must be conducted on two areas; the effect of SNX27 on KCa3.1 missorting to the apical membrane, and determining the reason why downregulating each of SNX1, SNX4, and SNX27 lead to a significant decrease in the 1-EBIO sensitive current but not in the clotrimazole sensitive current. If SNX27 is indeed responsible, or partially responsible for the basolateral localisation of KCa3.1, then SNX27 could increase the number of therapeutic targets for diseases involving KCa3.1 dysfunction. Due to the prevalence of KCa3.1 in several disease states (Section 1.4.4), it is vital to understand exactly how KCa3.1 is trafficked both to and from the plasma membrane. By understanding exactly how KCa3.1 is trafficked to the plasma membrane, the number of channels present in the plasma membrane can be more accurately controlled in cells. Additionally, by knowing how KCa3.1 is trafficked from the plasma membrane, it may become apparent that KCa3.1 can be “rescued” from degradatory pathways, and recycled to the plasma membrane. Alternatively, understanding how KCa3.1 is trafficked from the plasma membrane may lead to therapies revolving around increasing how long KCa3.1 can remain in the plasma membrane.

As these results suggest that the Retromer pathway is not involved in the trafficking of KCa3.1 to the basolateral membrane, this project is inconsequential for clinical situations involving KCa3.1. Furthermore, as the Retromer pathway is still largely not understood, any therapeutic remedies involving Retromer must be intensively studied to ensure that no unforeseen trafficking side effects occur. In the search for novel medicines to treat diseases caused by KCa3.1, other trafficking routes must be investigated, however routes involving the Retromer pathway can be discounted.

References

Abcam. (2015). Electrophoresis for western blot. *http://wwwabcamcom/protocols/electrophoresis-for-western-blot.*

Abdullaev IF, Rudkouskaya A, Mongin AA & Kuo YH. (2010). Calcium-activated potassium channels BK and IK1 are functionally expressed in human gliomas but do not regulate cell proliferation. *PloS one* **5,** e12304.

Adefolaju GA, Theron KE & Hosie MJ. (2015). BAX/BCL-2 mRNA and protein expression in human breast MCF-7 cells exposed to drug vehicles-methanol and dimethyl sulfoxide (DMSO) for 24 hrs. *Nigerian Medical Journal : Journal of the Nigeria Medical Association* **56,** 169-174.

Al-Hazza A, Linley JE, Aziz Q, Maclennan KA, Hunter M & Sandle GI. (2012). Potential role of reduced basolateral potassium ($IK_{Ca}3.1$) channel expression in the pathogenesis of diarrhoea in ulcerative colitis. *The Journal of Pathology* **226,** 463-470.

Aleksandrov AA & Riordan JR. (1998). Regulation of CFTR ion channel gating by MgATP. *FEBS letters* **431,** 97-101.

Aleksic I, Ren M, Czer LS, Freimark D, Dalichau H, Blanche C, Trento A & Barath P. (1996). Liposome-mediated transfer of genes containing HLA-class II alpha chain into cultured embryonic chick cardiac myocytes and COS7 cells. *The Thoracic and Cardiovascular Surgeon* **44,** 81-85.

Amasheh S, Barmeyer C, Koch CS, Tavalali S, Mankertz J, Epple HJ, Gehring MM, Florian P, Kroesen AJ, Zeitz M, Fromm M & Schulzke JD. (2004). Cytokine-dependent transcriptional down-regulation of epithelial sodium channel in ulcerative colitis. *Gastroenterology* **126,** 1711-1720.

Anderson KR, Sutton MG & Lie JT. (1979). Histopathological types of cardiac fibrosis in myocardial disease. *The Journal of Pathology* **128,** 79-85.

Andolfo I, Alper SL, De Franceschi L, Auriemma C, Russo R, De Falco L, Vallefuoco F, Esposito MR, Vandorpe DH, Shmukler BE, Narayan R, Montanaro D, D'Armiento M, Vetro A, Limongelli I, Zuffardi O, Glader BE, Schrier SL, Brugnara C, Stewart GW, Delaunay J & Iolascon A. (2013). Multiple clinical forms of dehydrated hereditary stomatocytosis arise from mutations in PIEZO1. *Blood* **121,** 3925-3935, s3921-3912.

Apodaca G, Gallo LI & Bryant DM. (2012). Role of membrane traffic in the generation of epithelial cell asymmetry. *Nature Cell Biology* **14,** 1235-1243.

Arighi CN, Hartnell LM, Aguilar RC, Haft CR & Bonifacino JS. (2004). Role of the mammalian retromer in sorting of the cation-independent mannose 6-phosphate receptor. *The Journal of Cell Biology* **165,** 123-133.

Ataga KI, Smith WR, De Castro LM, Swerdlow P, Saunthararajah Y, Castro O, Vichinsky E, Kutlar A, Orringer EP, Rigdon GC & Stocker JW. (2008). Efficacy and safety of the Gardos channel blocker, senicapoc (ICA-17043), in patients with sickle cell anemia. Blood 111, 3991-3997

Babbey CM, Ahktar N, Wang E, Chen CC, Grant BD & Dunn KW. (2006). Rab10 regulates membrane transport through early endosomes of polarized Madin-Darby canine kidney cells. *Molecular Biology of the Cell* **17,** 3156-3175.

Bahia PK, Suzuki R, Benton DC, Jowett AJ, Chen MX, Trezise DJ, Dickenson AH & Moss GW. (2005). A functional role for small-conductance calcium-activated potassium channels in sensory pathways including nociceptive processes. *The Journal of Neuroscience : the official journal of the Society for Neuroscience* **25,** 3489-3498.

Balana B, Maslennikov I, Kwiatkowski W, Stern KM, Bahima L, Choe S & Slesinger PA. (2011). Mechanism underlying selective regulation of G protein-gated inwardly rectifying potassium channels by the psychostimulant-sensitive sorting nexin 27. *Proceedings of the National Academy of Sciences of the United States of America* **108,** 5831-5836.

Balut CM, Gao Y, Murray SA, Thibodeau PH & Devor DC. (2010). ESCRT-dependent targeting of plasma membrane localized KCa3.1 to the lysosomes. *American Journal of Physiology Cell Physiology* **299,** C1015-1027.

Banerjee I, Yekkala K, Borg TK & Baudino TA. (2006). Dynamic interactions between myocytes, fibroblasts, and extracellular matrix. *Annals of the New York Academy of Sciences* **1080,** 76-84.

Barlowe C, Orci L, Yeung T, Hosobuchi M, Hamamoto S, Salama N, Rexach MF, Ravazzola M, Amherdt M & Schekman R. (1994). COPII: a membrane coat formed by Sec proteins that drive vesicle budding from the endoplasmic reticulum. *Cell* **77,** 895-907.

Barrett JN, Magleby KL & Pallotta BS. (1982). Properties of single calcium-activated potassium channels in cultured rat muscle. *The Journal of Physiology* **331,** 211-230.

Bartuzi P, Billadeau DD, Favier R, Rong S, Dekker D, Fedoseienko A, Fieten H, Wijers M, Levels JH, Huijkman N, Kloosterhuis N, van der Molen H, Brufau G, Groen AK, Elliott AM, Kuivenhoven JA, Plecko B, Grangl G, McGaughran J, Horton JD, Burstein E, Hofker MH & van de Sluis B. (2016). CCC- and WASH-mediated endosomal sorting of LDLR is required for normal clearance of circulating LDL. *Nature Communications* **7,** 10961.

Bertuccio CA, Lee SL, Wu G, Butterworth MB, Hamilton KL & Devor DC. (2014). Anterograde trafficking of KCa3.1 in polarized epithelia is Rab1- and Rab8-dependent and recycling endosome-independent. *PloS One* **9,** e92013.

Boettger MK, Till S, Chen MX, Anand U, Otto WR, Plumpton C, Trezise DJ, Tate SN, Bountra C, Coward K, Birch R & Anand P. (2002). Calcium-activated potassium channel SK1- and IK1-like

immunoreactivity in injured human sensory neurones and its regulation by neurotrophic factors. *Brain : a Journal of Neurology* **125,** 252-263.

Bonifacino JS & Dell'Angelica EC. (1999). Molecular bases for the recognition of tyrosine-based sorting signals. *The Journal of Cell Biology* **145,** 923-926.

Brown DA, Crise B & Rose JK. (1989). Mechanism of membrane anchoring affects polarized expression of two proteins in MDCK cells. *Science (New York, NY)* **245,** 1499-1501.

Brugnara C, de Franceschi L & Alper SL. (1993). Inhibition of Ca^{2+}-dependent K^+ transport and cell dehydration in sickle erythrocytes by clotrimazole and other imidazole derivatives. *The Journal of Clinical Investigation* **92,** 520-526.

Bryant DM, Kerr MC, Hammond LA, Joseph SR, Mostov KE, Teasdale RD & Stow JL. (2007). EGF induces macropinocytosis and SNX1-modulated recycling of E-cadherin. *Journal of Cell Science* **120,** 1818-1828.

Bujny MV, Popoff V, Johannes L & Cullen PJ. (2007). The retromer component sorting nexin-1 is required for efficient retrograde transport of Shiga toxin from early endosome to the trans Golgi network. Journal of cell science 120, 2010-2021.

Bulk E, Ay AS, Hammadi M, Ouadid-Ahidouch H, Schelhaas S, Hascher A, Rohde C, Thoennissen NH, Wiewrodt R, Schmidt E, Marra A, Hillejan L, Jacobs AH, Klein HU, Dugas M, Berdel WE, Muller-Tidow C & Schwab A. (2015). Epigenetic dysregulation of KCa 3.1 channels induces poor prognosis in lung cancer. *International Journal of Cancer* **137,** 1306-1317.

Cameron B & Landreth GE. (2010). Inflammation, microglia, and Alzheimer's disease. *Neurobiology of Disease* **37,** 503-509.

Carlton J, Bujny M, Peter BJ, Oorschot VM, Rutherford A, Mellor H, Klumperman J, McMahon HT & Cullen PJ. (2004). Sorting nexin-1 mediates tubular endosome-to-TGN transport through coincidence sensing of high- curvature membranes and 3-phosphoinositides. *Current Biology : CB* **14,** 1791-1800.

Carlton JG, Bujny MV, Peter BJ, Oorschot VM, Rutherford A, Arkell RS, Klumperman J, McMahon HT & Cullen PJ. (2005). Sorting nexin-2 is associated with tubular elements of the early endosome, but is not essential for retromer-mediated endosome-to-TGN transport. *Journal of Cell Science* **118,** 4527-4539.

Chabrillat ML, Wilhelm C, Wasmeier C, Sviderskaya EV, Louvard D & Coudrier E. (2005). Rab8 regulates the actin-based movement of melanosomes. *Molecular Biology of the Cell* **16,** 1640-1650.

Chankova SG, Dimova E, Dimitrova M & Bryant PE. (2007). Induction of DNA double-strand breaks by zeocin in Chlamydomonas reinhardtii and the role of increased DNA double-strand breaks

rejoining in the formation of an adaptive response. *Radiation and Environmental Biophysics* **46,** 409-416.

Chen D, Xiao H, Zhang K, Wang B, Gao Z, Jian Y, Qi X, Sun J, Miao L & Yang C. (2010). Retromer is required for apoptotic cell clearance by phagocytic receptor recycling. *Science (New York, NY)* **327,** 1261-1264.

Chen I, Howarth M, Lin W & Ting AY. (2005). Site-specific labeling of cell surface proteins with biophysical probes using biotin ligase. *Nature Methods* **2,** 99-104.

Chen W, Feng Y, Chen D & Wandinger-Ness A. (1998). Rab11 is required for trans-golgi network-to-plasma membrane transport and a preferential target for GDP dissociation inhibitor. *Molecular Biology of the Cell* **9,** 3241-3257.

Chen YJ, Wallace BK, Yuen N, Jenkins DP, Wulff H & O'Donnell ME. (2015). Blood-brain barrier KCa3.1 channels: evidence for a role in brain Na uptake and edema in ischemic stroke. *Stroke* **46,** 237-244.

Chishti AH, Kim AC, Marfatia SM, Lutchman M, Hanspal M, Jindal H, Liu SC, Low PS, Rouleau GA, Mohandas N, Chasis JA, Conboy JG, Gascard P, Takakuwa Y, Huang SC, Benz EJ, Jr., Bretscher A, Fehon RG, Gusella JF, Ramesh V, Solomon F, Marchesi VT, Tsukita S, Tsukita S, Hoover KB & et al. (1998). The FERM domain: a unique module involved in the linkage of cytoplasmic proteins to the membrane. Trends in biochemical sciences 23, 281-282.

Cohen FS & Pintavirooj C. (2004). Invariant surface alignment in the presence of affine and some nonlinear transformations. *Medical Image Analysis* **8,** 151-164.

Coleman SH, Madrid R, Van Damme N, Mitchell RS, Bouchet J, Servant C, Pillai S, Benichou S & Guatelli JC. (2006). Modulation of cellular protein trafficking by human immunodeficiency virus type 1 Nef: role of the acidic residue in the ExxxLL motif. *Journal of Virology* **80,** 1837-1849.

Collins BM, Norwood SJ, Kerr MC, Mahony D, Seaman MN, Teasdale RD & Owen DJ. (2008). Structure of Vps26B and mapping of its interaction with the retromer protein complex. *Traffic (Copenhagen, Denmark)* **9,** 366-379.

Collins BM, Skinner CF, Watson PJ, Seaman MN & Owen DJ. (2005). Vps29 has a phosphoesterase fold that acts as a protein interaction scaffold for retromer assembly. *Nature Structural & Molecular Biology* **12,** 594-602.

Cullen PJ. (2008). Endosomal sorting and signalling: an emerging role for sorting nexins. *Nature Reviews Molecular Cell Biology* **9,** 574-582.

Dalgaard OZ. (1957). Bilateral polycystic disease of the kidneys; a follow-up of 284 patients and their families. *Danish Medical Bulletin* **4,** 128-133.

Day CA, Baetz NW, Copeland CA, Kraft LJ, Han B, Tiwari A, Drake KR, De Luca H, Chinnapen DJ, Davidson MW, Holmes RK, Jobling MG, Schroer TA, Lencer WI & Kenworthy AK. (2015). Microtubule motors power plasma membrane tubulation in clathrin-independent endocytosis. *Traffic (Copenhagen, Denmark)* **16,** 572-590.

De Franceschi L, Saadane N, Trudel M, Alper SL, Brugnara C & Beuzard Y. (1994). Treatment with oral clotrimazole blocks Ca^{2+}-activated K^+ transport and reverses erythrocyte dehydration in transgenic SAD mice. A model for therapy of sickle cell disease. *The Journal of Clinical Investigation* **93,** 1670-1676.

Deborde S, Perret E, Gravotta D, Deora A, Salvarezza S, Schreiner R & Rodriguez-Boulan E. (2008). Clathrin is a key regulator of basolateral polarity. *Nature* **452,** 719-723.

Deora AA, Gravotta D, Kreitzer G, Hu J, Bok D & Rodriguez-Boulan E. (2004). The basolateral targeting signal of CD147 (EMMPRIN) consists of a single leucine and is not recognized by retinal pigment epithelium. *Molecular Biology of the Cell* **15,** 4148-4165.

Derivery E & Gautreau A. (2010). Evolutionary conservation of the WASH complex, an actin polymerization machine involved in endosomal fission. *Communicative & Integrative biology* **3,** 227-230.

Derivery E, Sousa C, Gautier JJ, Lombard B, Loew D & Gautreau A. (2009). The Arp2/3 activator WASH controls the fission of endosomes through a large multiprotein complex. *Developmental Cell* **17,** 712-723.

Devor DC, Singh AK, Frizzell RA & Bridges RJ. (1996). Modulation of Cl^- secretion by benzimidazolones. I. Direct activation of a Ca^{2+}-dependent K^+ channel. *The American Journal of Physiology* **271,** L775-784.

Devor DC, Singh AK, Gerlach AC, Frizzell RA & Bridges RJ. (1997). Inhibition of intestinal Cl^- secretion by clotrimazole: direct effect on basolateral membrane K^+ channels. *The American Journal of Physiology* **273,** C531-540.

Dong C, Yang L, Zhang X, Gu H, Lam ML, Claycomb WC, Xia H & Wu G. (2010). Rab8 interacts with distinct motifs in alpha2B- and beta2-adrenergic receptors and differentially modulates their transport. *The Journal of Biological Chemistry* **285,** 20369-20380.

Dong G, Hutagalung AH, Fu C, Novick P & Reinisch KM. (2005). The structures of exocyst subunit Exo70p and the Exo84p C-terminal domains reveal a common motif. *Nature Structural & Molecular Biology* **12,** 1094-1100.

Doray B, Lee I, Knisely J, Bu G & Kornfeld S. (2007). The gamma/sigma1 and alpha/sigma2 hemicomplexes of clathrin adaptors AP-1 and AP-2 harbor the dileucine recognition site. *Molecular Biology of the Cell* **18,** 1887-1896.

Durham AC. (1983). A survey of readily available chelators for buffering calcium ion concentrations in physiological solutions. *Cell Calcium* **4,** 33-46.

Eaton WA & Hofrichter J. (1987). Hemoglobin S gelation and sickle cell disease. *Blood* **70,** 1245-1266.

Ehrenfeld GM, Shipley JB, Heimbrook DC, Sugiyama H, Long EC, van Boom JH, van der Marel GA, Oppenheimer NJ & Hecht SM. (1987). Copper-dependent cleavage of DNA by bleomycin. *Biochemistry* **26,** 931-942.

El Khoury J, Toft M, Hickman SE, Means TK, Terada K, Geula C & Luster AD. (2007). Ccr2 deficiency impairs microglial accumulation and accelerates progression of Alzheimer-like disease. *Nature Medicine* **13,** 432-438.

Ellgaard L & Helenius A. (2003). Quality control in the endoplasmic reticulum. *Nature reviews Molecular Cell Biology* **4,** 181-191.

Engbers JD, Anderson D, Asmara H, Rehak R, Mehaffey WH, Hameed S, McKay BE, Kruskic M, Zamponi GW & Turner RW. (2012). Intermediate conductance calcium-activated potassium channels modulate summation of parallel fiber input in cerebellar Purkinje cells. *Proceedings of the National Academy of Sciences of the United States of America* **109,** 2601-2606.

Espira L & Czubryt MP. (2009). Emerging concepts in cardiac matrix biology. *Canadian Journal of Physiology and Pharmacology* **87,** 996-1008.

Fagerberg L, Hallstrom BM, Oksvold P, Kampf C, Djureinovic D, Odeberg J, Habuka M, Tahmasebpoor S, Danielsson A, Edlund K, Asplund A, Sjostedt E, Lundberg E, Szigyarto CA, Skogs M, Takanen JO, Berling H, Tegel H, Mulder J, Nilsson P, Schwenk JM, Lindskog C, Danielsson F, Mardinoglu A, Sivertsson A, von Feilitzen K, Forsberg M, Zwahlen M, Olsson I, Navani S, Huss M, Nielsen J, Ponten F & Uhlen M. (2014). Analysis of the human tissue-specific expression by genome-wide integration of transcriptomics and antibody-based proteomics. *Molecular & Cellular Proteomics : MCP* **13,** 397-406.

Fanger CM, Ghanshani S, Logsdon NJ, Rauer H, Kalman K, Zhou J, Beckingham K, Chandy KG, Cahalan MD & Aiyar J. (1999). Calmodulin mediates calcium-dependent activation of the intermediate conductance KCa channel, $IK_{Ca}1$. *The Journal of Biological Chemistry* **274,** 5746-5754.

Farquhar MG & Palade GE. (1963). Junctional complexes in various epithelia. *The Journal of Cell Biology* **17,** 375-412.

Farquhar RE, Rodrigues E & Hamilton KL. (2017). The Role of the Cytoskeleton and Myosin-Vc in the Targeting of KCa3.1 to the Basolateral Membrane of Polarized Epithelial Cells. *Frontiers in Physiology* **7,** 639.

Felgner PL, Gadek TR, Holm M, Roman R, Chan HW, Wenz M, Northrop JP, Ringold GM & Danielsen M. (1987). Lipofection: a highly efficient, lipid-mediated DNA-transfection procedure. *Proceedings of the National Academy of Sciences of the United States of America* **84,** 7413-7417.

Fjorback AW, Seaman M, Gustafsen C, Mehmedbasic A, Gokool S, Wu C, Militz D, Schmidt V, Madsen P, Nyengaard JR, Willnow TE, Christensen EI, Mobley WB, Nykjaer A & Andersen OM. (2012). Retromer binds the FANSHY sorting motif in SorLA to regulate amyloid precursor protein sorting and processing. *The Journal of Neuroscience : the official journal of the Society for Neuroscience* **32,** 1467-1480.

Frost A, Perera R, Roux A, Spasov K, Destaing O, Egelman EH, De Camilli P & Unger VM. (2008). Structural basis of membrane invagination by F-BAR domains. *Cell* **132,** 807-817.

Fujita H, Tuma PL, Finnegan CM, Locco L & Hubbard AL. (1998). Endogenous syntaxins 2, 3 and 4 exhibit distinct but overlapping patterns of expression at the hepatocyte plasma membrane. *The Biochemical Journal* **329 (Pt 3),** 527-538.

Fuller SD, Bravo R & Simons K. (1985). An enzymatic assay reveals that proteins destined for the apical or basolateral domains of an epithelial cell line share the same late Golgi compartments. *The EMBO Journal* **4,** 297-307.

Gallon M, Clairfeuille T, Steinberg F, Mas C, Ghai R, Sessions RB, Teasdale RD, Collins BM & Cullen PJ. (2014). A unique PDZ domain and arrestin-like fold interaction reveals mechanistic details of endocytic recycling by SNX27-retromer. *Proceedings of the National Academy of Sciences of the United States of America* **111,** E3604-3613.

Ganguli NC. (1956). A quantitative method for the estimation of serum proteins by paper disk electrophoresis. *Clinica Chimica Acta; International Journal of Clinical Chemistry* **1,** 413-416.

Gao Y, Balut CM, Bailey MA, Patino-Lopez G, Shaw S & Devor DC. (2010). Recycling of the Ca^{2+}-activated K^{+} channel, KCa2.3, is dependent upon RME-1, Rab35/EPI64C, and an N-terminal domain. *The Journal of Biological Chemistry* **285,** 17938-17953.

Gardos G. (1958). The function of calcium in the potassium permeability of human erythrocytes. *Biochimica et Biophysica Acta* **30,** 653-654.

Gassama-Diagne A, Yu W, ter Beest M, Martin-Belmonte F, Kierbel A, Engel J & Mostov K. (2006). Phosphatidylinositol-3,4,5-trisphosphate regulates the formation of the basolateral plasma membrane in epithelial cells. *Nature Cell Biology* **8,** 963-970.

Gerlach AC, Syme CA, Giltinan L, Adelman JP & Devors DC. (2001). ATP-dependent activation of the intermediate conductance, Ca^{2+}-activated K^{+} channel, hIK1, is conferred by a C-terminal domain. *The Journal of Biological Chemistry* **276,** 10963-10970.

Geyer M, Fackler OT & Peterlin BM. (2002). Subunit H of the V-ATPase involved in endocytosis shows homology to beta-adaptins. *Molecular Biology of the Cell* **13,** 2045-2056.

Gibson JS, Speake PF & Ellory JC. (1998). Differential oxygen sensitivity of the K^+-Cl^- cotransporter in normal and sickle human red blood cells. *The Journal of Physiology* **511 (Pt 1),** 225-234.

Glogowska E, Lezon-Geyda K, Maksimova Y, Schulz VP & Gallagher PG. (2015). Mutations in the Gardos channel (KCNN4) are associated with hereditary xerocytosis. *Blood* **126,** 1281-1284.

Gluzman Y. (1981). SV40-transformed simian cells support the replication of early SV40 mutants. *Cell* **23,** 175-182.

Gomez TS & Billadeau DD. (2009). A FAM21-containing WASH complex regulates retromer-dependent sorting. *Developmental Cell* **17,** 699-711.

Gomez TS, Gorman JA, Artal-Martinez de Narvajas A, Koenig AO & Billadeau DD. (2012). Trafficking defects in WASH-knockout fibroblasts originate from collapsed endosomal and lysosomal networks. *Molecular Biology of the Cell* **23,** 3215-3228.

Greig ER, Boot-Handford RP, Mani V & Sandle GI. (2004). Decreased expression of apical Na^+ channels and basolateral Na^+, K^+-ATPase in ulcerative colitis. *The Journal of Pathology* **204,** 84-92.

Grgic I, Kiss E, Kaistha BP, Busch C, Kloss M, Sautter J, Muller A, Kaistha A, Schmidt C, Raman G, Wulff H, Strutz F, Grone HJ, Kohler R & Hoyer J. (2009). Renal fibrosis is attenuated by targeted disruption of KCa3.1 potassium channels. *Proceedings of the National Academy of Sciences of the United States of America* **106,** 14518-14523.

Griffin CT, Trejo J & Magnuson T. (2005). Genetic evidence for a mammalian retromer complex containing sorting nexins 1 and 2. *Proceedings of the National Academy of Sciences of the United States of America* **102,** 15173-15177.

Grindstaff KK, Yeaman C, Anandasabapathy N, Hsu SC, Rodriguez-Boulan E, Scheller RH & Nelson WJ. (1998). Sec6/8 complex is recruited to cell-cell contacts and specifies transport vesicle delivery to the basal-lateral membrane in epithelial cells. *Cell* **93,** 731-740.

Gross JL, de Azevedo MJ, Silveiro SP, Canani LH, Caramori ML & Zelmanovitz T. (2005). Diabetic nephropathy: diagnosis, prevention, and treatment. *Diabetes Care* **28,** 164-176.

Guezguez B, Vigneron P, Alais S, Jaffredo T, Gavard J, Mege RM & Dunon D. (2006). A dileucine motif targets MCAM-l cell adhesion molecule to the basolateral membrane in MDCK cells. *FEBS Letters* **580,** 3649-3656.

Guo W, Roth D, Walch-Solimena C & Novick P. (1999). The exocyst is an effector for Sec4p, targeting secretory vesicles to sites of exocytosis. *The EMBO Journal* **18,** 1071-1080.

Guo W, Sacher M, Barrowman J, Ferro-Novick S & Novick P. (2000). Protein complexes in transport vesicle targeting. *Trends in Cell Biology* **10,** 251-255.

Hakomori S & Handa K. (2002). Glycosphingolipid-dependent cross-talk between glycosynapses interfacing tumor cells with their host cells: essential basis to define tumor malignancy. *FEBS Letters* **531,** 88-92.

Harbour ME, Breusegem SY, Antrobus R, Freeman C, Reid E & Seaman MN. (2010). The cargo-selective retromer complex is a recruiting hub for protein complexes that regulate endosomal tubule dynamics. *Journal of Cell Science* **123,** 3703-3717.

Harbour ME, Breusegem SY & Seaman MN. (2012). Recruitment of the endosomal WASH complex is mediated by the extended 'tail' of Fam21 binding to the retromer protein Vps35. *The Biochemical Journal* **442,** 209-220.

Harris PC. (2006). Genetic studies: a key to understanding pathogenesis in PKD. *Nephrology News & Issues* **20,** 20-22.

Hasenfuss G. (1998). Animal models of human cardiovascular disease, heart failure and hypertrophy. *Cardiovascular Research* **39,** 60-76.

Helfer E, Harbour ME, Henriot V, Lakisic G, Sousa-Blin C, Volceanov L, Seaman MN & Gautreau A. (2013). Endosomal recruitment of the WASH complex: active sequences and mutations impairing interaction with the retromer. *Biology of the Cell* **105,** 191-207.

Hierro A, Rojas AL, Rojas R, Murthy N, Effantin G, Kajava AV, Steven AC, Bonifacino JS & Hurley JH. (2007). Functional architecture of the retromer cargo-recognition complex. *Nature* **449,** 1063-1067.

Hirtz D, Thurman DJ, Gwinn-Hardy K, Mohamed M, Chaudhuri AR & Zalutsky R. (2007). How common are the "common" neurologic disorders? *Neurology* **68,** 326-337.

Hoffman JF, Joiner W, Nehrke K, Potapova O, Foye K & Wickrema A. (2003). The hSK4 (KCNN4) isoform is the Ca^{2+}-activated K^{+} channel (Gardos channel) in human red blood cells. *Proceedings of the National Academy of Sciences of the United States of America* **100,** 7366-7371.

Horazdovsky BF, Davies BA, Seaman MN, McLaughlin SA, Yoon S & Emr SD. (1997). A sorting nexin-1 homologue, Vps5p, forms a complex with Vps17p and is required for recycling the vacuolar protein-sorting receptor. *Molecular Biology of the Cell* **8,** 1529-1541.

Hsu SC, Hazuka CD, Roth R, Foletti DL, Heuser J & Scheller RH. (1998). Subunit composition, protein interactions, and structures of the mammalian brain sec6/8 complex and septin filaments. *Neuron* **20,** 1111-1122.

Hsu SC, Ting AE, Hazuka CD, Davanger S, Kenny JW, Kee Y & Scheller RH. (1996). The mammalian brain rsec6/8 complex. *Neuron* **17,** 1209-1219.

Ishii TM, Silvia C, Hirschberg B, Bond CT, Adelman JP & Maylie J. (1997). A human intermediate conductance calcium-activated potassium channel. *Proceedings of the National Academy of Sciences of the United States of America* **94,** 11651-11656.

Isoyama S & Nitta-Komatsubara Y. (2002). Acute and chronic adaptation to hemodynamic overload and ischemia in the aged heart. *Heart Failure Reviews* **7,** 63-69.

Jackson LP, Kelly BT, McCoy AJ, Gaffry T, James LC, Collins BM, Honing S, Evans PR & Owen DJ. (2010). A large-scale conformational change couples membrane recruitment to cargo binding in the AP2 clathrin adaptor complex. *Cell* **141,** 1220-1229.

Jacobs DT, Weigert R, Grode KD, Donaldson JG & Cheney RE. (2009). Myosin Vc is a molecular motor that functions in secretory granule trafficking. *Molecular Biology of the Cell* **20,** 4471-4488.

Jia D, Gomez TS, Billadeau DD & Rosen MK. (2012). Multiple repeat elements within the FAM21 tail link the WASH actin regulatory complex to the retromer. *Molecular Biology of the Cell* **23,** 2352-2361.

Jia D, Gomez TS, Metlagel Z, Umetani J, Otwinowski Z, Rosen MK & Billadeau DD. (2010). WASH and WAVE actin regulators of the Wiskott-Aldrich syndrome protein (WASP) family are controlled by analogous structurally related complexes. *Proceedings of the National Academy of Sciences of the United States of America* **107,** 10442-10447.

Jiang Y, Lee A, Chen J, Cadene M, Chait BT & MacKinnon R. (2002). Crystal structure and mechanism of a calcium-gated potassium channel. *Nature* **417,** 515-522.

Jiang Y, Lee A, Chen J, Ruta V, Cadene M, Chait BT & MacKinnon R. (2003). X-ray structure of a voltage-dependent K^+ channel. *Nature* **423,** 33-41.

Joiner WJ, Wang LY, Tang MD & Kaczmarek LK. (1997). hSK4, a member of a novel subfamily of calcium-activated potassium channels. *Proceedings of the National Academy of Sciences of the United States of America* **94,** 11013-11018.

Jones HM, Hamilton KL & Devor DC. (2005). Role of an S4-S5 linker lysine in the trafficking of the Ca^{2+}-activated K^+ channels IK1 and SK3. *The Journal of Biological Chemistry* **280,** 37257-37265.

Jones HM, Hamilton KL, Papworth GD, Syme CA, Watkins SC, Bradbury NA & Devor DC. (2004). Role of the NH2 terminus in the assembly and trafficking of the intermediate conductance Ca^{2+}-activated K^{+} channel hIK1. *The Journal of Biological CShemistry* **279,** 15531-15540.

Joyce CR. (1958). Uptake of potassium and sodium by parts of packed human blood cell column. *Quarterly Journal of Experimental Physiology and Cognate Medical Sciences* **43,** 299-309.

Kajii Y, Muraoka S, Hiraoka S, Fujiyama K, Umino A & Nishikawa T. (2003). A developmentally regulated and psychostimulant-inducible novel rat gene mrt1 encoding PDZ-PX proteins isolated in the neocortex. *Molecular Psychiatry* **8,** 434-444.

Kanwar YS, Wada J, Sun L, Xie P, Wallner EI, Chen S, Chugh S & Danesh FR. (2008). Diabetic nephropathy: mechanisms of renal disease progression. *Experimental Biology and Medicine (Maywood, NJ)* **233,** 4-11.

Kelly AE, Kranitz H, Dotsch V & Mullins RD. (2006). Actin binding to the central domain of WASP/Scar proteins plays a critical role in the activation of the Arp2/3 complex. *The Journal of Biological Chemistry* **281,** 10589-10597.

Kenworthy AK & Edidin M. (1998). Distribution of a glycosylphosphatidylinositol-anchored protein at the apical surface of MDCK cells examined at a resolution of <100 A using imaging fluorescence resonance energy transfer. *The Journal of Cell Biology* **142,** 69-84.

Klein H, Garneau L, Banderali U, Simoes M, Parent L & Sauve R. (2007). Structural determinants of the closed KCa3.1 channel pore in relation to channel gating: results from a substituted cysteine accessibility analysis. *The Journal of General Physiology* **129,** 299-315.

Klumperman J, Schweizer A, Clausen H, Tang BL, Hong W, Oorschot V & Hauri HP. (1998). The recycling pathway of protein ERGIC-53 and dynamics of the ER-Golgi intermediate compartment. *Journal of Cell Science* **111 (Pt 22),** 3411-3425.

Kohler M, Hirschberg B, Bond CT, Kinzie JM, Marrion NV, Maylie J & Adelman JP. (1996). Small-conductance, calcium-activated potassium channels from mammalian brain. *Science (New York, NY)* **273,** 1709-1714.

Kurzban GP, Gitlin G, Bayer EA, Wilchek M & Horowitz PM. (1990). Biotin binding changes the conformation and decreases tryptophan accessibility of streptavidin. *Journal of Protein Chemistry* **9,** 673-682.

Lafont F, Lecat S, Verkade P & Simons K. (1998). Annexin XIIIb associates with lipid microdomains to function in apical delivery. *The Journal of Cell Biology* **142,** 1413-1427.

Lafont F, Verkade P, Galli T, Wimmer C, Louvard D & Simons K. (1999). Raft association of SNAP receptors acting in apical trafficking in Madin-Darby canine kidney cells. *Proceedings of the National Academy of Sciences of the United States of America* **96,** 3734-3738.

Langevin J, Morgan MJ, Sibarita JB, Aresta S, Murthy M, Schwarz T, Camonis J & Bellaiche Y. (2005). Drosophila exocyst components Sec5, Sec6, and Sec15 regulate DE-Cadherin trafficking from recycling endosomes to the plasma membrane. *Developmental Cell* **9,** 365-376.

Lauf PK, Bauer J, Adragna NC, Fujise H, Zade-Oppen AM, Ryu KH & Delpire E. (1992). Erythrocyte K-Cl cotransport: properties and regulation. *The American Journal of Physiology* **263,** C917-932.

Lauffer BE, Melero C, Temkin P, Lei C, Hong W, Kortemme T & von Zastrow M. (2010). SNX27 mediates PDZ-directed sorting from endosomes to the plasma membrane. *The Journal of Cell Biology* **190,** 565-574.

Lee S, Chang J & Blackstone C. (2016). FAM21 directs SNX27-retromer cargoes to the plasma membrane by preventing transport to the Golgi apparatus. *Nature Communications* **7,** 10939.

Lee WS, Ngo-Anh TJ, Bruening-Wright A, Maylie J & Adelman JP. (2003). Small conductance Ca^{2+}-activated K^{+} channels and calmodulin: cell surface expression and gating. *The Journal of Biological Chemistry* **278,** 25940-25946.

Lew VL & Bookchin RM. (2005). Ion transport pathology in the mechanism of sickle cell dehydration. *Physiological Reviews* **85,** 179-200.

Li J, Callaway DJ & Bu Z. (2009). Ezrin induces long-range interdomain allostery in the scaffolding protein NHERF1. Journal of molecular biology 392, 166-180.

Lin MT, Adelman JP & Maylie J. (2012). Modulation of endothelial SK3 channel activity by Ca^{2+}-dependent caveolar trafficking. *American Journal of Physiology Cell Physiology* **303,** C318-327.

Lipschutz JH, Guo W, O'Brien LE, Nguyen YH, Novick P & Mostov KE. (2000). Exocyst is involved in cystogenesis and tubulogenesis and acts by modulating synthesis and delivery of basolateral plasma membrane and secretory proteins. *Molecular Biology of the Cell* **11,** 4259-4275.

Lisanti MP, Caras IW, Davitz MA & Rodriguez-Boulan E. (1989). A glycophospholipid membrane anchor acts as an apical targeting signal in polarized epithelial cells. *The Journal of Cell Biology* **109,** 2145-2156.

Liu Y, Zhao L, Ma W, Cao X, Chen H, Feng D, Liang J, Yin K & Jiang X. (2015). The Blockage of KCa3.1 Channel Inhibited Proliferation, Migration and Promoted Apoptosis of Human Hepatocellular Carcinoma Cells. *Journal of Cancer* **6,** 643-651.

Lunn ML, Nassirpour R, Arrabit C, Tan J, McLeod I, Arias CM, Sawchenko PE, Yates JR, 3rd & Slesinger PA. (2007). A unique sorting nexin regulates trafficking of potassium channels via a PDZ domain interaction. *Nature Neuroscience* **10,** 1249-1259.

Luo G, Zhang J & Guo W. (2014). The role of Sec3p in secretory vesicle targeting and exocyst complex assembly. *Molecular Biology of the Cell* **25,** 3813-3822.

Machesky LM, Mullins RD, Higgs HN, Kaiser DA, Blanchoin L, May RC, Hall ME & Pollard TD. (1999). Scar, a WASp-related protein, activates nucleation of actin filaments by the Arp2/3 complex. *Proceedings of the National Academy of Sciences of the United States of America* **96,** 3739-3744.

MacKinnon R. (2003). Potassium channels. *FEBS letters* **555,** 62-65.

Madara JL. (1998). Regulation of the movement of solutes across tight junctions. *Annual Review of Physiology* **60,** 143-159.

Madrid R, Le Maout S, Barrault MB, Janvier K, Benichou S & Merot J. (2001). Polarized trafficking and surface expression of the AQP4 water channel are coordinated by serial and regulated interactions with different clathrin-adaptor complexes. *The EMBO Journal* **20,** 7008-7021.

Maezawa I, Jenkins DP, Jin BE & Wulff H. (2012). Microglial KCa3.1 Channels as a Potential Therapeutic Target for Alzheimer's Disease. *International Journal of Alzheimer's Disease* **2012,** 868972.

Maezawa I, Zimin PI, Wulff H & Jin LW. (2011). Amyloid-beta protein oligomer at low nanomolar concentrations activates microglia and induces microglial neurotoxicity. *The Journal of Biological Chemistry* **286,** 3693-3706.

Majoul I, Straub M, Hell SW, Duden R & Soling HD. (2001). KDEL-cargo regulates interactions between proteins involved in COPI vesicle traffic: measurements in living cells using FRET. *Developmental Cell* **1,** 139-153.

Malik-Hall M, Ganellin CR, Galanakis D & Jenkinson DH. (2000). Compounds that block both intermediate-conductance (IK_{Ca}) and small-conductance (SK_{Ca}) calcium-activated potassium channels. *British Journal of Pharmacology* **129,** 1431-1438.

Marchand JB, Kaiser DA, Pollard TD & Higgs HN. (2001). Interaction of WASP/Scar proteins with actin and vertebrate Arp2/3 complex. *Nature Cell Biology* **3,** 76-82.

Mari M, Bujny MV, Zeuschner D, Geerts WJ, Griffith J, Petersen CM, Cullen PJ, Klumperman J & Geuze HJ. (2008). SNX1 defines an early endosomal recycling exit for sortilin and mannose 6-phosphate receptors. *Traffic (Copenhagen, Denmark)* **9,** 380-393.

Matern HT, Yeaman C, Nelson WJ & Scheller RH. (2001). The Sec6/8 complex in mammalian cells: characterization of mammalian Sec3, subunit interactions, and expression of subunits in polarized cells. *Proceedings of the National Academy of Sciences of the United States of America* **98,** 9648-9653.

Matsudaira P. (1987). Sequence from picomole quantities of proteins electroblotted onto polyvinylidene difluoride membranes. *The Journal of Biological Chemistry* **262,** 10035-10038.

Matter K, Hunziker W & Mellman I. (1992). Basolateral sorting of LDL receptor in MDCK cells: the cytoplasmic domain contains two tyrosine-dependent targeting determinants. *Cell* **71,** 741-753.

McCracken AA & Brodsky JL. (1996). Assembly of ER-associated protein degradation in vitro: dependence on cytosol, calnexin, and ATP. *The Journal of Cell Biology* **132,** 291-298.

Miller DR, Rickles FR, Lichtman MA, La Celle PL, Bates J & Weed RI. (1971). A new variant of hereditary hemolytic anemia with stomatocytosis and erythrocyte cation abnormality. *Blood* **38,** 184-204.

Miranda KC, Khromykh T, Christy P, Le TL, Gottardi CJ, Yap AS, Stow JL & Teasdale RD. (2001). A dileucine motif targets E-cadherin to the basolateral cell surface in Madin-Darby canine kidney and LLC-PK1 epithelial cells. *The Journal of Biological Chemistry* **276,** 22565-22572.

Mironov AA, Mironov AA, Jr., Beznoussenko GV, Trucco A, Lupetti P, Smith JD, Geerts WJ, Koster AJ, Burger KN, Martone ME, Deerinck TJ, Ellisman MH & Luini A. (2003). ER-to-Golgi carriers arise through direct en bloc protrusion and multistage maturation of specialized ER exit domains. *Developmental Cell* **5,** 583-594.

Misek DE, Bard E & Rodriguez-Boulan E. (1984). Biogenesis of epithelial cell polarity: intracellular sorting and vectorial exocytosis of an apical plasma membrane glycoprotein. *Cell* **39,** 537-546.

Morais-Cabral JH, Zhou Y & MacKinnon R. (2001). Energetic optimization of ion conduction rate by the K^+ selectivity filter. *Nature* **414,** 37-42.

Nagel RL & Lawrence C. (1991). The distinct pathobiology of sickle cell-hemoglobin C disease. Therapeutic implications. *Hematology/Oncology Clinics of North America* **5,** 433-451.

Neylon CB, Lang RJ, Fu Y, Bobik A & Reinhart PH. (1999). Molecular cloning and characterization of the intermediate-conductance Ca^{2+}-activated K^+ channel in vascular smooth muscle: relationship between K_{Ca} channel diversity and smooth muscle cell function. *Circulation Research* **85,** e33-43.

Norwood SJ, Shaw DJ, Cowieson NP, Owen DJ, Teasdale RD & Collins BM. (2011). Assembly and solution structure of the core retromer protein complex. *Traffic (Copenhagen, Denmark)* **12,** 56-71.

Nothwehr SF, Bruinsma P & Strawn LA. (1999). Distinct domains within Vps35p mediate the retrieval of two different cargo proteins from the yeast prevacuolar/endosomal compartment. *Molecular Biology of the Cell* **10,** 875-890.

Novick P, Field C & Schekman R. (1980). Identification of 23 complementation groups required for post-translational events in the yeast secretory pathway. *Cell* **21,** 205-215.

Oh J, Julias JG, Ferris AL & Hughes SH. (2002). Construction and characterization of a replication-competent retroviral shuttle vector plasmid. *Journal of Virology* **76,** 1762-1768.

Ohkura T, Momose F, Ichikawa R, Takeuchi K & Morikawa Y. (2014). Influenza A virus hemagglutinin and neuraminidase mutually accelerate their apical targeting through clustering of lipid rafts. *Journal of Virology* **88,** 10039-10055.

Owen DJ & Evans PR. (1998). A structural explanation for the recognition of tyrosine-based endocytotic signals. *Science (New York, NY)* **282,** 1327-1332.

Pearson MA, Reczek D, Bretscher A & Karplus PA. (2000). Structure of the ERM protein moesin reveals the FERM domain fold masked by an extended actin binding tail domain. Cell 101, 259-270.

Pedarzani P, Mosbacher J, Rivard A, Cingolani LA, Oliver D, Stocker M, Adelman JP & Fakler B. (2001). Control of electrical activity in central neurons by modulating the gating of small conductance Ca^{2+}-activated K^{+} channels. *The Journal of Biological Chemistry* **276,** 9762-9769.

Pena TL & Rane SG. (1999). The fibroblast intermediate conductance K(Ca) channel, FIK, as a prototype for the cell growth regulatory function of the IK channel family. *The Journal of Membrane Biology* **172,** 249-257.

Peter BJ, Kent HM, Mills IG, Vallis Y, Butler PJ, Evans PR & McMahon HT. (2004). BAR domains as sensors of membrane curvature: the amphiphysin BAR structure. *Science (New York, NY)* **303,** 495-499.

Pfeffer SR. (2010). How the Golgi works: a cisternal progenitor model. *Proceedings of the National Academy of Sciences of the United States of America* **107,** 19614-19618.

Pocha SM, Wassmer T, Niehage C, Hoflack B & Knust E. (2011). Retromer controls epithelial cell polarity by trafficking the apical determinant Crumbs. *Current Biology : CB* **21,** 1111-1117.

Ponting CP. (1997). Evidence for PDZ domains in bacteria, yeast, and plants. Protein science : a publication of the Protein Society 6, 464-468.s

Procino G, Barbieri C, Tamma G, De Benedictis L, Pessin JE, Svelto M & Valenti G. (2008). AQP2 exocytosis in the renal collecting duct -- involvement of SNARE isoforms and the regulatory role of Munc18b. *Journal of Cell Science* **121,** 2097-2106.

Qi W, Chen X, Poronnik P & Pollock CA. (2006). The renal cortical fibroblast in renal tubulointerstitial fibrosis. *The International Journal of Biochemistry & Cell Biology* **38,** 1-5.

Qian F, Germino FJ, Cai Y, Zhang X, Somlo S & Germino GG. (1997). PKD1 interacts with PKD2 through a probable coiled-coil domain. *Nature Genetics* **16,** 179-183.

Rabjerg M, Olivan-Viguera A, Hansen LK, Jensen L, Sevelsted-Moller L, Walter S, Jensen BL, Marcussen N & Kohler R. (2015). High expression of KCa3.1 in patients with clear cell renal carcinoma predicts high metastatic risk and poor survival. *PloS One* **10,** e0122992.

Rapetti-Mauss R, Lacoste C, Picard V, Guitton C, Lombard E, Loosveld M, Nivaggioni V, Dasilva N, Salgado D, Desvignes JP, Beroud C, Viout P, Bernard M, Soriani O, Vinti H, Lacroze V, Feneant-Thibault M, Thuret I, Guizouarn H & Badens C. (2015). A mutation in the Gardos channel is associated with hereditary xerocytosis. *Blood* **126,** 1273-1280.

Rapetti-Mauss R, Soriani O, Vinti H, Badens C & Guizouarn H. (2016). Senicapoc: a potent candidate for the treatment of a subset of hereditary xerocytosis caused by mutations in the Gardos channel. Haematologica 101, e431-e435.

Rapoport TA, Jungnickel B & Kutay U. (1996). Protein transport across the eukaryotic endoplasmic reticulum and bacterial inner membranes. *Annual Review of Biochemistry* **65,** 271-303.

Rath A, Glibowicka M, Nadeau VG, Chen G & Deber CM. (2009). Detergent binding explains anomalous SDS-PAGE migration of membrane proteins. *Proceedings of the National Academy of Sciences of the United States of America* **106,** 1760-1765.

Reddy JV & Seaman MN. (2001). Vps26p, a component of retromer, directs the interactions of Vps35p in endosome-to-Golgi retrieval. *Molecular Biology of the Cell* **12,** 3242-3256.

Regeer RR & Markovich D. (2004). A dileucine motif targets the sulfate anion transporter sat-1 to the basolateral membrane in renal cell lines. *American journal of physiology Cell physiology* **287,** C365-372.

Reynolds JA & Tanford C. (1970). Binding of dodecyl sulfate to proteins at high binding ratios. Possible implications for the state of proteins in biological membranes. *Proceedings of the National Academy of Sciences of the United States of America* **66,** 1002-1007.

Rhoda MD, Apovo M, Beuzard Y & Giraud F. (1990). Ca^{2+} permeability in deoxygenated sickle cells. *Blood* **75,** 2453-2458.

Rivera-Molina F & Toomre D. (2013). Live-cell imaging of exocyst links its spatiotemporal dynamics to various stages of vesicle fusion. *The Journal of Cell Biology* **201,** 673-680.

Robinson MS, Sahlender DA & Foster SD. (2010). Rapid inactivation of proteins by rapamycin-induced rerouting to mitochondria. *Developmental Cell* **18,** 324-331.

Rodionov DG & Bakke O. (1998). Medium chains of adaptor complexes AP-1 and AP-2 recognize leucine-based sorting signals from the invariant chain. *The Journal of Biological Chemistry* **273,** 6005-6008.

Rodriguez-Boulan E & Musch A. (2005). Protein sorting in the Golgi complex: shifting paradigms. *Biochimica et Biophysica Acta* **1744,** 455-464.

Rojas R, Kametaka S, Haft CR & Bonifacino JS. (2007). Interchangeable but essential functions of SNX1 and SNX2 in the association of retromer with endosomes and the trafficking of mannose 6-phosphate receptors. *Molecular and Cellular Biology* **27,** 1112-1124.

Roncarati R, Decimo I & Fumagalli G. (2005). Assembly and trafficking of human small conductance Ca^{2+}-activated K^+ channel SK3 are governed by different molecular domains. *Molecular and Cellular Neurosciences* **28,** 314-325.

Rotte A, Pasham V, Mack AF, Bhandaru M, Qadri SM, Eichenmuller M, Ruth P & Lang F. (2011). Ca^{2+} activated K^+ channel KCa3.1 as a determinant of gastric acid secretion. *Cellular Physiology and Biochemistry: International Journal of Experimental Cellular Physiology, Biochemistry, and Pharmacology* **27,** 597-604.

Ryabov AD, Firsova YN, Ershov A & Dementiev IA. (1999). Spectrophotometric kinetic study and analytical implications of the glucose oxidase-catalyzed reduction of [MIII(LL)2Cl2]+ complexes by D-glucose (M = Os and Ru, LL = 2,2'-bipyridine and 1,10-phenanthroline type ligands). *Journal of Biological Inorganic Chemistry: JBIC: a publication of the Society of Biological Inorganic Chemistry* **4,** 175-182.

Sandle GI, McNicholas CM & Lomax RB. (1994). Potassium channels in colonic crypts. *Lancet (London, England)* **343,** 23-25.

Scheiffele P, Peranen J & Simons K. (1995). N-glycans as apical sorting signals in epithelial cells. *Nature* **378,** 96-98.

Schumacher MA, Rivard AF, Bachinger HP & Adelman JP. (2001). Structure of the gating domain of a Ca^{2+}-activated K^+ channel complexed with Ca^{2+}/calmodulin. *Nature* **410,** 1120-1124.

Schwab A, Nechyporuk-Zloy V, Gassner B, Schulz C, Kessler W, Mally S, Römer M & Stock C. (2012). Dynamic redistribution of calcium sensitive potassium channels ($hK_{Ca}3.1$) in migrating cells. *Journal of Cellular Physiology* **227,** 686-696.

Seaman MN, Marcusson EG, Cereghino JL & Emr SD. (1997). Endosome to Golgi retrieval of the vacuolar protein sorting receptor, Vps10p, requires the function of the VPS29, VPS30, and VPS35 gene products. *The Journal of Cell Biology* **137,** 79-92.

Seaman MN, McCaffery JM & Emr SD. (1998). A membrane coat complex essential for endosome-to-Golgi retrograde transport in yeast. *The Journal of Cell Biology* **142,** 665-681.

Seet LF & Hong W. (2006). The Phox (PX) domain proteins and membrane traffic. *Biochimica et Biophysica Acta* **1761,** 878-896.

Shapiro AL, Vinuela E & Maizel JV, Jr. (1967). Molecular weight estimation of polypeptide chains by electrophoresis in SDS-polyacrylamide gels. *Biochemical and Biophysical Research Communications* **28,** 815-820.

Sharma N, Low SH, Misra S, Pallavi B & Weimbs T. (2006). Apical targeting of syntaxin 3 is essential for epithelial cell polarity. *The Journal of Cell Biology* **173,** 937-948.

Shi H, Rojas R, Bonifacino JS & Hurley JH. (2006). The retromer subunit Vps26 has an arrestin fold and binds Vps35 through its C-terminal domain. *Nature Structural & Molecular Biology* **13,** 540-548.

Simons K & Fuller SD. (1985). Cell surface polarity in epithelia. *Annual Review of Cell Biology* **1,** 243-288.

Singh V, Yang J, Cha B, Chen TE, Sarker R, Yin J, Avula LR, Tse M & Donowitz M. (2015). Sorting nexin 27 regulates basal and stimulated brush border trafficking of NHE3. *Molecular Biology of the Cell* **26,** 2030-2043.

Smith PK, Krohn RI, Hermanson GT, Mallia AK, Gartner FH, Provenzano MD, Fujimoto EK, Goeke NM, Olson BJ & Klenk DC. (1985). Measurement of protein using bicinchoninic acid. *Analytical Biochemistry* **150,** 76-85.

Solis GP, Hulsbusch N, Radon Y, Katanaev VL, Plattner H & Stuermer CA. (2013). Reggies/flotillins interact with Rab11a and SNX4 at the tubulovesicular recycling compartment and function in transferrin receptor and E-cadherin trafficking. *Molecular Biology of the Cell* **24,** 2689-2702.

Sollner T, Bennett MK, Whiteheart SW, Scheller RH & Rothman JE. (1993). A protein assembly-disassembly pathway in vitro that may correspond to sequential steps of synaptic vesicle docking, activation, and fusion. *Cell* **75,** 409-418.

Steinberg F, Gallon M, Winfield M, Thomas EC, Bell AJ, Heesom KJ, Tavare JM & Cullen PJ. (2013). A global analysis of SNX27-retromer assembly and cargo specificity reveals a function in glucose and metal ion transport. *Nature Cell Biology* **15,** 461-471.

Strochlic TI, Setty TG, Sitaram A & Burd CG. (2007). Grd19/Snx3p functions as a cargo-specific adapter for retromer-dependent endocytic recycling. *The Journal of Cell Biology* **177,** 115-125.

Sun AQ, Swaby I, Xu S & Suchy FJ. (2001). Cell-specific basolateral membrane sorting of the human liver Na^+-dependent bile acid cotransporter. *American Journal of Physiology Gastrointestinal and Liver Physiology* **280,** G1305-1313.

Syme CA, Hamilton KL, Jones HM, Gerlach AC, Giltinan L, Papworth GD, Watkins SC, Bradbury NA & Devor DC. (2003). Trafficking of the Ca^{2+}-activated K^+ channel, hIK1, is dependent upon a C-terminal leucine zipper. *The Journal of Biological Chemistry* **278,** 8476-8486.

Tasevski V, Benn D, Peters G, Luttrell B & Simpson A. (1998). The Fischer rat thyroid cell line FRTL-5 exhibits a nondiploid karyotype. *Thyroid : official journal of the American Thyroid Association* **8,** 623-626.

Tashima Y, Taguchi R, Murata C, Ashida H, Kinoshita T & Maeda Y. (2006). PGAP2 is essential for correct processing and stable expression of GPI-anchored proteins. *Molecular Biology of the Cell* **17,** 1410-1420.

Teasdale RD & Collins BM. (2012). Insights into the PX (phox-homology) domain and SNX (sorting nexin) protein families: structures, functions and roles in disease. *The Biochemical Journal* **441,** 39-59.

Temkin P, Lauffer B, Jager S, Cimermancic P, Krogan NJ & von Zastrow M. (2011). SNX27 mediates retromer tubule entry and endosome-to-plasma membrane trafficking of signalling receptors. *Nature Cell Biology* **13,** 715-721.

Tepass U, Tanentzapf G, Ward R & Fehon R. (2001). Epithelial cell polarity and cell junctions in Drosophila. *Annual Review of Genetics* **35,** 747-784.

TerBush DR, Maurice T, Roth D & Novick P. (1996). The Exocyst is a multiprotein complex required for exocytosis in Saccharomyces cerevisiae. *The EMBO Journal* **15,** 6483-6494.

TerBush DR & Novick P. (1995). Sec6, Sec8, and Sec15 are components of a multisubunit complex which localizes to small bud tips in Saccharomyces cerevisiae. *The Journal of Cell Biology* **130,** 299-312.

Thomas DC, Brewer CB & Roth MG. (1993). Vesicular stomatitis virus glycoprotein contains a dominant cytoplasmic basolateral sorting signal critically dependent upon a tyrosine. *The Journal of Biological Chemistry* **268,** 3313-33

Thorpe GH, Kricka LJ, Moseley SB & Whitehead TP. (1985). Phenols as enhancers of the chemiluminescent horseradish peroxidase-luminol-hydrogen peroxide reaction: application in luminescence-monitored enzyme immunoassays. *Clinical Chemistry* **31,** 1335-1341.

Torres VE & Harris PC. (2009). Autosomal dominant polycystic kidney disease: the last 3 years. *Kidney International* **76,** 149-168.

Torres VE, Rossetti S & Harris PC. (2007). Update on autosomal dominant polycystic kidney disease. *Minerva Medica* **98,** 669-691.

Traer CJ, Rutherford AC, Palmer KJ, Wassmer T, Oakley J, Attar N, Carlton JG, Kremerskothen J, Stephens DJ & Cullen PJ. (2007). SNX4 coordinates endosomal sorting of TfnR with dynein-mediated transport into the endocytic recycling compartment. *Nature Cell Biology* **9,** 1370-1380.

Trinh NT, Prive A, Maille E, Noel J & Brochiero E. (2008). EGF and K^+ channel activity control normal and cystic fibrosis bronchial epithelia repair. *American Journal of Physiology Lung Cellular and Molecular Physiology* **295,** L866-880.

Turner KL & Sontheimer H. (2014). KCa3.1 modulates neuroblast migration along the rostral migratory stream (RMS) in vivo. *Cerebral Cortex (New York, NY : 1991)* **24,** 2388-2400.

Turner RW, Kruskic M, Teves M, Scheidl-Yee T, Hameed S & Zamponi GW. (2015). Neuronal expression of the intermediate conductance calcium-activated potassium channel KCa3.1 in the mammalian central nervous system. *Pflugers Archiv : European Journal of Physiology* **467,** 311-328.

USRD. (2009). U.S. Renal Data System. USRD 2009 Annual Data Report: Atlas of chronic kidney disease and end-stage renal disease in the United States. *National Institutes of Health, National Institute of Diabetes and Digestive and Kidney Diseases: Bethesda, MD, USA*.

Ussing HH & Zerahn K. (1951). Active transport of sodium as the source of electric current in the short-circuited isolated frog skin. *Acta Physiologica Scandinavica* **23,** 110-127.

Vallon V, Grahammer F, Volkl H, Sandu CD, Richter K, Rexhepaj R, Gerlach U, Rong Q, Pfeifer K & Lang F. (2005). KCNQ1-dependent transport in renal and gastrointestinal epithelia. *Proceedings of the National Academy of Sciences of the United States of America* **102,** 17864-17869.

van Weering JR, Sessions RB, Traer CJ, Kloer DP, Bhatia VK, Stamou D, Carlsson SR, Hurley JH & Cullen PJ. (2012). Molecular basis for SNX-BAR-mediated assembly of distinct endosomal sorting tubules. *The EMBO Journal* **31,** 4466-4480.

Wandinger-Ness A, Bennett MK, Antony C & Simons K. (1990). Distinct transport vesicles mediate the delivery of plasma membrane proteins to the apical and basolateral domains of MDCK cells. *The Journal of Cell Biology* **111,** 987-1000.

Wang CC, Shi H, Guo K, Ng CP, Li J, Gan BQ, Chien Liew H, Leinonen J, Rajaniemi H, Zhou ZH, Zeng Q & Hong W. (2007). VAMP8/endobrevin as a general vesicular SNARE for regulated exocytosis of the exocrine system. *Molecular Biology of the Cell* **18,** 1056-1063.

Wang LP, Wang Y, Zhao LM, Li GR & Deng XL. (2013a). Angiotensin II upregulates K(Ca)3.1 channels and stimulates cell proliferation in rat cardiac fibroblasts. *Biochemical Pharmacology* **85,** 1486-1494.

Wang TY & Silvius JR. (2003). Sphingolipid partitioning into ordered domains in cholesterol-free and cholesterol-containing lipid bilayers. *Biophysical Journal* **84,** 367-378.

Wang X, Zhao Y, Zhang X, Badie H, Zhou Y, Mu Y, Loo LS, Cai L, Thompson RC, Yang B, Chen Y, Johnson PF, Wu C, Bu G, Mobley WC, Zhang D, Gage FH, Ranscht B, Zhang YW, Lipton SA, Hong W & Xu H. (2013b). Loss of sorting nexin 27 contributes to excitatory synaptic dysfunction by modulating glutamate receptor recycling in Down's syndrome. *Nature Medicine* **19,** 473-480.

Wassmer T, Attar N, Bujny MV, Oakley J, Traer CJ & Cullen PJ. (2007). A loss-of-function screen reveals SNX5 and SNX6 as potential components of the mammalian retromer. *Journal of Cell Science* **120,** 45-54.

Wassmer T, Attar N, Harterink M, van Weering JR, Traer CJ, Oakley J, Goud B, Stephens DJ, Verkade P, Korswagen HC & Cullen PJ. (2009). The retromer coat complex coordinates endosomal sorting and dynein-mediated transport, with carrier recognition by the trans-Golgi network. *Developmental Cell* **17,** 110-122.

Watanabe S, Umeki N, Ikebe R & Ikebe M. (2008). Impacts of Usher syndrome type IB mutations on human myosin VIIa motor function. *Biochemistry* **47,** 9505-9513.

Weber K & Osborn M. (1969). The reliability of molecular weight determinations by dodecyl sulfate-polyacrylamide gel electrophoresis. *The Journal of Biological Chemistry* **244,** 4406-4412.

Weber KT. (2000). Fibrosis and hypertensive heart disease. *Current Opinion in Cardiology* **15,** 264-272.

Wei T, Yi M, Gu W, Hou L, Lu Q, Yu Z & Chen H. (2016). The Potassium Channel KCa3.1 Represents a Valid Pharmacological Target for Astrogliosis-Induced Neuronal Impairment in a Mouse Model of Alzheimer's Disease. *Frontiers in Pharmacology* **7,** 528.

Winter BJ, Balut CM, Butterworth MB, Gao Y, Devor DC & Hamilton KL. (2011). Basolateral trafficking of KCa3.1 in a polarized epithelium. The FASEB Journal 25, 860.813.

Wu S, Mehta SQ, Pichaud F, Bellen HJ & Quiocho FA. (2005). Sec15 interacts with Rab11 via a novel domain and affects Rab11 localization in vivo. *Nature Structural & Molecular Biology* **12,** 879-885.

Wulff H, Miller MJ, Hansel W, Grissmer S, Cahalan MD & Chandy KG. (2000). Design of a potent and selective inhibitor of the intermediate-conductance Ca^{2+}-activated K^{+} channel, IKCa1: a potential immunosuppressant. *Proceedings of the National Academy of Sciences of the United States of America* **97,** 8151-8156.

Xia XM, Fakler B, Rivard A, Wayman G, Johnson-Pais T, Keen JE, Ishii T, Hirschberg B, Bond CT, Lutsenko S, Maylie J & Adelman JP. (1998). Mechanism of calcium gating in small-conductance calcium-activated potassium channels. *Nature* **395,** 503-507.

Xu XF, Chen ZT, Gao N, Zhang JL & An J. (2009). Myosin Vc, a member of the actin motor family associated with Rab8, is involved in the release of DV2 from HepG2 cells. *Intervirology* **52,** 258-265.

Yamazaki D, Aoyama M, Ohya S, Muraki K, Asai K & Imaizumi Y. (2006). Novel functions of small conductance Ca^{2+}-activated K^{+} channel in enhanced cell proliferation by ATP in brain endothelial cells. *The Journal of Biological Chemistry* **281,** 38430-38439.

Yang JS, Lee SY, Spano S, Gad H, Zhang L, Nie Z, Bonazzi M, Corda D, Luini A & Hsu VW. (2005). A role for BARS at the fission step of COPI vesicle formation from Golgi membrane. *The EMBO Journal* **24,** 4133-4143.

Yao D, Ehrlich M, Henis YI & Leof EB. (2002). Transforming growth factor-beta receptors interact with AP2 by direct binding to beta2 subunit. *Molecular Biology of the Cell* **13,** 4001-4012.

Yeaman C, Le Gall AH, Baldwin AN, Monlauzeur L, Le Bivic A & Rodriguez-Boulan E. (1997). The O-glycosylated stalk domain is required for apical sorting of neurotrophin receptors in polarized MDCK cells. *The Journal of Cell Biology* **139,** 929-940.

Yi M, Yu P, Lu Q, Geller HM, Yu Z & Chen H. (2016). KCa3.1 constitutes a pharmacological target for astrogliosis associated with Alzheimer's disease. *Molecular and Cellular Neurosciences* **76,** 21-32.

Yoder BK, Hou X & Guay-Woodford LM. (2002). The polycystic kidney disease proteins, polycystin-1, polycystin-2, polaris, and cystin, are co-localized in renal cilia. *Journal of the American Society of Nephrology : JASN* **13,** 2508-2516.

Zhang M & Wang W. (2003). Organization of signaling complexes by PDZ-domain scaffold proteins. *Accounts of Chemical Research* **36,** 530-538.

Zhang X, Wang G, Dupre DJ, Feng Y, Robitaille M, Lazartigues E, Feng YH, Hebert TE & Wu G. (2009). Rab1 GTPase and dimerization in the cell surface expression of angiotensin II type 2 receptor. *The Journal of Pharmacology and Experimental Therapeutics* **330,** 109-117.

Zhao LM, Wang LP, Wang HF, Ma XZ, Zhou DX & Deng XL. (2015). The role of KCa3.1 channels in cardiac fibrosis induced by pressure overload in rats. *Pflugers Archiv : European Journal of Physiology* **467,** 2275-2285.

Zhao X, Nothwehr S, Lara-Lemus R, Zhang BY, Peter H & Arvan P. (2007). Dominant-negative behavior of mammalian Vps35 in yeast requires a conserved PRLYL motif involved in retromer assembly. *Traffic (Copenhagen, Denmark)* **8,** 1829-1840.

Zimmerberg J & McLaughlin S. (2004). Membrane curvature: how BAR domains bend bilayers. *Current Biology : CB* **14,** R250-252.

Zimmerman SP, Hueschen CL, Malide D, Milgram SL & Playford MP. (2013). Sorting nexin 27 (SNX27) associates with zonula occludens-2 (ZO-2) and modulates the epithelial tight junction. *The Biochemical Journal* **455,** 95-106.

Zurzolo C, Gentile R, Mascia A, Garbi C, Polistina C, Aloj L, Avvedimento VE & Nitsch L. (1991). The polarized epithelial phenotype is dominant in hybrids between polarized and unpolarized rat thyroid cell lines. *Journal of Cell Science* **98 (Pt 1),** 65-73.